

1971

The effects of cold work and subsequent annealing upon the microstructure and magnetic properties of zr-doped 6-80 molybdenum permalloy

Charles Rudolf Frohlich Jr.
Lehigh University

Follow this and additional works at: <https://preserve.lehigh.edu/etd>

 Part of the [Materials Science and Engineering Commons](#)

Recommended Citation

Frohlich, Charles Rudolf Jr., "The effects of cold work and subsequent annealing upon the microstructure and magnetic properties of zr-doped 6-80 molybdenum permalloy" (1971). *Theses and Dissertations*. 3967.
<https://preserve.lehigh.edu/etd/3967>

This Thesis is brought to you for free and open access by Lehigh Preserve. It has been accepted for inclusion in Theses and Dissertations by an authorized administrator of Lehigh Preserve. For more information, please contact preserve@lehigh.edu.

THE EFFECTS OF COLD WORK AND SUBSEQUENT
ANNEALING UPON THE MICROSTRUCTURE AND MAGNETIC
PROPERTIES OF A ZR-DOPED 6-80 MOLYBDENUM PERMALLOY

by
Charles Rudolf Frohlich Jr.

1.

ABSTRACT

An alloy containing 80.0% Ni, 12.65% Fe, 6.74% Mo, 0.36% Zr, and 0.25% Mn by weight was cast, solution annealed, and cold rolled into thin strips reduced in area by 0, 50, 75, and 90%. In addition samples of each worked condition were annealed to produce recrystallized and aged structures. Light metallography, electron microscopy, microprobe analysis, and magnetic testing were performed to determine the effects of cold working and annealing upon the microstructure and magnetic properties of the alloy.

Cold working produced a high initial hardness together with a high coercive force. Recrystallization of the cold worked structures occurred on annealing at 600°C and above, and caused significant decreases in hardness and coercive force. An activation energy of 80.5 kcal/g mole was found for the recrystallization process in 50%, 75%, and 90% reduced specimens. The transformation occurred more rapidly in more highly cold worked structures as evidenced by the increase in the pre-exponential constant of the Arrhenius equation.

For longer times at the recrystallization temperature and above, transmission electron microscopy and electron diffraction revealed a small number of spherical Ni_4Mo particles. These particles had essentially no effect on magnetic properties because of their relatively coarse size and spacing, and because

the rapid recrystallization and attendant increase in perfection overshadowed their pinning effect on domain walls. Beginning at 700°C ribbon-shaped particles of Ni_5Zr intermetallic compound, apparently coherent and with a definite habit, also precipitated out of solid solution. Both precipitates were a result of continuous precipitation within grains and were not formed by a cellular or discontinuous precipitation reaction. A peak in coercive force at 800°C is attributed to domain wall pinning associated with the fine distribution of rodlike Ni_5Zr particles. Cold working 90% and aging at 800°C was found to increase coercive force by almost 0.2 oersted.

Magnetic hysteresis was observed to be increased by both cold working and age hardening. Annealing, however, decreased hysteresis and improved squareness. The temperature of annealing was found to be more critical in determining magnetic properties than was time at a specified temperature.

THE EFFECTS OF COLD WORK AND
SUBSEQUENT ANNEALING UPON THE MICROSTRUCTURE
AND MAGNETIC PROPERTIES OF A ZR-DOPED 6-80 MOLYBDENUM PERMALLOY

by
Charles R. Frohlich Jr.

A Thesis
Presented to the Graduate Committee
of Lehigh University
in Candidacy for the Degree of
Master of Science
in
Metallurgy and Materials Science

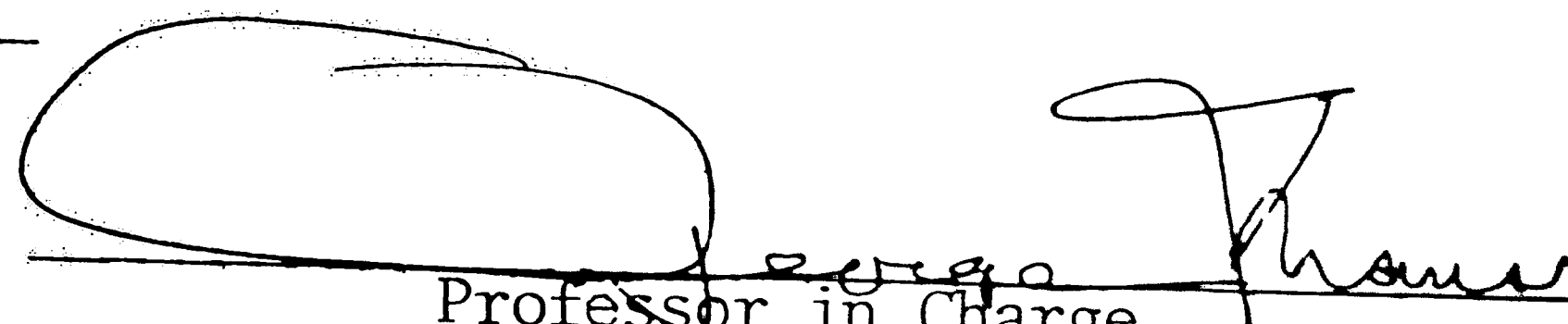
Lehigh University

1971

CERTIFICATE OF APPROVAL

This thesis is accepted and approved in partial fulfillment of the requirements for the degree of Master of Science.

May 10, 1971
Date


Professor in Charge

G. P. Conrad

Chairman of the Department
of Metallurgy and Materials
Science

ACKNOWLEDGEMENTS

The author expresses his sincere gratitude to Professor George Krauss for his encouragement and guidance throughout this work. He also thanks J. L. Bestel of the Western Electric Engineering Research Center for his ideas and assistance.

Of the many people at the Western Electric Engineering Research Center whose special talents contributed to this thesis, a special thanks goes to S. J. Buzash for his help in metallography and assistance on details too numerous to list, to R. E. Woods for his untiring work on the electron microscope, and to R. L. Tavani for his aid in sample preparation and photographic techniques. The author similarly is indebted to B. Broyde who got him started on this project, and to G. Y. Chin and T. C. Tisone of Bell Telephone Laboratories whose theory, suggestions, and material assistance proved invaluable.

Acknowledgement also goes to the following Western Electric people:

- P. A. Crawford for electron microprobe analysis.
- B. L. Madsen and D. A. Green for fluorescence analysis.
- P. F. Elarde of Chicago for hysteresis loop measurements.

and K. M. Olsen of BTL, Murray Hill for ingot processing. The complete typing of this manuscript by Cathie Grier is sincerely appreciated.

Last but not least the author thanks his wife, Gayle, for her enthusiasm and encouragement over the past two years.

TABLE OF CONTENTS

	<u>PAGE</u>
ACKNOWLEDGEMENTS.	iii
LIST OF FIGURES	v
LIST OF TABLES.	vii
ABSTRACT.	1
INTRODUCTION.	3
EXPERIMENTAL PROCEDURE	9
RESULTS AND DISCUSSION	13
Hardness Test.	13
Magnetic Measurements	15
Optical Microscope Studies	20
Electron Microprobe Analysis	21
Electron Microscope Investigation.	22
CONCLUSIONS	30
FIGURES	32
BIBLIOGRAPHY	64
VITA	66

LIST OF FIGURES

Figure		Page
1	Hardness vs. Annealing Temperature for a 15-minute Anneal	32
2	Hardness vs. Annealing Temperature for a 30-minute Anneal	33
3	Hardness vs. Annealing Temperature for a 1-hour Anneal	34
4	Hardness vs. Annealing Temperature for a 2-hour Anneal	35
5	Coercive Force vs. Annealing Temperature for a 15-minute Anneal	36
6	Coercive Force vs. Annealing Temperature for a 30-minute Anneal	37
7	Coercive Force vs. Annealing Temperature for a 1-hour Anneal	38
8	Coercive Force vs. Annealing Temperature for a 2-hour Anneal	39
9	Coercive Force vs. Annealing Temperature for a 4-hour Anneal	40
10	Coercive Force vs. Annealing Time at 600°C	41
11	Coercive Force vs. Annealing Time at 700°C	42
12	Coercive Force vs. Annealing Time at 800°C	43
13	Coercive Force vs. Annealing Time at 900°C	44
14	Hysteresis Loops for 0% and 50% Cold Worked Alloys Annealed as Indicated	45
15	Hysteresis Loops for 75% and 90% Cold Worked Alloys Annealed as Indicated	46
16	Hysteresis Loops for 75% Cold Worked Alloy Annealed as Indicated	47

Figure		Page
17	Time for 50% Recrystallization vs. $1/T$	48
18	Microstructures of 0% and 50% Cold Worked Alloys	49
19	Microstructure of 0% Cold Work Alloy Annealed for 15 Minutes at Various Temperatures	50
20	Microstructures of Alloys Annealed at 800°C for 30 Minutes	51
21	X-Ray Raster and Back-Scatter Displays of 50% Cold Worked Structure Annealed at 850°C for 1 Hour	52
22	Electron Micrographs of 90% Cold Worked Alloy Annealed at 600°C for Various Times	53
23	Electron Micrographs of 90% Cold Worked Alloy Annealed for 2 Hours at Various Temperatures	54
24	Electron Micrographs of 90% Cold Worked Alloy Annealed at 700°C for Various Times	55
25	Electron Micrographs and Diffraction Pattern of 90% Cold Worked Alloy Annealed at 700°C for 30 Minutes	56
26	Electron Micrographs of 90% Cold Worked Alloy Annealed at 700°C for 30 Minutes	57
27	Electron Micrographs of 90% Cold Worked Alloy Annealed at 800°C for Various Times	58
28	Electron Micrographs of 90% Cold Worked Alloy Annealed at Various Times and Temperatures	59
29	Electron Micrographs of 90% Cold Worked Alloy Annealed at 850°C for 2 Hours	60
30	Electron Diffraction Patterns of 90% Cold Worked Alloy Annealed at Various Times and Temperatures	61

LIST OF TABLES

Table		Page
I	Electron Diffraction Data for a 90% Cold Work - Unannealed Structure	62
II	Electron Diffraction Data for a 90% Cold Work - 600°C - 2 Hour Anneal Structure	62
III	Electron Diffraction Data for a 90% Cold Work - 850°C - 2 Hour Anneal Structure	63

ABSTRACT

An alloy containing 80.0% Ni, 12.65% Fe, 6.74% Mo, 0.36% Zr, and 0.25% Mn by weight was cast, solution annealed, and cold rolled into thin strips reduced in area by 0, 50, 75, and 90%. In addition samples of each worked condition were annealed to produce recrystallized and aged structures. Light metallography, electron microscopy, microprobe analysis, and magnetic testing were performed to determine the effects of cold working and annealing upon the microstructure and magnetic properties of the alloy.

Cold working produced a high initial hardness together with a high coercive force. Recrystallization of the cold worked structures occurred on annealing at 600°C and above, and caused significant decreases in hardness and coercive force. An activation energy of 80.5 kcal/g mole was found for the recrystallization process in 50%, 75%, and 90% reduced specimens. The transformation occurred more rapidly in more highly cold worked structures as evidenced by the increase in the pre-exponential constant of the Arrhenius equation.

For longer times at the recrystallization temperature and above, transmission electron microscopy and electron diffraction revealed a small number of spherical Ni_4Mo particles. These particles had essentially no effect on magnetic properties because of their relatively coarse size and spacing, and because

the rapid recrystallization and attendant increase in perfection overshadowed their pinning effect on domain walls. Beginning at 700°C ribbon-shaped particles of Ni_5Zr intermetallic compound, apparently coherent and with a definite habit, also precipitated out of solid solution. Both precipitates were a result of continuous precipitation within grains and were not formed by a cellular or discontinuous precipitation reaction. A peak in coercive force at 800°C is attributed to domain wall pinning associated with the fine distribution of rodlike Ni_5Zr particles. Cold working 90% and aging at 800°C was found to increase coercive force by almost 0.2 oersted.

Magnetic hysteresis was observed to be increased by both cold working and age hardening. Annealing, however, decreased hysteresis and improved squareness. The temperature of annealing was found to be more critical in determining magnetic properties than was time at a specified temperature.

INTRODUCTION

In electronic telephone switching systems, all instructions are magnetically stored as programs in memory units (program stores) and changes are made by electrically rewriting the programs. In addition to the program store, these systems require a more temporary memory known as the call store. This second memory serves as a magnetic blackboard on which information can be written during the course of a call and later erased. Together with a central processor (logic unit) the program and call stores supply the common-control functions required to operate the switching network in a telephone central office. In an effort to combine both memory functions in a single unit, a stored-program control has been developed, the heart of which is the piggyback twistor memory (PBT).

The basic element of the PBT memory is a twistor wire consisting of two dissimilar magnetic tapes wrapped on a 3 mil copper wire. One of the tapes, a 4-79 molybdenum permalloy (78.8% Ni, 16.1% Fe, 4.1% Mo, 0.9% Mn), is the "sense" tape and is wrapped directly on the copper wire helically at 45 degrees. The other tape, a gold-iron-cobalt alloy, acts as the "storage" tape and is wrapped in piggyback fashion over the Mo-permalloy sensing tape. The major advantage of this construction is that permanent magnets in the storage tape can be rapidly and electrically switched from one direction to another.

The Mo-permalloy sense tapes and the Au-Fe-Co storage tapes are of particular interest because their different properties and functions determine the efficiency of the twistor. Au-Fe-Co tape is magnetically hard and difficult to magnetize. In it are written the tiny permanent magnets used for memory elements. In an attempt to obtain significant information on the Au-Fe-Co alloys, Uhl ³ and Lynch ⁴ have investigated the effects of alloying and processing on the microstructure and related magnetic properties. Uhl found that upon annealing, a discontinuous or cellular precipitation reaction produced incoherent gold precipitate and at the same time, effectively recrystallized the cold worked matrix. The more highly cold worked structures obtained higher coercive force peak values due to a finer, more closely spaced precipitate and a finer grained recrystallized matrix. Lynch added the effects of gold variation in the alloy and found that changes in gold concentration up to 14% Au increased H_c . In addition it was established that the dependence of coercive force upon % cold work was primarily due to the smaller recrystallized grains in more severely deformed materials rather than the size of the precipitates.

In contrast to the Au-Fe-Co alloy the permalloy sense tape is magnetically soft. It detects the direction of magnetization of the storage magnets in the mating tape. Essentially, a PBT write operation sends a bit current through the wire to change the

magnetization of the magnets at selected bits. When current is stopped, the field of each storage magnet causes the magnetization of the underlying sense tape segment to align itself with the magnet's field. Hence the Mo-permalloy tape is soft enough to be switched by the field lines of the storage tape magnets above it and the information is written in the memory. In reading, a read current (approximately 1/2 write current) generates a magnetic field which overcomes the static field of the storage tape magnets, causing sensing tape segments to again reverse their magnetization and hence release information. The important point is that while the applied field used for reading is strong enough to overcome the static field from a storage magnet, it is not strong enough to change the magnetization of the magnet itself, i.e., it is non-destructive to the stored information.

As an outgrowth of problems encountered with the magnetostrictive behavior of the presently used 4-79 Mo-permalloy during processing, and extreme sensitivity of coercive force to annealing temperature, it has become necessary to develop a new material whose properties are less susceptible to temperature and handling variations. Based on functional testing of the twistor memory with a 4% Au - 12% Fe - 85% Co alloy as the magnetically hard tape, it has been determined that for optimum operation the permalloy should exhibit:

1. low magnetostriction to maintain its magnetic properties during wrapping
2. a square hysteresis loop to increase the signal-to-noise ratio
3. a coercive force of approximately 0.6 oersted
4. development of the required magnetic properties during an 800-850°C anneal (which terminates the twistor fabrication process)
5. good working characteristics in order to be reduced to tape form without excessive difficulty

Because the Mo-permalloy tape has proven successful in operation, the initial phase of a new material development has attempted to improve the known properties of the Mo-permalloy.

Tisone, Chin and Grupen¹ have found that by changing the known 4-79 Mo-permalloy system to a 6-80 Mo-permalloy (80.5% Ni, 13.5% Fe, 6% Mo) an extremely low coercive force can be obtained. However, because of its very low H_C , the tape is in danger of being switched by the earth magnetic or stray magnetic fields. Also, switching times are so rapid that present memory read-out schemes are lagging. Small additions of zirconium to the 6-80 composition increased the coercive force following precipitation produced by annealing between 800 and 850°C. This precipitation was designed on the basis that the alloying element would be only slightly soluble, form an intermetallic compound type precipitate which does not preferentially precipitate at grain boundaries, and would not degrade the mechanical workability or the magnetic properties of the parent alloy.

Additional studies¹ showed that a 6-80 Mo-permalloy with about 0.3% Zr (from hereon called Zr-permalloy) was found to have properties closely approximating those of the optimum permalloy established as a guide for the investigation. Aging studies revealed significant precipitation from 700-800°C and a maximum solubility of Zr at 800°C of between 0.1% and 0.3%. Low stress sensitivity, high squareness, and a large decrease in shuttle signal were also obtained with the alloy. With desirable magnetic properties and enhanced operating characteristics now achieved, the most favorable areas for further investigation appear to be in considering details of the precipitation reaction, the influence of Zr content, and the effects of processing variables on precipitation (and hence magnetic properties).

When a material is cold worked, many imperfections are introduced into the lattice. Dislocations, dislocation jogs, and interstitials are created, and existing grains are subdivided by low angle boundaries or dislocation tangles. These lattice imperfections and increased number of boundaries impede magnetic domain wall motion when the material is magnetized. The domain walls are forced either to go through or around the obstacles, resulting in an increased magnetizing force necessary to move the walls and hence in a high initial coercive force. If the material is annealed at an elevated temperature for a substantial time, recovery, recrystallization, and/or grain growth will occur such

That many of the imperfections anneal out, polygonization occurs, new strain-free grains are nucleated in the cold worked matrix, and the strain-free grains grow into larger, equiaxed grains. During these processes the coercive force is reduced by the disappearance of imperfections that interfere with moving domain walls. A secondary rise in coercive force may further be observed if an element of low solubility in the solid solution precipitates out during the annealing process. The precipitate particles have the same effect as imperfections in that they pin domain walls (but to a lesser extent), and H_c again rises. Thus by controlling alloying element concentration, amount of cold work, and annealing times and temperatures, the coercive force can be changed.

It is the purpose of this thesis to investigate the effects of cold work and annealing on the microstructure and magnetic properties of the Zr-doped 6-80 Mo-permalloy. The extent to which coercive force is influenced by precipitation in the alloy, a detailed analysis of the precipitation reaction, the influence of percent reduction, annealing times, and temperatures on magnetic hysteresis, and the relationship of measured changes in hardness and coercive force to the observed changes in microstructure upon heating the cold worked material are all aspects of the problem that received attention.

EXPERIMENTAL PROCEDURE

A 1" ingot of Zr-doped 6-80 Mo-permalloy containing 80.0% Ni, 12.65% Fe, 6.74% Mo, 0.36% Zr, and 0.25% Mn was obtained from the Bell Telephone Laboratories at Allentown. X-ray fluorescence analysis and D. C. arc technique were subsequently performed at the Western Electric Engineering Research Center and qualitatively verified the presence and concentration of each of the elements, along with the homogeneity of the ingot. In order to reduce the ingot into tape form, it was first worked slightly by hot swaging to break up the dendritic structure. Following homogenization at 1100°C for 40 hours in an H₂ atmosphere the ingot was further cold swaged and successively rolled to a 0.020" thick tape. Intermediate strand anneals at 870°C were made between rolling operations. The processing was concluded by cold rolling equal lengths of the 0.020" thick strip to 0.010", 0.005", and 0.002" representing 50%, 75%, and 90% cold work, respectively.

A portion of each tape was cut into 3/8" X 1/2" samples so that three specimens were available for each annealing time-temperature treatment. Combinations of time, temperature, and % cold work were produced by annealing the above samples at 400, 500, 600, 700, 800, 850 and 900°C for 15 min., 30 min., 1, 2, and 4 hours. A Lindberg 3-zone horizontal tube furnace was employed for annealing. The temperature was monitored by a potentiometer connected

to a platinum - 10% rhodium platinum thermocouple at the center zone of the furnace. In order to prevent curling, and to minimize oxidation and premature slow cooling during transfer from furnace to quench, all tape samples were placed between two high-purity alumina plates and the plates were fed into the furnace via an alumina combustion boat. An inert atmosphere of forming gas (90% N_2 -10% H_2) flowed through the furnace at all times. At the conclusion of each anneal the specimens were immediately quenched in a brine bath maintained at 15°C to preserve the high temperature microstructure. Microhardness measurements were subsequently performed on all samples with a Leitz microhardness tester and a diamond pyramid indenter as verification that the annealing had occurred in meaningful time and temperature ranges.

Two techniques were used to determine magnetic properties. A Magneatest D. C. precision coercive force meter was employed to measure coercive force. Calibrated to 2 millioersted accuracy, it was positioned and adjusted so that the magnetic earth field and stray magnetic and A. C. fields were compensated. Samples 3/8" X 1/2" were tested for all time-temperature-% cold work combinations. Hysteresis loops of selected samples were constructed by an all electronic magnetic hysteresisgraph. During aging each sample was wrapped tightly in a stainless steel envelope to insure that any oxidation occurring in transferring the sample from furnace to quench would be minimized. These samples were 3/8" X 10" so that

they could be accommodated in the instrument and at the same time, simulate an infinite solenoid with a large length-to-width ratio of approximately 30 to 1. Complete B-H curves were obtained.

Metallographic specimens were mounted, mechanically ground and polished, and chemically etched with a solution of 10gm CuSO_4 , 50 ml H_2O , and 50 ml HCl . Resulting photomicrographs were taken at magnifications of 200X and 1000X.

Electron microprobe analysis was performed on sections both free of and containing a second phase to determine if compositional differences existed between the two areas. A 0.020" specimen annealed at 800°C for 1 hour was ground, polished, and etched, sections both with and without second phase particles were angularly scanned, and the intensities of characteristic X-rays from Ni, Fe, Mo, and Zr were recorded.

Transmission electron microscope studies were made for high resolution observation of microstructural changes and as a means of identifying the precipitates. Specimens cold worked 90% (approximately 3/8" X 3/4") were thinned in a dual-jet electrolytic polisher operated at 20 volts with a current density of 0.1 amp per sq. cm. The electrolyte was a solution of 50% perchloric acid-50% acetic acid by volume. A window technique was employed in obtaining selective electrochemical etching by coating the sample perimeter with Microstop stop-off lacquer. This left a "window" approximately 3/8" X 1/4" which was thinned and polished until a

small hole just appeared. Soaking in methanol for 15 minutes enabled removal of the lacquer. The actual transmission specimens were then obtained by carefully cutting around the hole (while leaving the hole intact) so that an O-ring of approximately 1/8" O. D. resulted. This was mounted in a copper grid and the extremely thin material adjacent to the hole was then observed under the electron microscope. The electron micrographs were taken between 10,000 and 20,000X. In utilizing the diffraction mode on the transmission electron microscope diffraction patterns were obtained on areas with and without precipitate. A measure of the resulting d-spacings, consideration of all applicable intermetallic compounds and studies on like systems, and comparison of the measured spacings to established ASTM diffraction values yielded an identification of the compounds present.

RESULTS AND DISCUSSION

1. Hardness Test

The results of microhardness measurements made on all samples annealed between 400 and 900°C for annealing times of between 15 minutes and 2 hours are presented in Figures 1 to 4. The curves for 50%, 75% and 90% cold worked structures exhibit a sigmoidal configuration characteristic of a recrystallization process. At any temperature above 500°C the % recrystallization at that temperature increased with the amount of cold work introduced in accord with increased nucleation rates of strain-free grains expected in more drastically deformed structures. As the annealing time increases, the curves of the highly deformed structures become superimposed on one another beyond 600°C until at two hours and above, recrystallization is initiated at or slightly below 600°C and is essentially complete by 700°C. Such behavior indicates that the same process occurs in all the samples between approximately 500 and 700°C. There was no change observed in the hardness of the 0% cold worked structure with annealing, except a gradual softening due to grain growth after heating at 700°C. Guy⁵ reports recrystallization temperatures of 595°C for alloys containing 70% Ni and above, which is in good agreement with the value of 600°C obtained in this investigation from both hardness and coercive force studies. The higher hardnesses of samples with greater reductions in area are consistent with the greater dislocation densities and more complex dislocation configurations expected for greater amounts of cold work.

Transmission electron microscopy clearly shows that recrystallization accompanies the hardness decreases with increasing temperature. This evidence is presented in Section 5 of the Results and Discussion. No precipitation peak in the higher temperature range was detected by hardness measurements as it was in the magnetic investigation. This was attributed to the fact that the hardness is not nearly as sensitive a function of precipitation as is coercive force.

2. Magnetic Measurements

The coercive force changes as a function of annealing temperature and time are shown in Figures 5 to 9. Initially the 50%, 75% and 90% deformed specimens have high H_C values which are attributable to the many imperfections introduced with rolling. For 15 minute anneals at increasing temperatures, it can be seen that the curves exhibit a sigmoidal configuration similar to the hardness curves. This drop in coercive force which parallels the drop in hardness within approximately the same temperature range provides additional evidence that recrystallization is indeed occurring. In a hardened material the residual strains and imperfections retard domain boundary migration and prevent randomization of the domains so that a relatively high H_C is needed for magnetization changes. The thermal activity of annealing promotes randomization of domain alignments so that when recovery and recrystallization eliminate the imperfections and strains that are obstacles to domain boundary movement, the annealed material is easier to magnetize and hence, H_C is reduced. Such behavior is observed for all the deformed and annealed samples between 500°C and 700°C. Very little change occurs in H_C for the 0% cold work structures in the same range.

As the time of annealing increases to 30 minutes, a peak is initiated at 800°C. With still longer times the peak continues to rise, the amount of increase being greater with the more highly

cold worked structures. The effect of increased H_C is observed above 700°C for longer annealing times. As subsequently shown by electron microscopy, the peak is a result of precipitation of Ni_5Zr and Ni_4Mo intermetallic compounds. During magnetization domain walls move so that favorably oriented domains grow and unfavorable domains are consumed. If structural defects or precipitate particles are present, the domain walls can be immobilized by the defects or particles blocking their motion, in effect pinning the walls. Because both wall energy and magnetostatic energy are reduced by the domain walls being attracted to particles, this attraction and ensuing resistance to motion causes H_C to be raised. Since more force must be applied to move the domain walls past the particles, the observed increase in H_C from 700°C to 800°C is caused by precipitation of the two phases. The drop in H_C after 800°C is a result of grain growth and the precipitates coalescing into larger, more widely spaced particles.

Figures 10 to 13 are isothermal plots of coercive force as a function of time. Again H_C is higher for the more cold worked samples. For the 600°C curves there is a gradual decrease in H_C with time due to the recrystallization process. A first indication of higher coercive force at 700°C is at 30 minutes and this correlates with the first appearance of a rodlike precipitate in electron micrographs. The effect is most pronounced in 800°C annealed specimens where after a steep rise in H_C at 30 minutes,

the increase continues more gradually up to 4 hours. Finally Figure 13 shows that at 900°C coalescence has caused H_C to remain essentially constant with time and decreased from the values at 800°C. Thus it is seen that the time at a temperature is not nearly as critical in determining H_C as is the temperature itself.

Immobilization of the domain boundaries by the deformation, strain, and subsequent precipitation lead to an energy loss which is manifested in magnetic hysteresis. Hysteresis loops made from a cross-section of time, temperature, and per cent cold work combinations are shown in Figures 14 to 16. An absence of many structural imperfections in the 0% cold work samples results in very little change with annealing in the hysteresis loops (Figure 14, top). On the other hand, annealing the 50% cold worked material produces both a decrease in H_C and hysteresis loss, as can be seen in the bottom series of the same figure. Comparison of the 0% and 50% cold worked structures having the same thermal histories shows extensively greater hysteresis associated with the initially deformed structure. A high remanance is characteristic of all the worked samples.

In Figure 15 the effect of recrystallization can be seen. When the structures are annealed from the cold worked state, squareness improves with annealing while hysteresis is reduced. In addition H_C is continually decreased so that the annealing out of strain and imperfections is responsible for the above observed

effects. At 800°C where maximum precipitation occurs, coercive force increases with time (Figure 16) as does the hysteresis. The effects of precipitate coalescence and grain growth can be seen by a comparison of the last two loops of Figure 16. The H_C values obtained from the hysteresis loops compared well with those measured in the Magnatest equipment.

From the curves in Figures 5 to 9 for the cold worked samples a plot of $\log t_{50}$ (time for 50% recrystallization) vs $1/T$ was constructed (Figure 17). The data fit a linear relationship and satisfied the Arrhenius equation

$$\text{Rate of transformation} = 1/t_{50} = Ae^{-Q/RT}$$

extremely well. For 50%, 75% and 90% reduction the parallel lines are indicative of the same process occurring, and a value of 80.5 kcal/mole was obtained for the activation energy. No published activation energies were found for this system or similar systems, but Uhl³ found an activation energy of 82.0 kcal/mole for the cellular precipitation reaction in a 50% cold worked 82% Co-12% Fe- 6% Au Alloy. Aust and Rutter⁶ have found in lead-silver and lead-gold solutions that the addition of very small amounts of gold or silver (1 ppm) to zone-refined lead raises the activation energy for recrystallization over 25 kcal/mole. The effects of solute in pinning high-angle boundaries and decreasing diffusion rates accounted for the higher activation energies when solute is present. In light of this evidence it is not unreasonable that the combina-

tion of Fe, Mo, Mn, and Zr in Ni in the permalloy could have similar effects. The faster rate of transformation as seen from the associated constants, A , in going from 50% to 90% cold work is attributed to the presence of more structural imperfections in the matrix acting as nucleation sites.

3. Optical Microscope Studies

Figure 18(a) shows the equiaxed grain structure of the annealed alloy and Figure 18(b) presents the elongated grains and distortion resulting from cold rolling. The rolling direction in Figure 18(b) is indicated by the arrow. Examination of these structures with polarized light reveals that even in the 0% cold work - no anneal sample, some particles are present at grain boundaries and infrequently within the grains. Furthermore, Figure 19 shows that the particles and grain structure coarsen with longer annealing times and higher temperatures. Electron diffraction analysis indicates that these particles are an Ni_4Mo compound, and the coercive force measurements of samples annealed at times and temperatures where the particles are known to be present indicate that the coarse particles are ineffective in impeding domain boundary motion.

Figure 20 shows that as the degree of cold work is increased, annealing produces Ni_4Mo particles which are finer, more closely spaced, and more uniformly distributed. This figure is also evidence of the smaller recrystallized grains present in the 90% cold worked structure as compared to the larger grains in the 0% and 50% cold worked samples.

4. Electron Microprobe Analysis

X-ray displays for Ni $K\alpha_1$, and Zr $L\alpha_1$, radiation from a 50% cold worked structure annealed at 850°C for one hour are presented in Figures 21(a) and 21(b). These two elements are essentially uniformly distributed and the displays show the relatively greater amount of Ni present as compared to Zr. Figure 22(c) is an electron back-scatter micrograph showing the topography of the etched surface.

The particles distributed throughout the matrix were too small to be resolved individually under a 1 micron beam. Nevertheless, X-ray diffraction scans from 20 to 74 degrees of a 0% cold worked structure annealed at 800°C for 1 hour resulted in increased Ni and Mo intensities of 8%, and decreased Zr and Fe intensities of 16%, for areas of the structure containing particles as compared to areas free of particles. This is taken as a qualitative indication that the particles are a compound of high composition of Ni and Mo in accord with electron diffraction evidence.

5. Electron Microscope Investigation

No acceptable transmission micrograph of the as-cold worked structure could be obtained because of great difficulties in producing foils with uniformly thin areas. Very high dislocation densities were present and many bend contours tended to mask the fine structure. Nevertheless the fine structures which are presented are characteristic of a highly cold worked material. No evidence of precipitates in the cold worked regions was visible, and the diffraction patterns contained no precipitate reflections.

The onset of recrystallization is observed in figure 22(a) for a sample annealed at 600°C for 15 minutes. Small newly-formed, strain-free grains have nucleated in the highly strained regions of the cold worked structure and appear as clear white areas surrounded by darker, unrecrystallized material. In Figure 22(b) annealing for 2 hours at 600°C has produced extensive recrystallization, but some highly distorted cold worked structure remains. As can be seen in the upper left portion of Figure 22(b), the transformation proceeds by high-angle grain boundaries migrating into the strained matrix. The recrystallized grains with a low dislocation density are growing into dark, strained areas with a high dislocation density, this difference in dislocation densities being the driving force for recrystallization. Figure 22(b) shows that the boundaries of the recrystallized grains move away from their centers of curvature into the residual cold worked matrix. Preci-

precipitation does not occur behind the moving grain boundaries, and hence a discontinuous precipitation reaction is not taking place in this material.

The areas shown in Figures 22(c) and 22(d) at different magnifications exhibit a completely recrystallized structure after a 4-hour anneal, and the grain growth which has occurred. Within the recrystallized matrix many small spherical particles are visible. In addition there is an abundance of annealing twins caused by irregularities in the growth of the strain-free grains from the deformed grains.

A series of 90% cold worked samples annealed for 2 hours at various temperatures is presented in Figure 23. The partially recrystallized matrix of a sample annealed at 600°C has already been presented in Figure 22(b). Figures 23(a) and (b) show that the grains present are completely recrystallized and have grown extensively after two hours at 850° and 900°C, respectively. Figure 23(b) is a perfectly recrystallized structure in which three grains meet in adjoining 120° angles (a triple point). Comparison of Figures 23(a) and (b) with Figure 22(d) emphasizes the increase in grain size which develops with prolonged annealing times at elevated temperatures.

At 700°C large recrystallized grains occur as shown in Figure 24. Some dislocations are still evident in the structure but the number is almost nil compared to the amount present in the

unrecrystallized material. Throughout the matrix particles have precipitated primarily within grains, rather than at grain boundaries. Hammond and Ansell¹² report that for an Fe-Ni base alloy with small additions of Al and Ti, Ni_3Al (γ') precipitates as spherical particles randomly oriented with respect to the matrix lattice. The associated spotty ring γ' diffraction patterns imply a randomly oriented phase, and because random γ' orientations and coherency are not compatible, the Ni_3Al particles are apparently not coherent during their formation. The spherical Ni_4Mo particles in the present alloy appear to develop in a similar manner. The tetragonal Ni_4Mo with a lattice parameter of 5.72 \AA is incoherent with the FCC NiFe matrix having $a_0 = 3.56 \text{ \AA}$.

At 700°C after a 30 minute anneal, an extremely fine-textured, rodlike precipitate first appeared within several grains. This additional precipitation occurs simultaneously with that of the Ni_4Mo , but only at temperatures of 700°C and above. As identified later, this striated phase is an FCC Ni_5Zr compound and can be clearly seen in Figures 25(a) and 28(a). Essentially uniformly distributed, the precipitate appears to be the primary cause for the coercive force peak at 800°C , and together with the Ni_4Mo , successfully inhibits domain wall motion so that coercive force is increased. The contrast effects associated with the elongated particles is emphasized by the high magnification brightfield micrograph of Figure 26(a). Furthermore, precision darkfield imaging

indeed shows the fine precipitate in another part of the specimen being illuminated by the tilted beam (Figure 26(b)). The series of Figure 27 presents the large recrystallized grains accompanying the precipitates at 800°C, and when compared to Figure 22, shows the grain size to be less sensitive a function of time at higher temperatures than at lower temperatures. The appearance of the Ni_5Zr compound is a result of an age hardening process related to the chemistry of the permalloy. Chilton and Barton¹⁰ have investigated a similar effect in 18Ni maraging steels containing aluminum, vanadium, or titanium. After aging, each steel contained a fine distribution of precipitate particles which consisted of two distinct phases. One was orthorhombic Ni_3Mo (the primary precipitate and had a ribbon-shaped morphology approximately 50 \AA wide and several hundred \AA long. The other, FCC Ni_3Al (or tetragonal sigma phases), consisted of small spherical particles but was much finer than the Ni_3Mo . In the present case the Ni_5Zr morphology is rodlike and the Ni_4Mo is spherical. Again the uniform distribution of this precipitate within each grain implies that homogeneous nucleation has occurred, and the absence of a moving reaction front indicates precipitation is continuous.

Although not established in this study, the Ni_5Zr appears to be coherent with the NiFe matrix. Both have a face-centered cubic structure and $a_0 = 6.71\text{\AA}$ for Ni_5Zr is a little less than double $a_0 = 3.56\text{\AA}$ for NiFe. The platelike or rodlike particles are usually indicative of coherent precipitate and a coherent interface implies a definite orientation relation between precipitate and matrix. In

the observed structures all the rodlike particles are oriented in the same direction. Coherent particles can contain relatively few atoms as compared to incoherent particles, and for a large number of small particles, the interparticle spacing is extremely small. Because of coherency strains between the precipitate and matrix, the effective size of the particles is increased by the surrounding volume of strained matrix. The increase in coercive force between 700°C and 800°C, therefore, is attributed to the many small Ni_5Zr particles offering resistance to domain wall motion. Figures 26(a) and 28(a) are excellent examples of the coexistence of the Ni_4Mo and Ni_5Zr precipitates.

The assorted micrographs of Figure 28 demonstrate various grain structures resulting from the high temperature anneals. At 900°C after 2 hours the grain structure is characteristic of a well-annealed metal with grain boundaries meeting at 120° angles. Apparently many of the precipitates have dissolved after this treatment. The micrographs of Figures 29(c) and 29(d) are brightfield and darkfield shots, respectively, of an area surrounding a hole in a 90% cold worked sample annealed for 2 hours at 850°C.

The optical micrographs and the electron micrographs (Figures 19 and 24) show that the Ni_4Mo particles at grain boundaries grow with time and temperature, but those within the grains do not grow as extensively once nucleated. This may be explained by the fact that volume diffusion in the lattice is much more difficult than

grain boundary diffusion due to short circuiting effects in the grain boundaries. Atoms are able to move faster in the grain boundaries and thus coalesce at grain boundary precipitates. The larger particles at 800°C were determined to be approximately 2500 Å in diameter. Nesbitt and Williams¹⁴ report the most effective precipitate for pinning domain walls would be needle-like shapes of fine particles between 500 Å and 1000 Å long. Therefore the smaller Ni₄Mo particles and the closely-spaced, rodlike Ni₅Zr precipitates are the most effective impediments. It was observed that temperature is more critical in determining precipitate size than is time at a given temperature.

The two intermetallic compound-type precipitates, along with the matrix, were identified from selected-area diffraction patterns. The data was analyzed with respect to all the phases expected to be present from compositional considerations. In Figure 30(a) is presented the diffraction pattern associated with the 90% cold worked-unannealed structure. Broad, fairly continuous rings indicate the cold work and residual stresses which are present. D-spacings determined from the rings index to a pattern of FCC NiFe with $a_0 = 3.56 \text{ Å}$ and are presented in Table I. These reflections are all produced by the matrix. Although the light micrographs do show some particles in the 0% cold work condition prior to rolling (evidently despite the fast cooling, all of the Ni₄Mo could not be kept in solid solution), it is most likely that the quantity was so small as not to produce any significant reflections.

The series of diffraction patterns in Figure 30 shows the changes occurring during recovery and recrystallization. As compared to the cold worked pattern, the rings in Figure 30(b) have sharpened extensively and the partially continuous rings are evidence that indeed fine grains are appearing. At the recrystallization temperature the rings are the sharpest, which is characteristic of a recrystallization process, and at 600°C for 2 hours, weak reflections of Ni_4Mo are obtained (Table II). (As observed from Tables II and III the d-spacings of NiFe and Ni_4Mo are almost identical. These superimposed reflections aid in producing the strong continuous rings in Figure 30(c). However, additional reflections from Ni_4Mo are also observed, which indicates the presence of this compound over and above NiFe . Chilton and Barton¹⁰ have developed an intricate method of segregating the origins of the two reflections, but the procedure is above the scope of this investigation.) The approximate uniform intensity in these rings supports the argument that the Ni_4Mo precipitate is randomly oriented and thus incoherent.

The first appearance of NiZr compound is observed in analyzing Figure 30(d), a 90% cold worked specimen annealed at 700°C for 4 hours. Its pattern indexes to FCC Ni_5Zr . This is in good agreement with the electron microscope observations which optically show the first appearance of a rodlike precipitate at 700°C. Strong

evidence of Ni_4Mo is still obtained and indicates the coexistence of the two precipitates. This was also verified optically as has been mentioned. The spotty nature of the pattern means that grain coarsening (growth) is beginning to occur.

At 850°C diffraction patterns show the strongest reflections from Ni_5Zr (Table III), which correlates well with the design that maximum precipitation occurs near 800°C and also with the peak values of coercive force at 800°C caused by age hardening. The non-uniformity of the rings from the Ni_5Zr supports the hypothesis that this precipitate is probably oriented and coherent with the matrix.

CONCLUSIONS

Cold working of a Zr-doped 6-80 Mo-permalloy increases the hardness and coercive force by the introduction of structural imperfections. These imperfections impede magnetic domain wall motion to increase H_C . Upon annealing, the distorted matrix recrystallizes and a steep drop in coercive force and hardness follows the optically observed recrystallization process occurring at about 600°C. When compared to the Arrhenius equation, the resulting H_C data yielded an activation energy of 80,500 cal/g mole for the 50%, 75%, and 90% cold worked structures. Hence the same process occurs in each and the observed faster rate of transformation in the more highly cold worked structures is attributed to a higher density of structural imperfections that act as nucleation sites.

For longer times at the recrystallization temperature and above, a small number of spherical particles of Ni_4Mo were continuously and incoherently precipitated within grains. As the degree of cold work increases, annealing produces new particles which are finer and more uniformly distributed, but still relatively few in number. In addition, smaller recrystallized grains appear in the more deformed structures. Because the particles are not closely spaced, and the recrystallized grains grow rapidly, the effect of the Ni_4Mo on magnetic properties in this early stage is essentially nil. Beginning at 700°C, a Ni_5Zr intermetallic compound also precipitates out of solid solution with a ribbon-shaped morphology.

It is postulated that this phase is coherent and oriented. A peak in coercive force at 800°C is attributed to the maximum precipitation of rodlike Ni_5Zr (approximately 1200Å long) together with a lesser contribution of intragranular spheres of Ni_4Mo (1000 - 2500 Å in diameter) pinning domain walls. Grain growth in the recrystallized matrix and precipitate coalescence beyond 800°C results in a decreased coercive force.

Hysteresis was found to be increased by both cold working and precipitation resulting from age hardening. Annealing, on the other hand, decreased hysteresis considerably and significantly improved the squareness. A high remanence was characteristic of all the cold worked samples. The temperature of annealing was found to be more critical in determining magnetic properties than was time at a specified temperature.

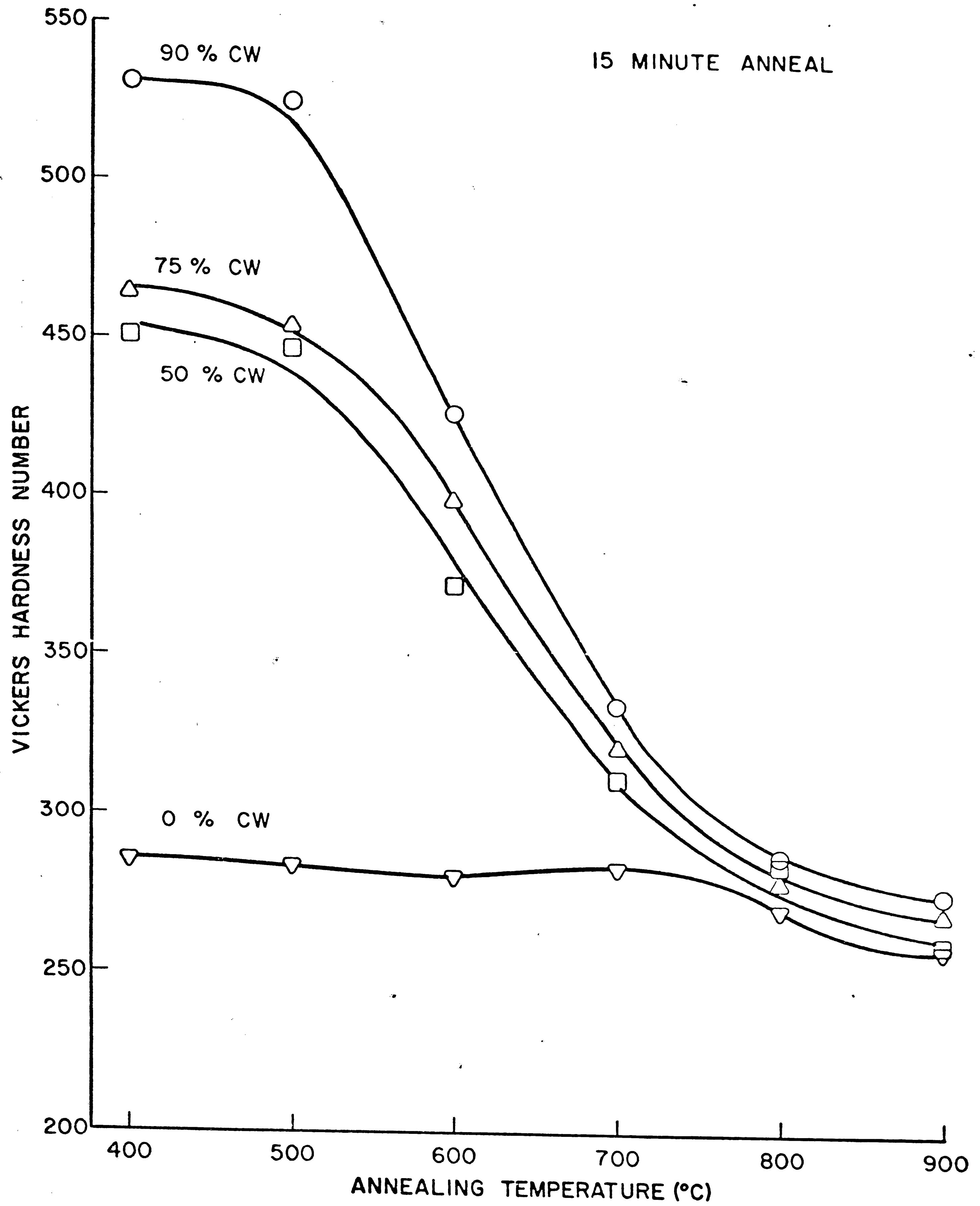


FIGURE 1
HARDNESS VS ANNEALING TEMPERATURE

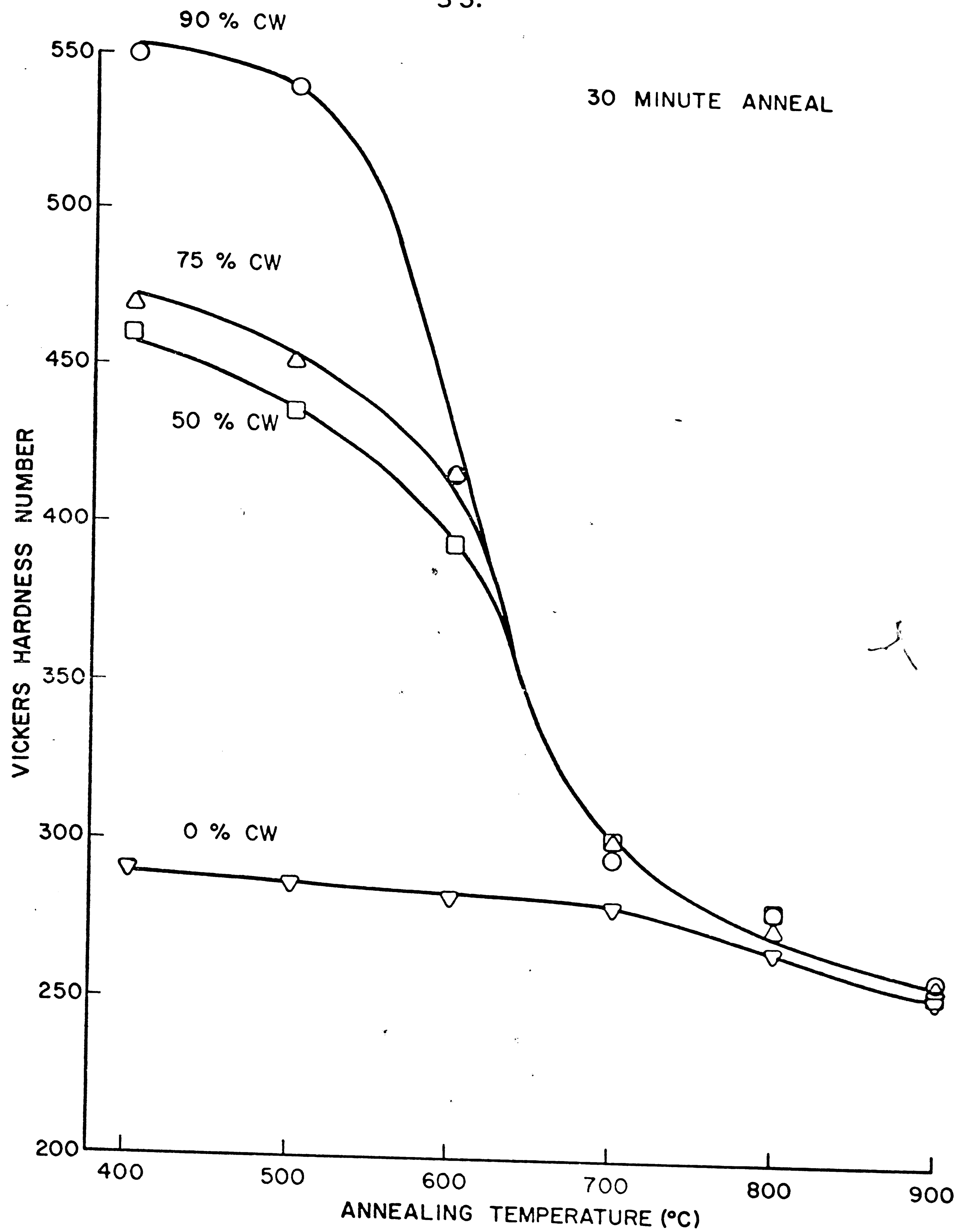


FIGURE 2
HARDNESS VS ANNEALING TEMPERATURE

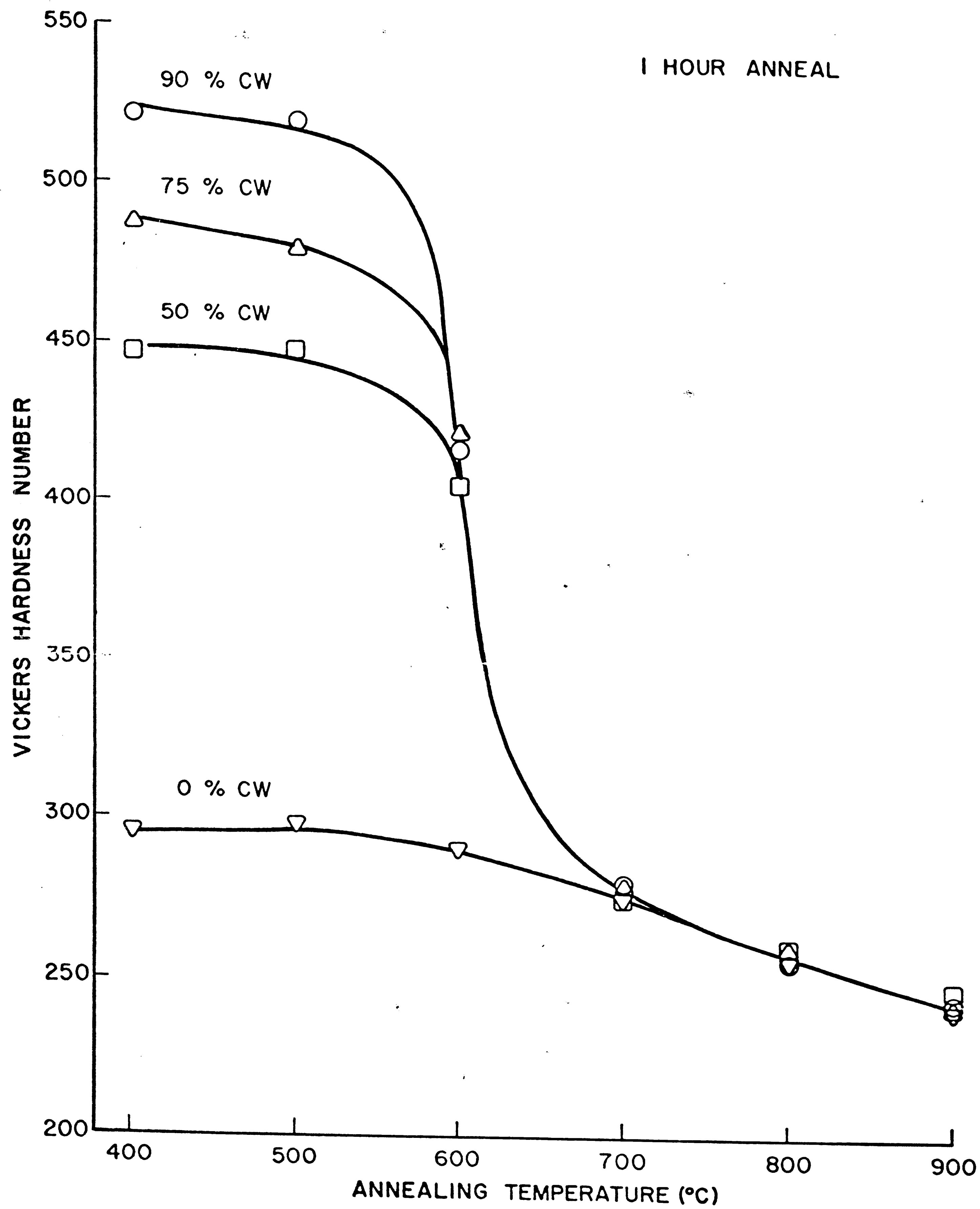


FIGURE 3
HARDNESS VS ANNEALING TEMPERATURE

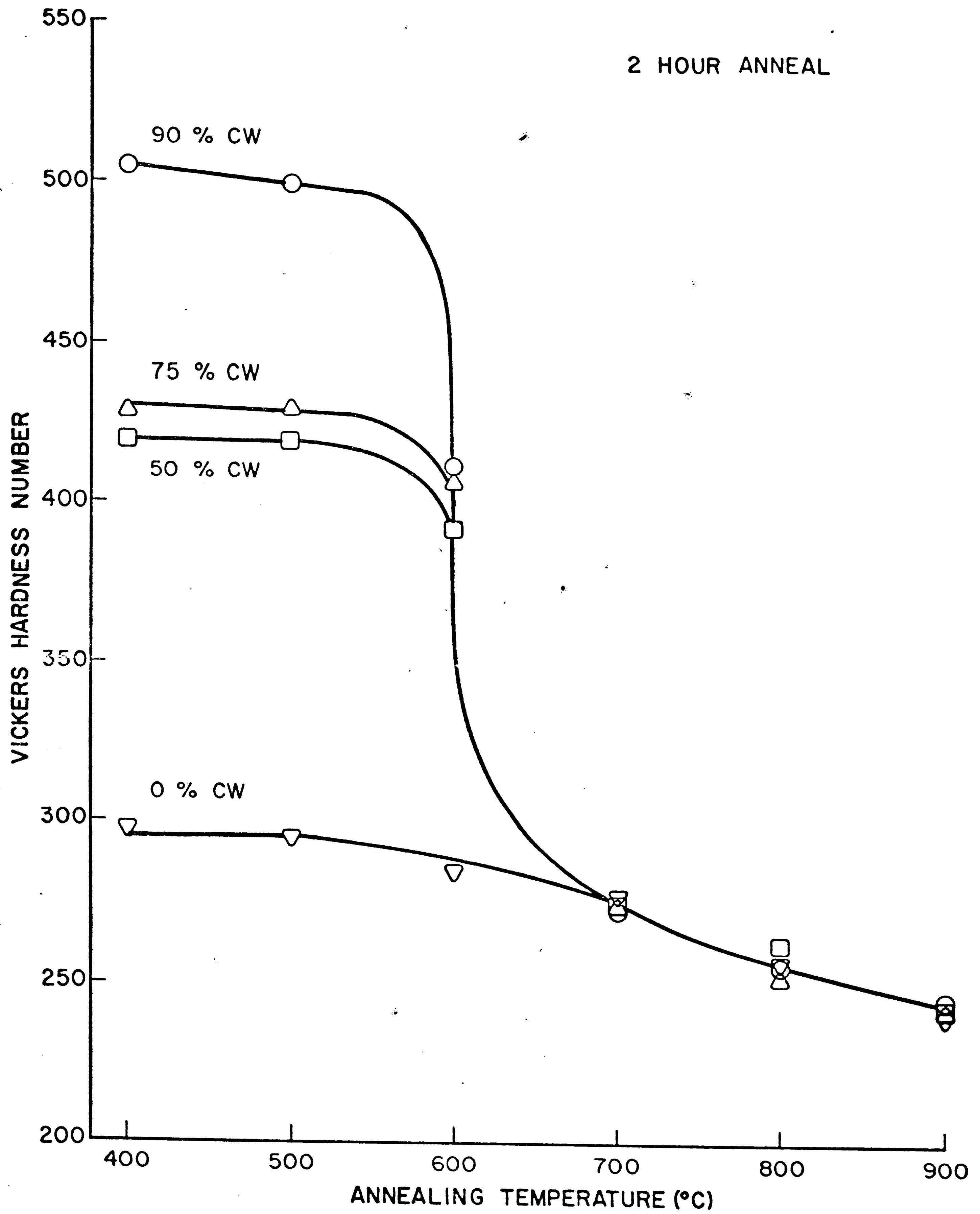


FIGURE 4

HARDNESS VS ANNEALING TEMPERATURE

36.

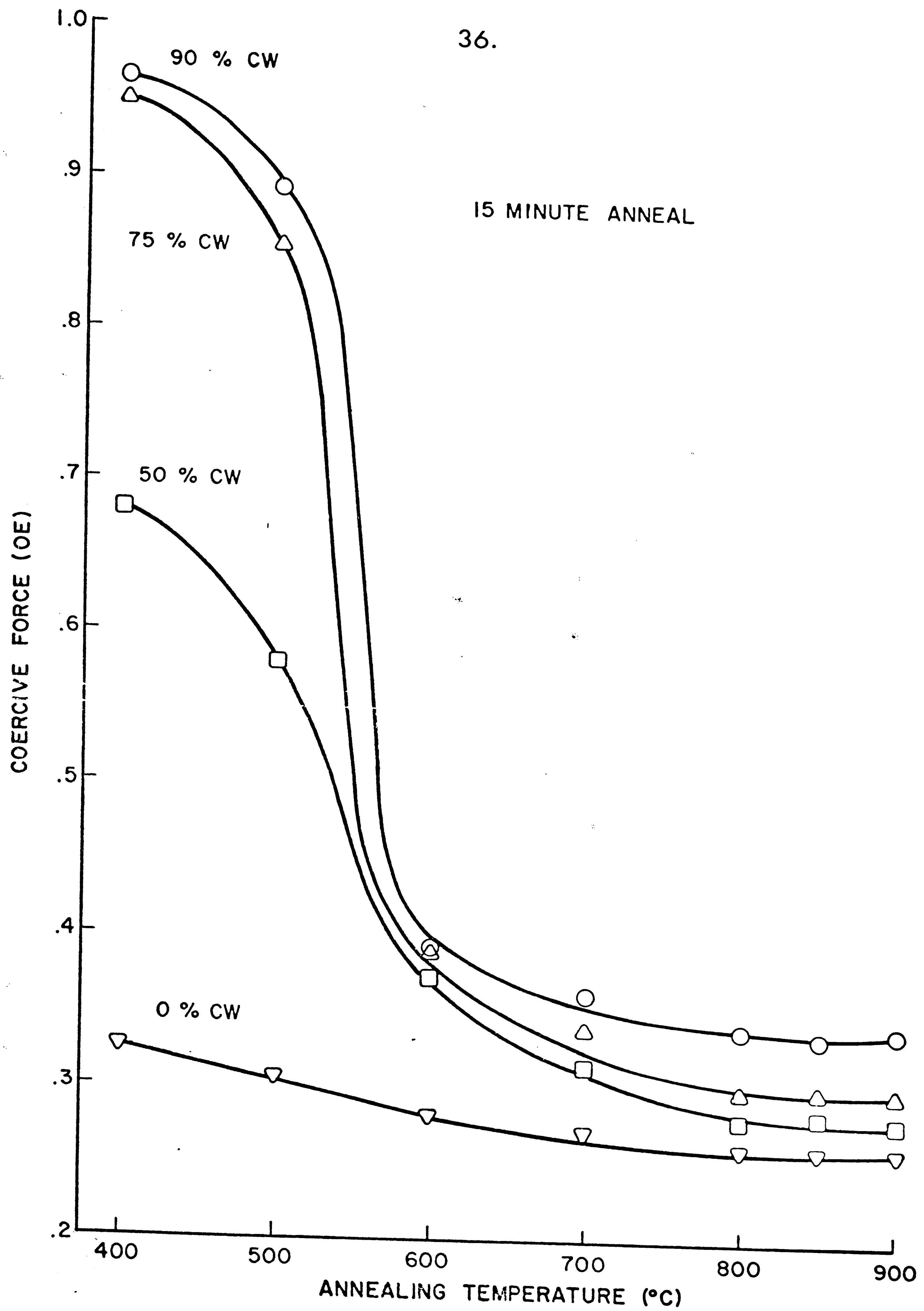


FIGURE 5
COERCIVE FORCE VS ANNEALING TEMPERATURE

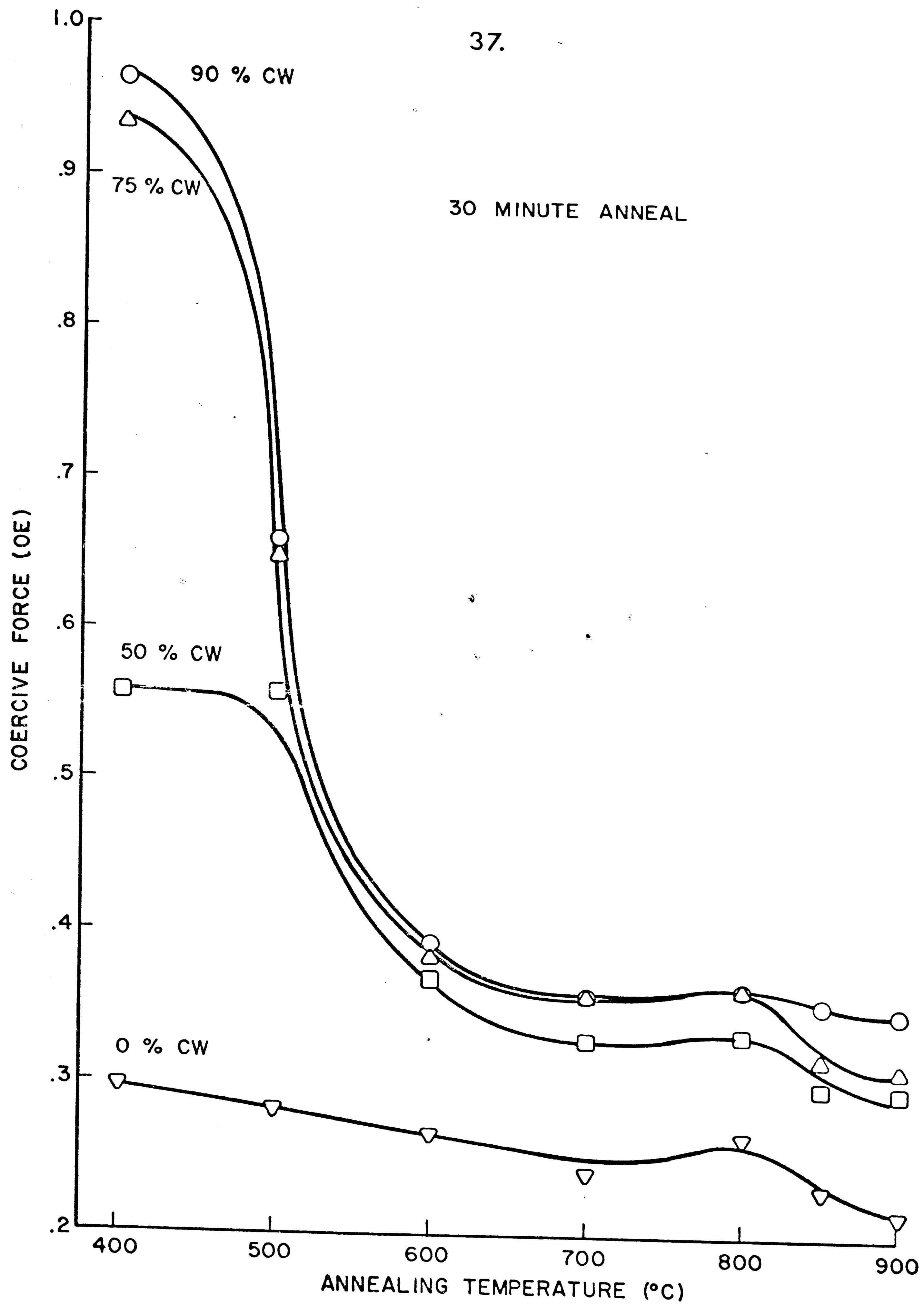


FIGURE 6
COERCIVE FORCE VS ANNEALING TEMPERATURE

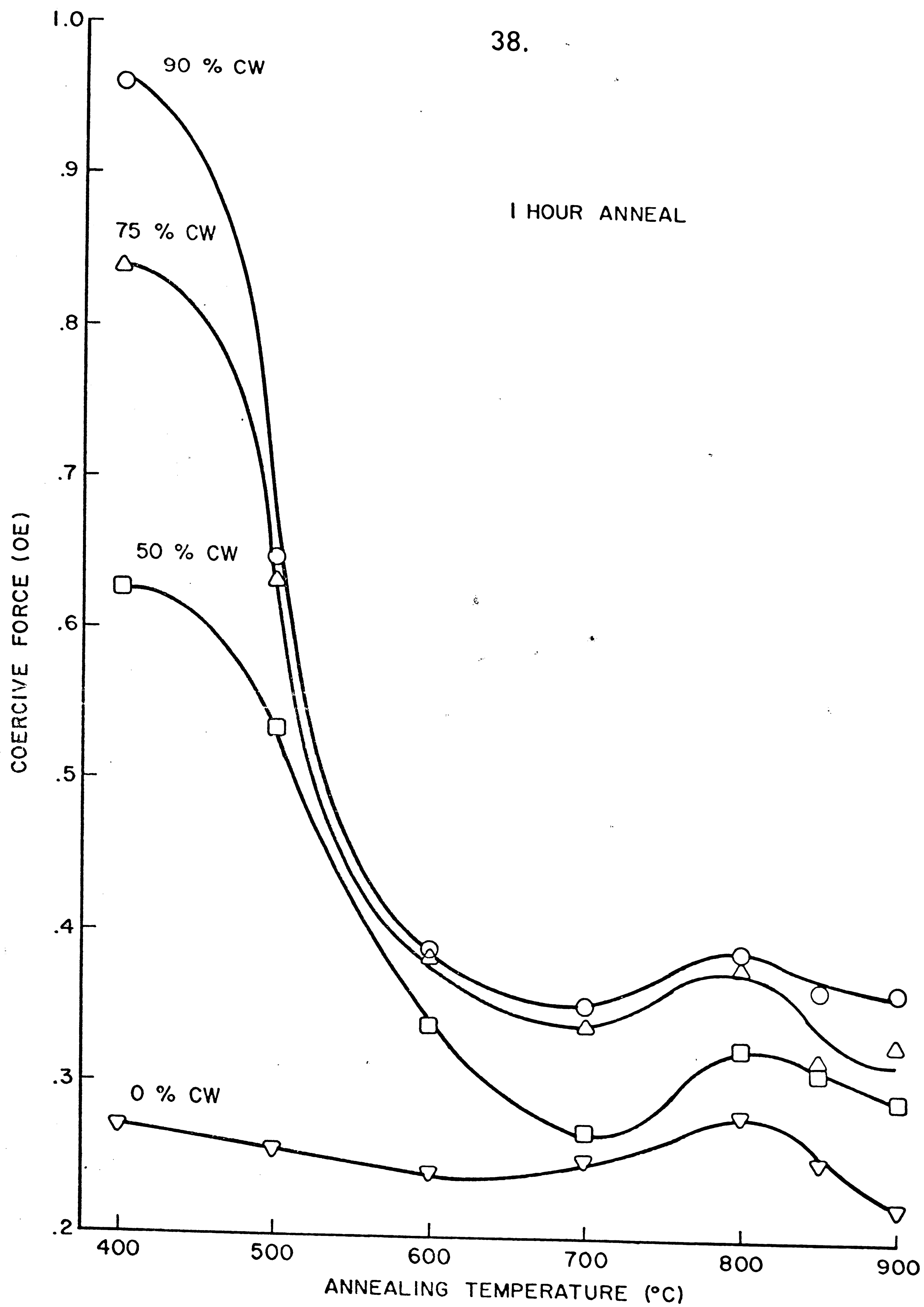


FIGURE 7
COERCIVE FORCE VS ANNEALING TEMPERATURE

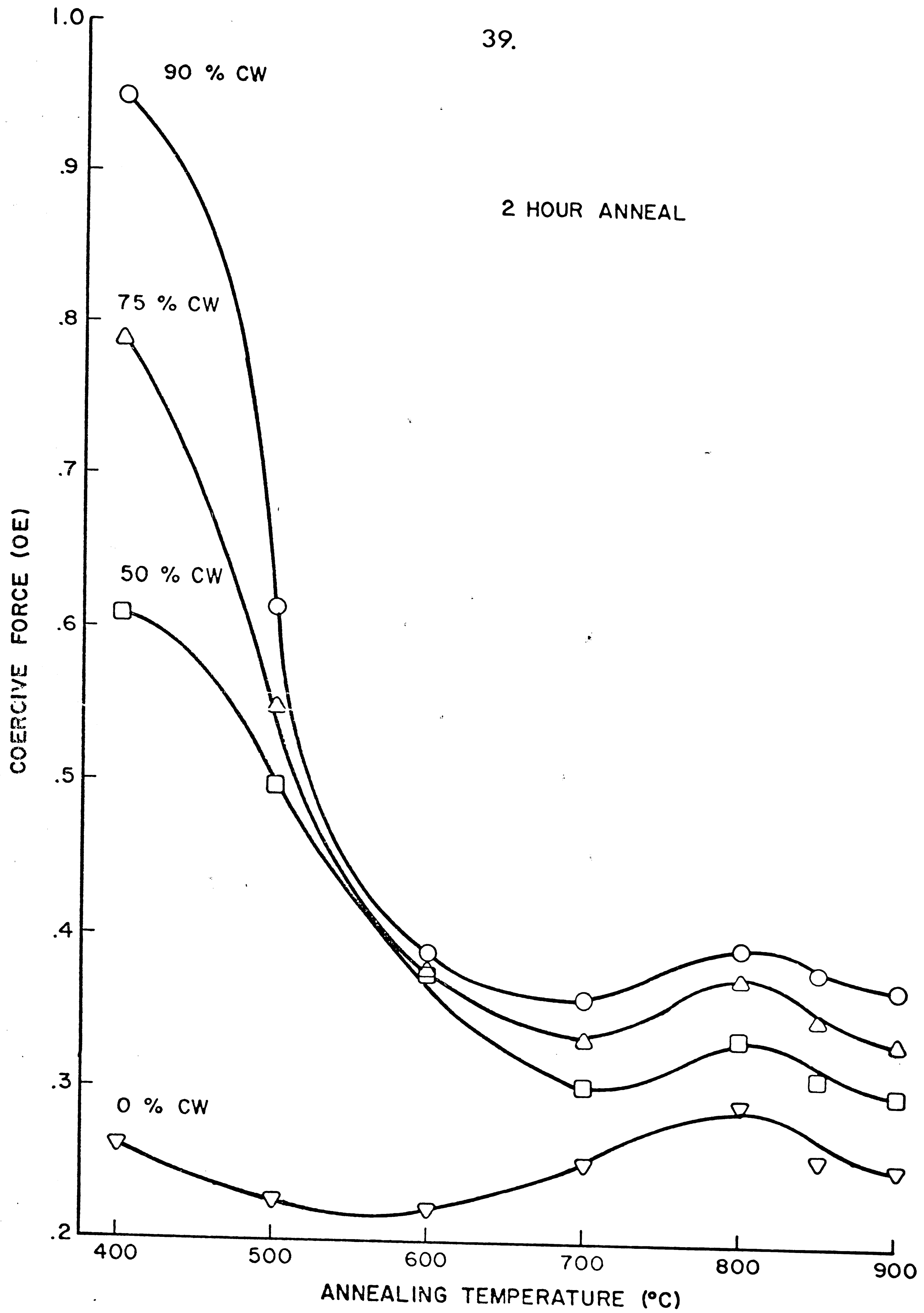


FIGURE 8
COERCIVE FORCE VS ANNEALING TEMPERATURE

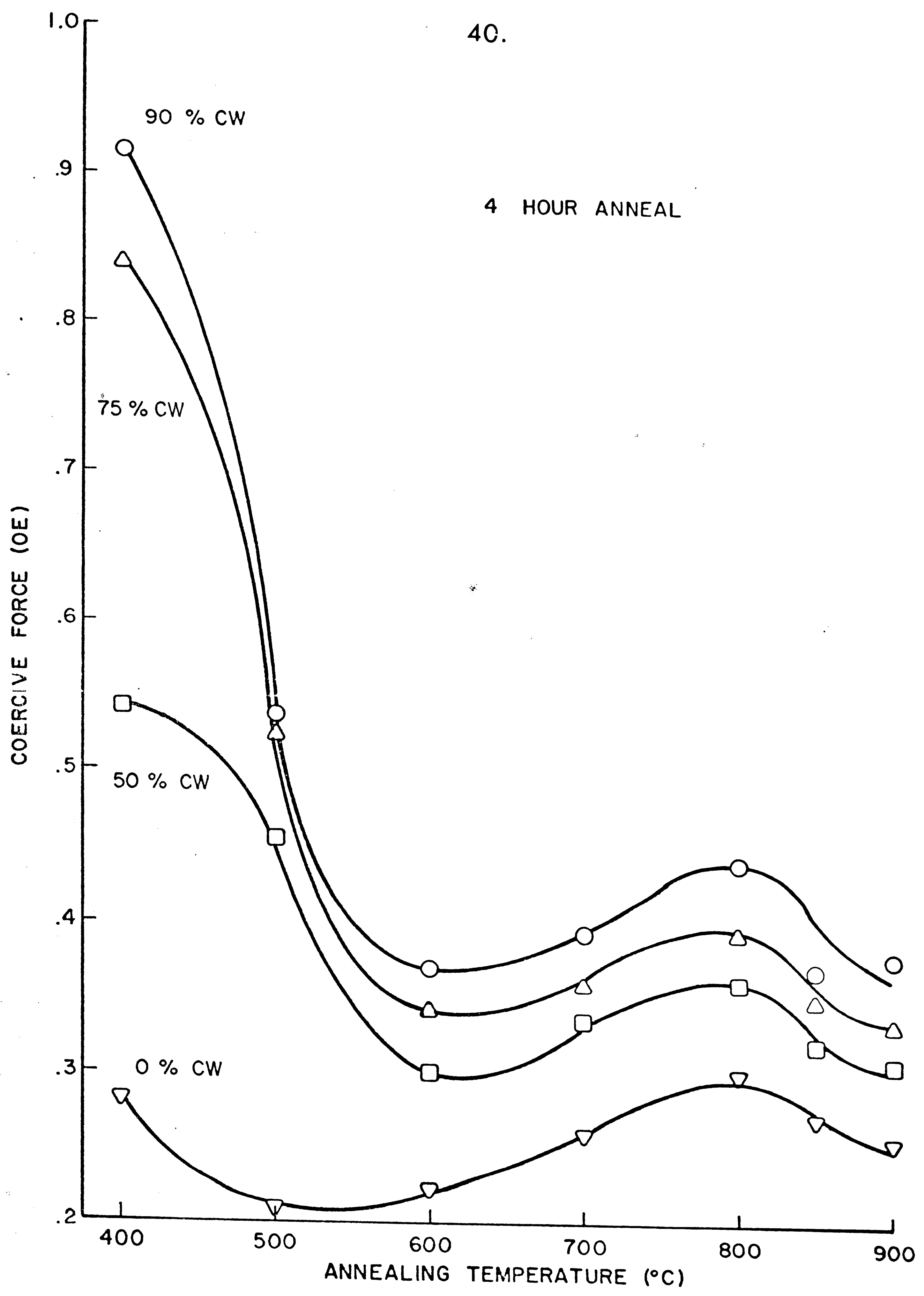


FIGURE 9
COERCIVE FORCE VS ANNEALING TEMPERATURE

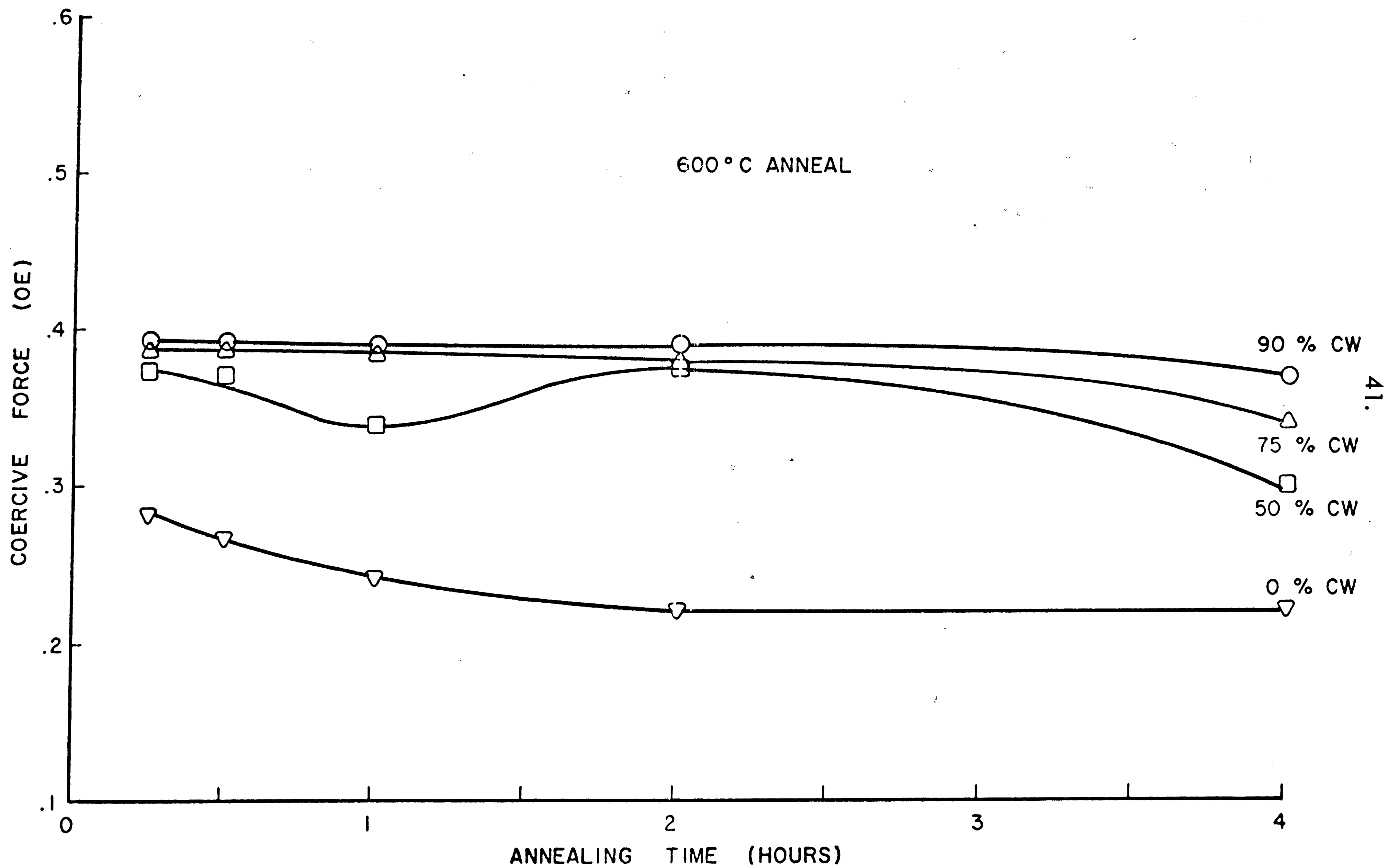


FIGURE 10
COERCIVE FORCE VS ANNEALING TIME

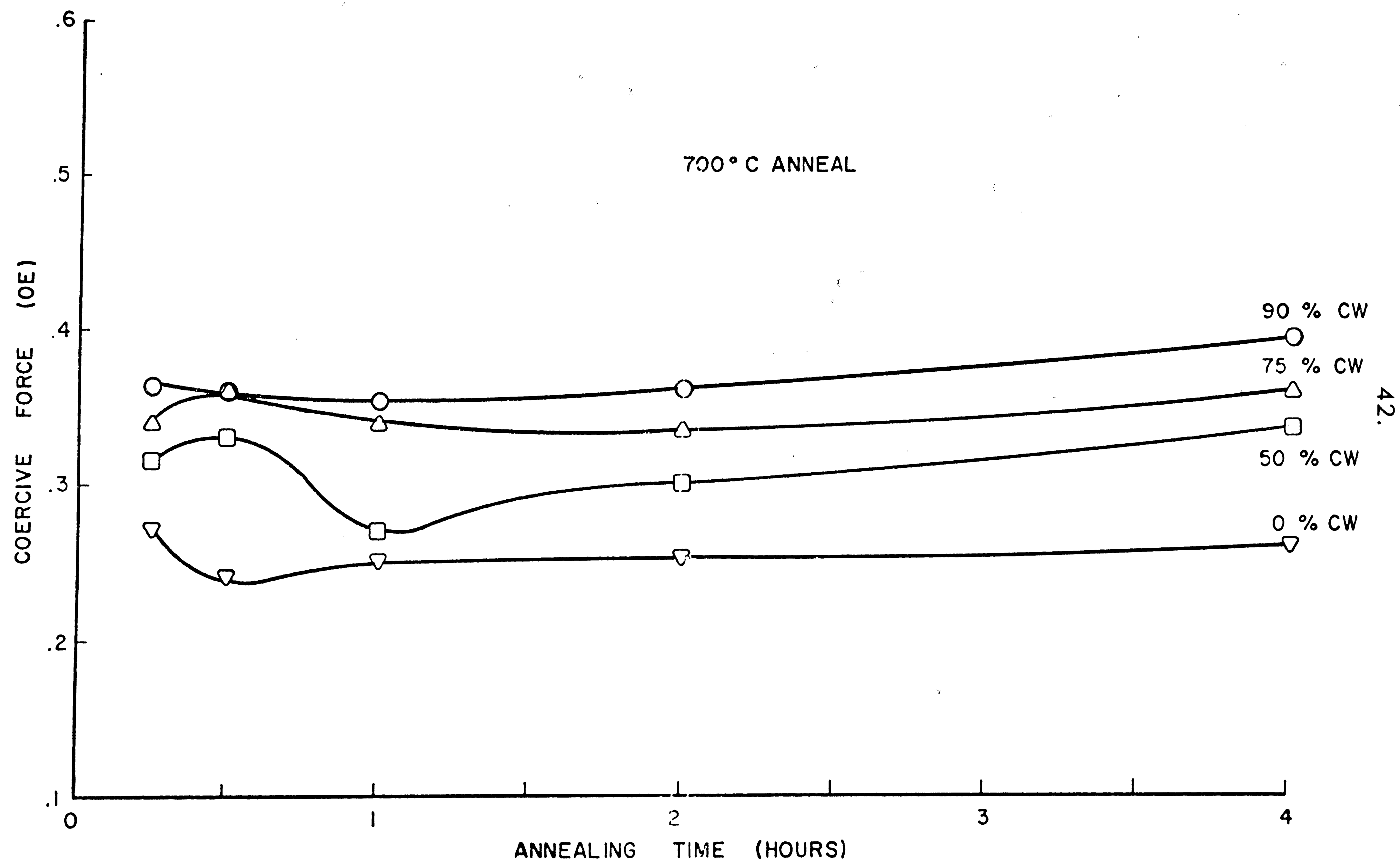
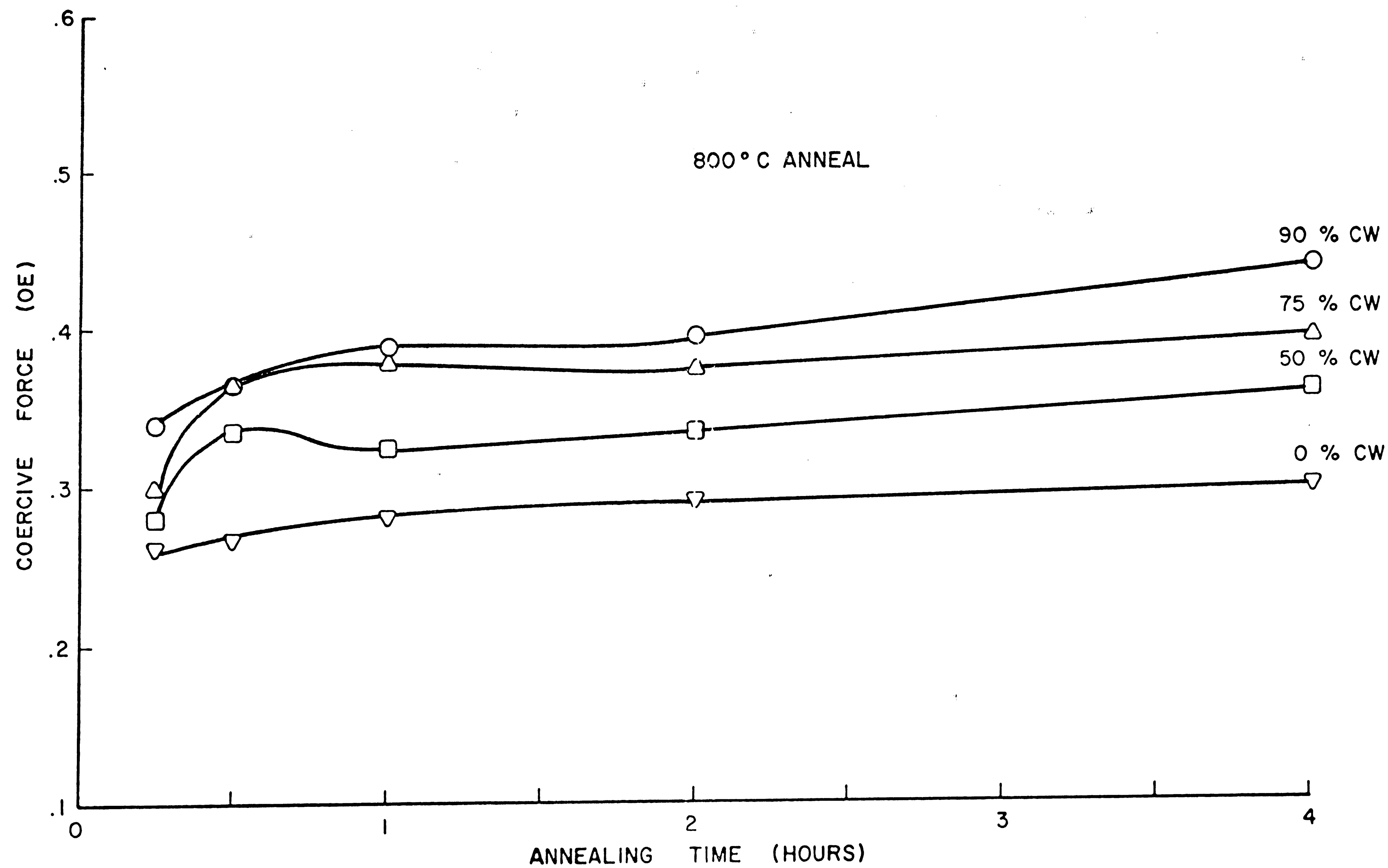


FIGURE 11
COERCIVE FORCE VS ANNEALING TIME



43.

FIGURE 12
COERCIVE FORCE VS ANNEALING TIME

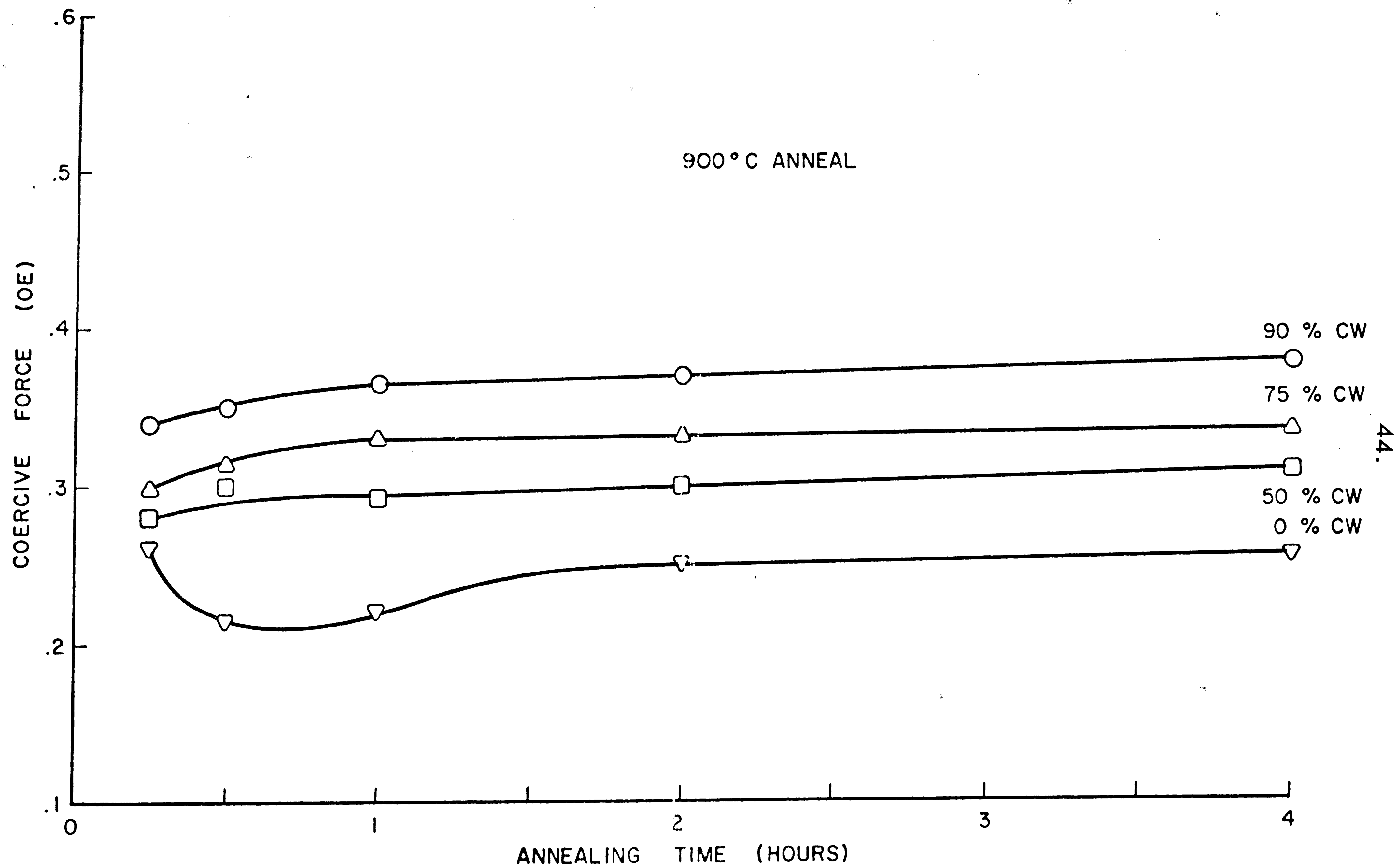
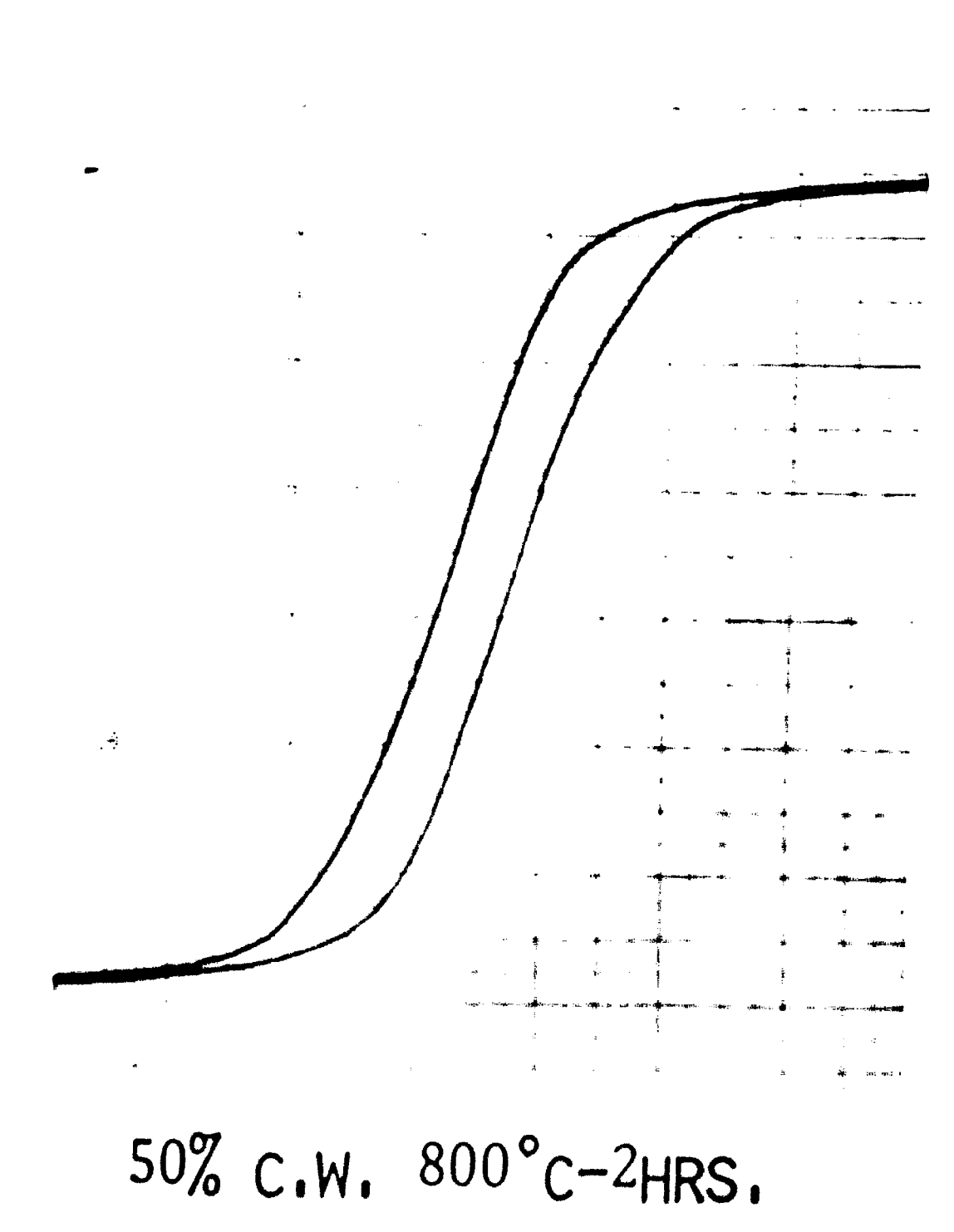
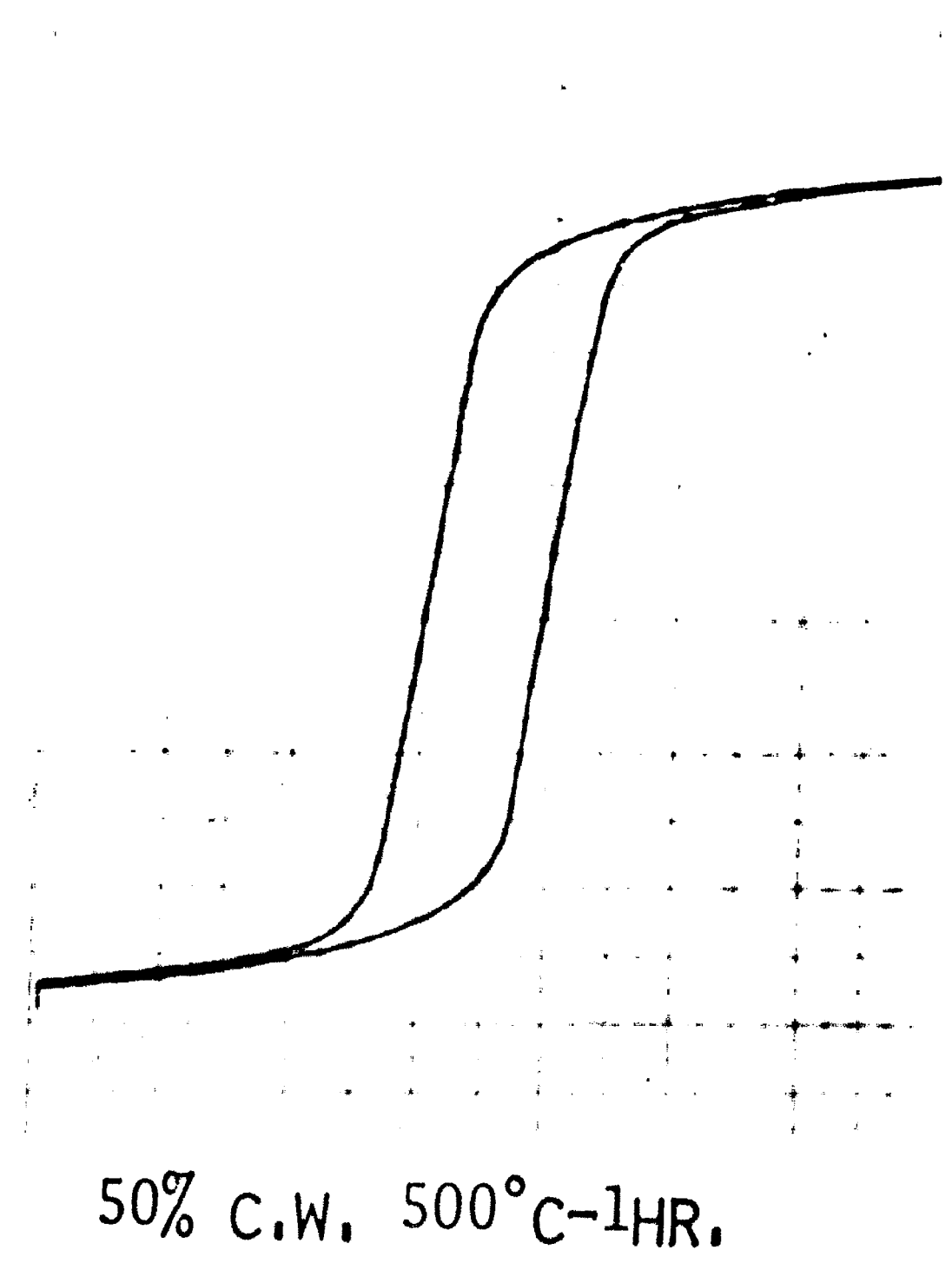
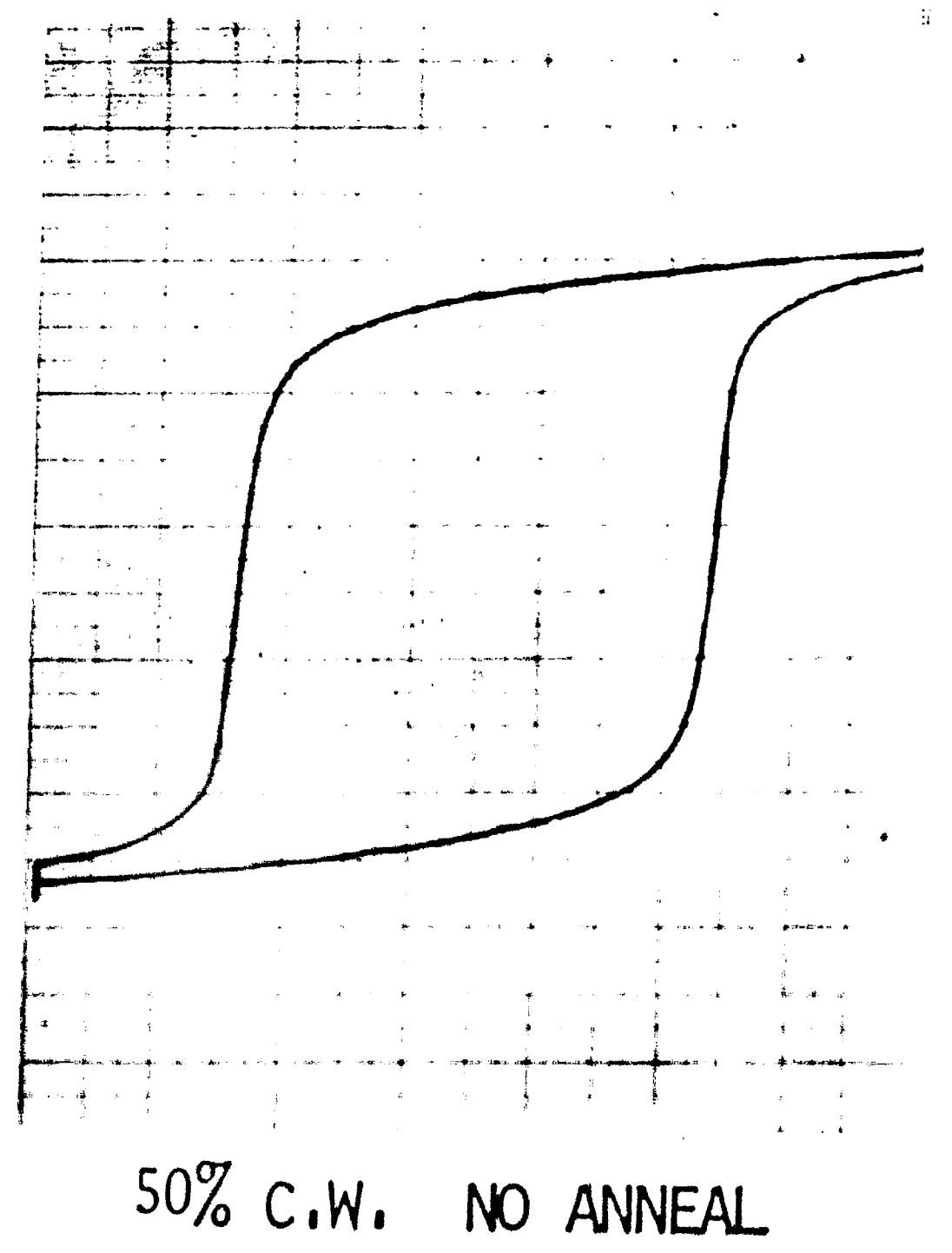
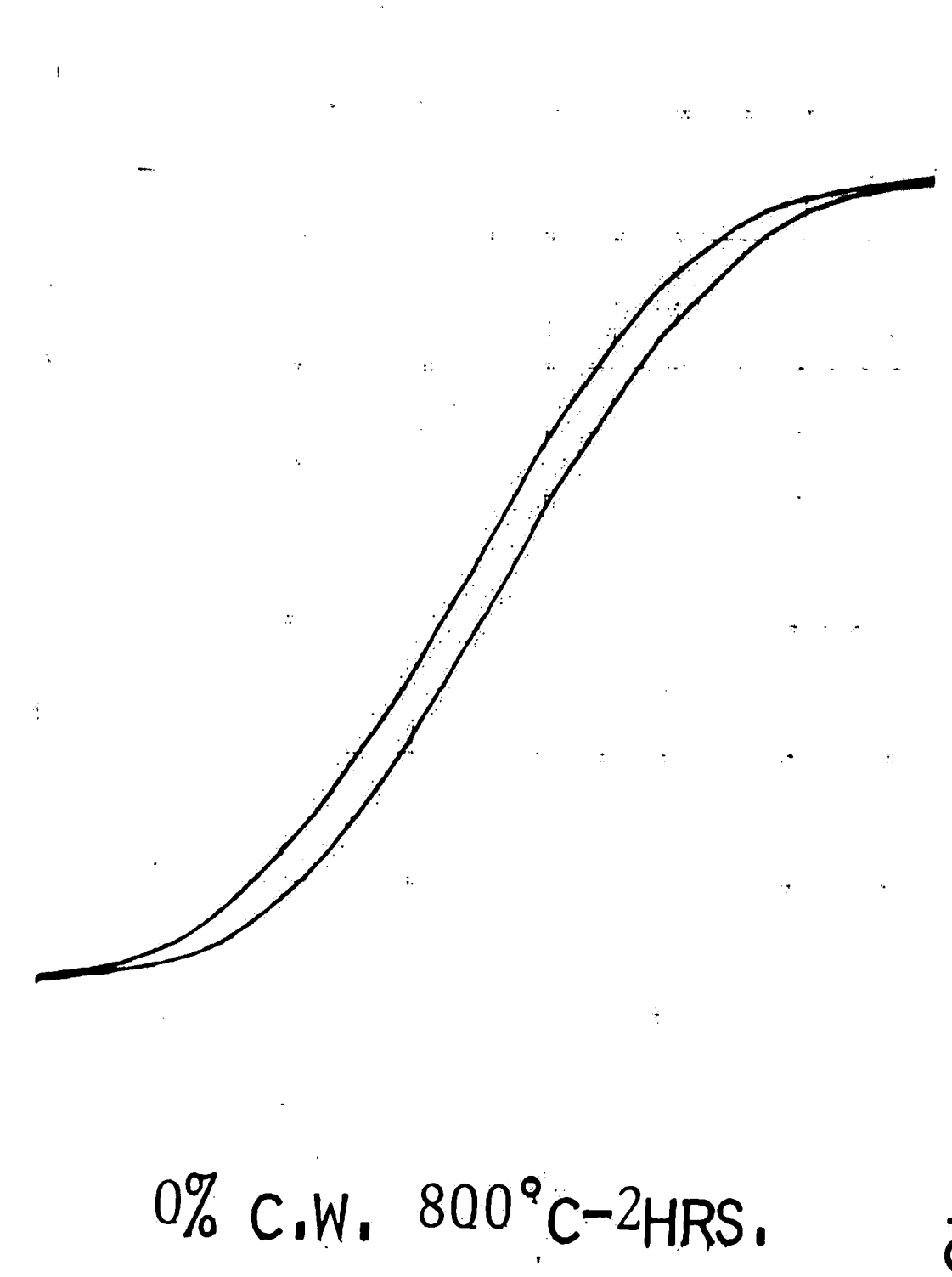
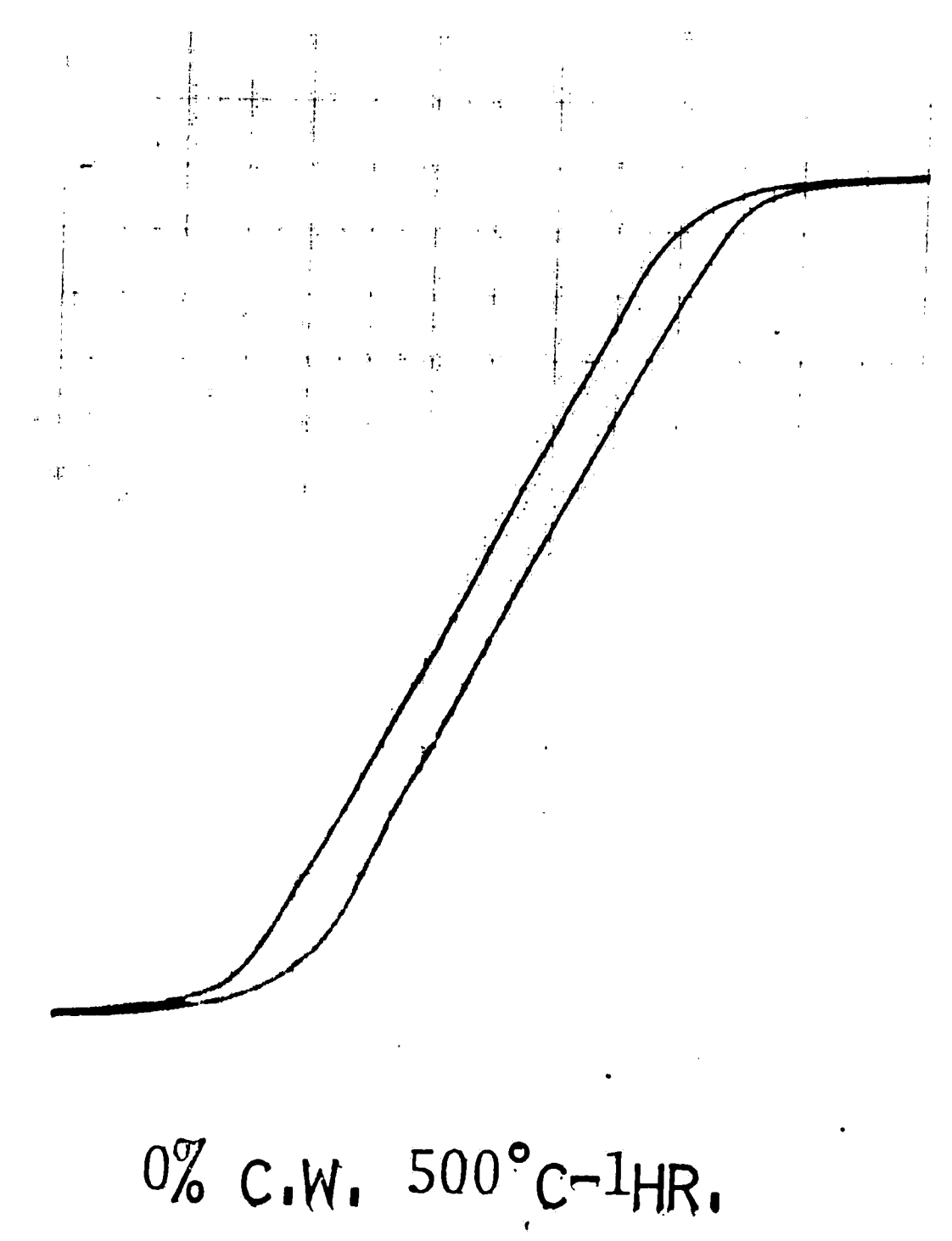
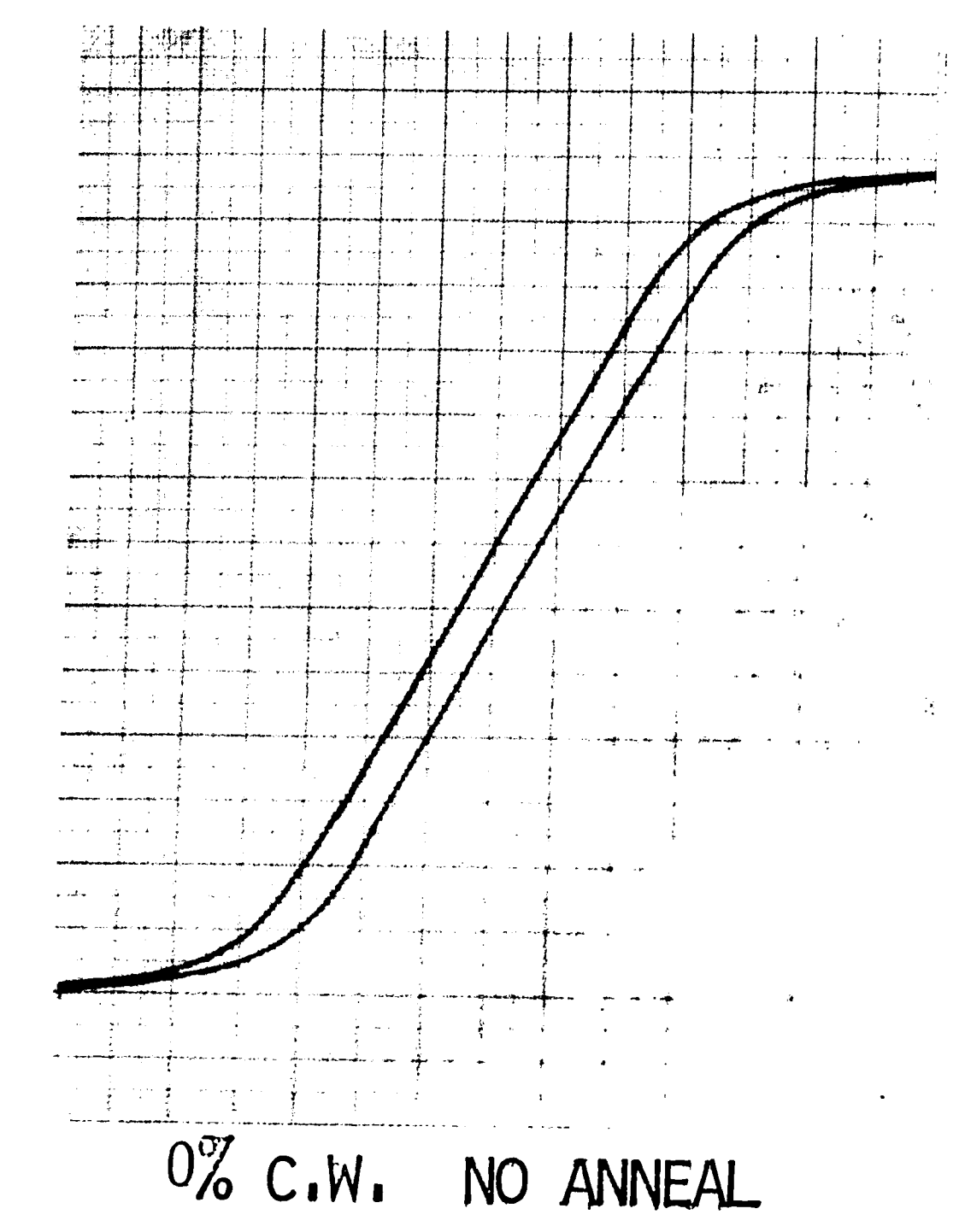


FIGURE 13
COERCIVE FORCE VS ANNEALING TIME

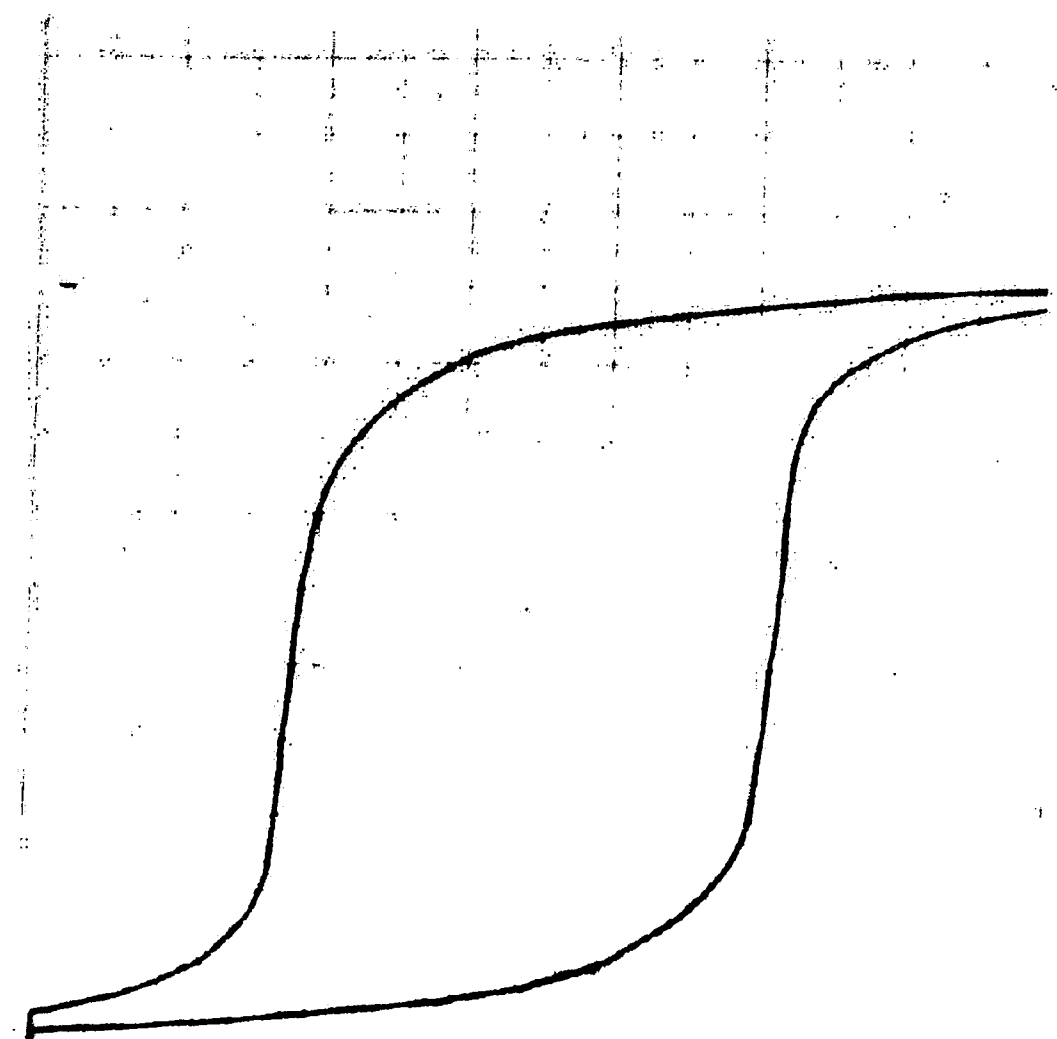
HYSTERESIS LOOPS FOR 0% AND 50% COLD WORKED
ALLOYS ANNEALED AS INDICATED

FIGURE 14

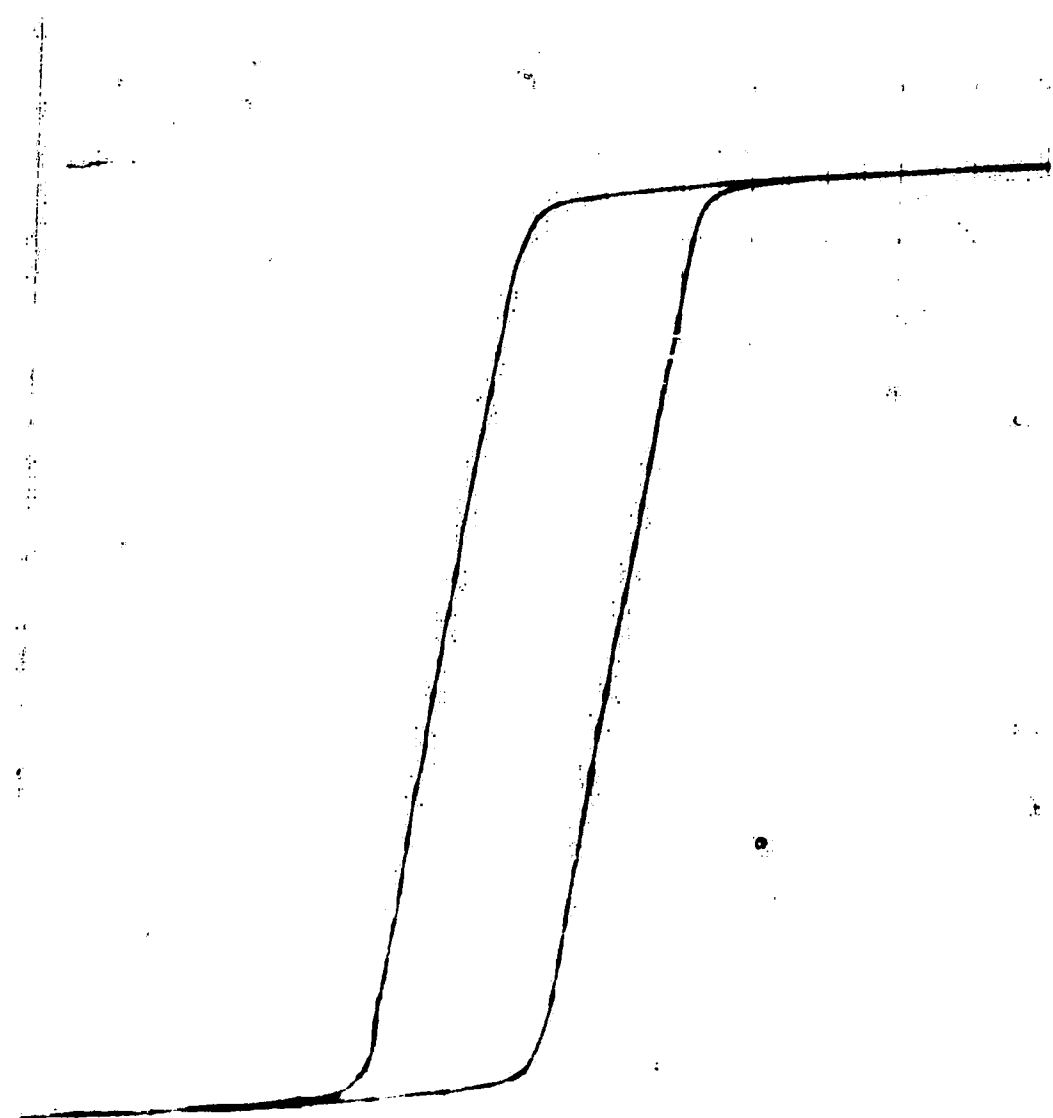


HYSTERESIS LOOPS FOR 75% AND 90% COLD WORKED
ALLOYS ANNEALED AS INDICATED

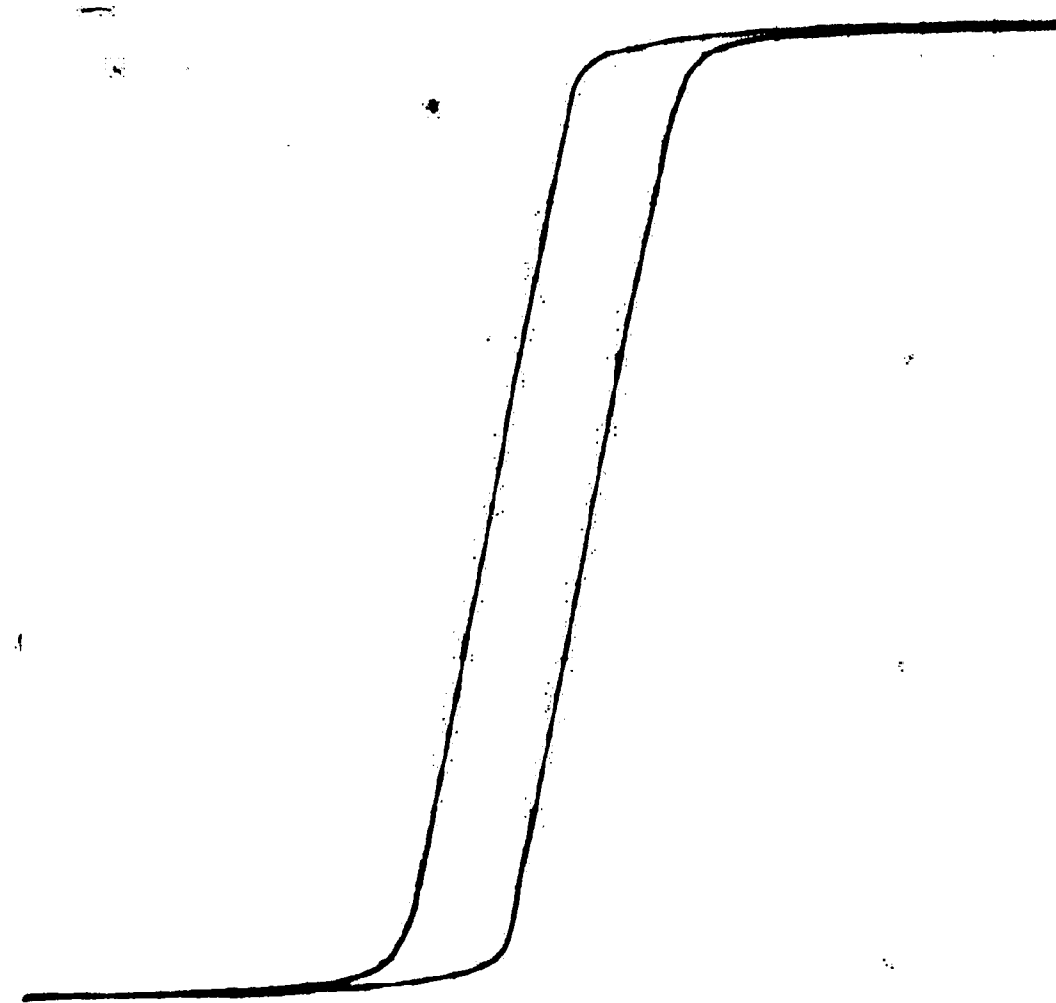
FIGURE 15



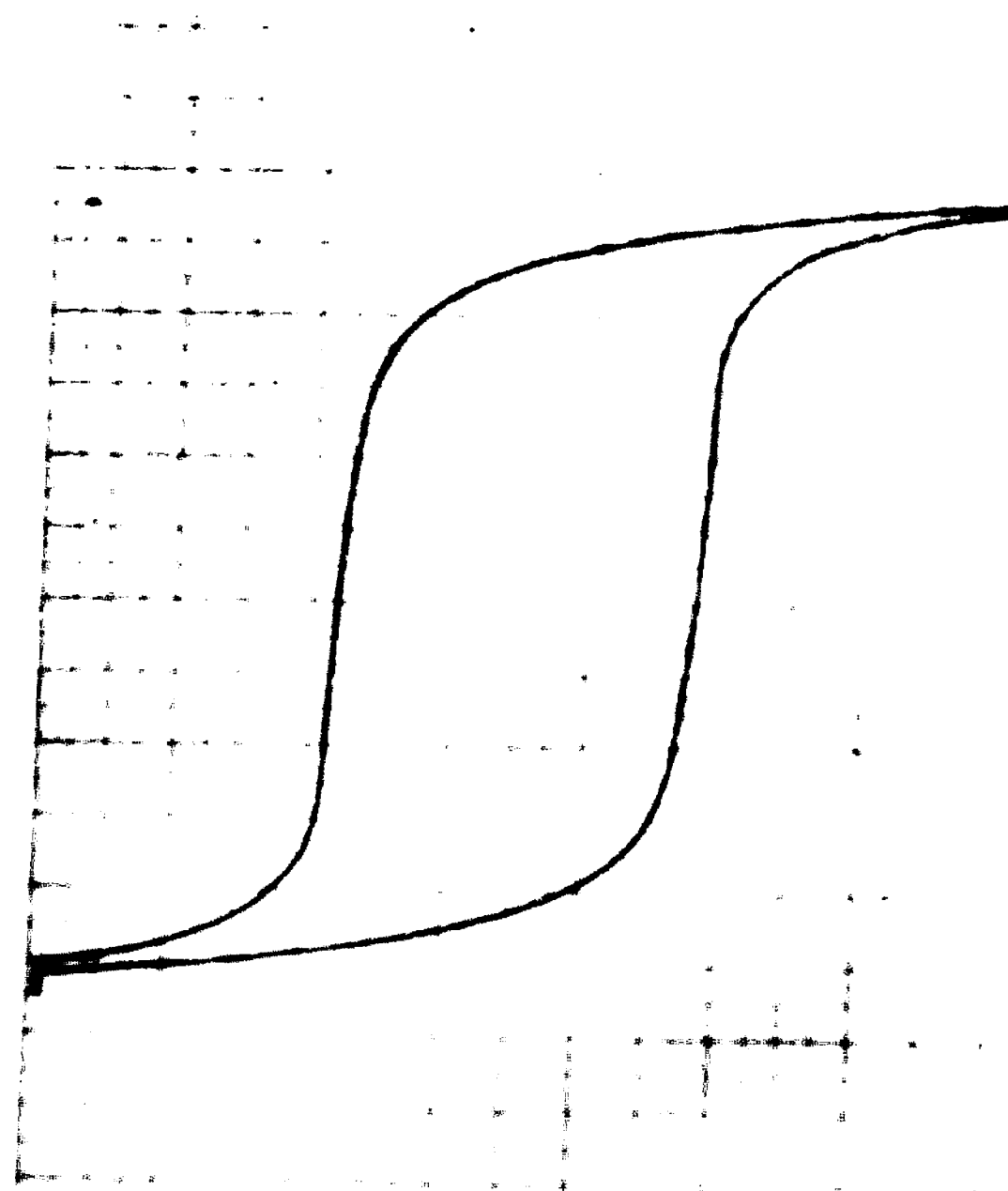
75% C.W. NO ANNEAL



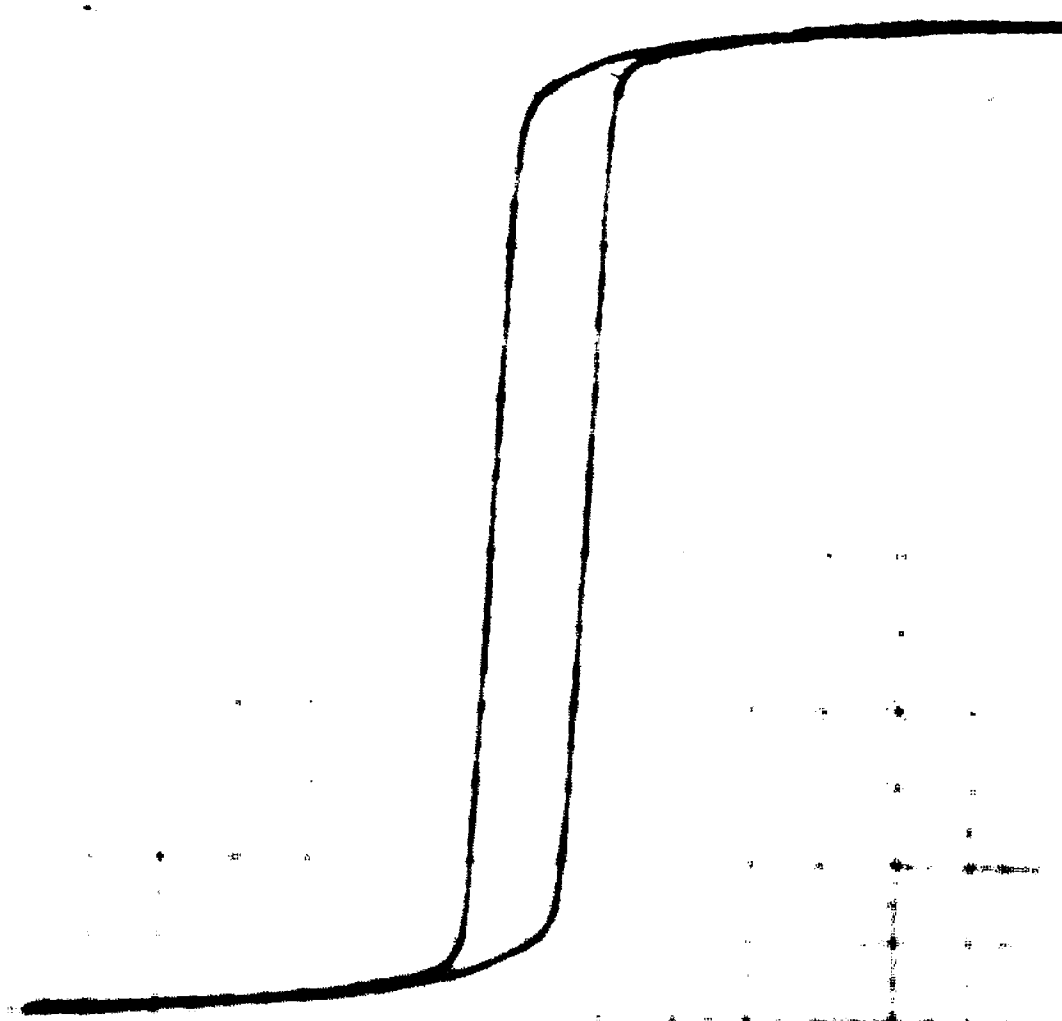
75% C.W. 500°C-2HRS.



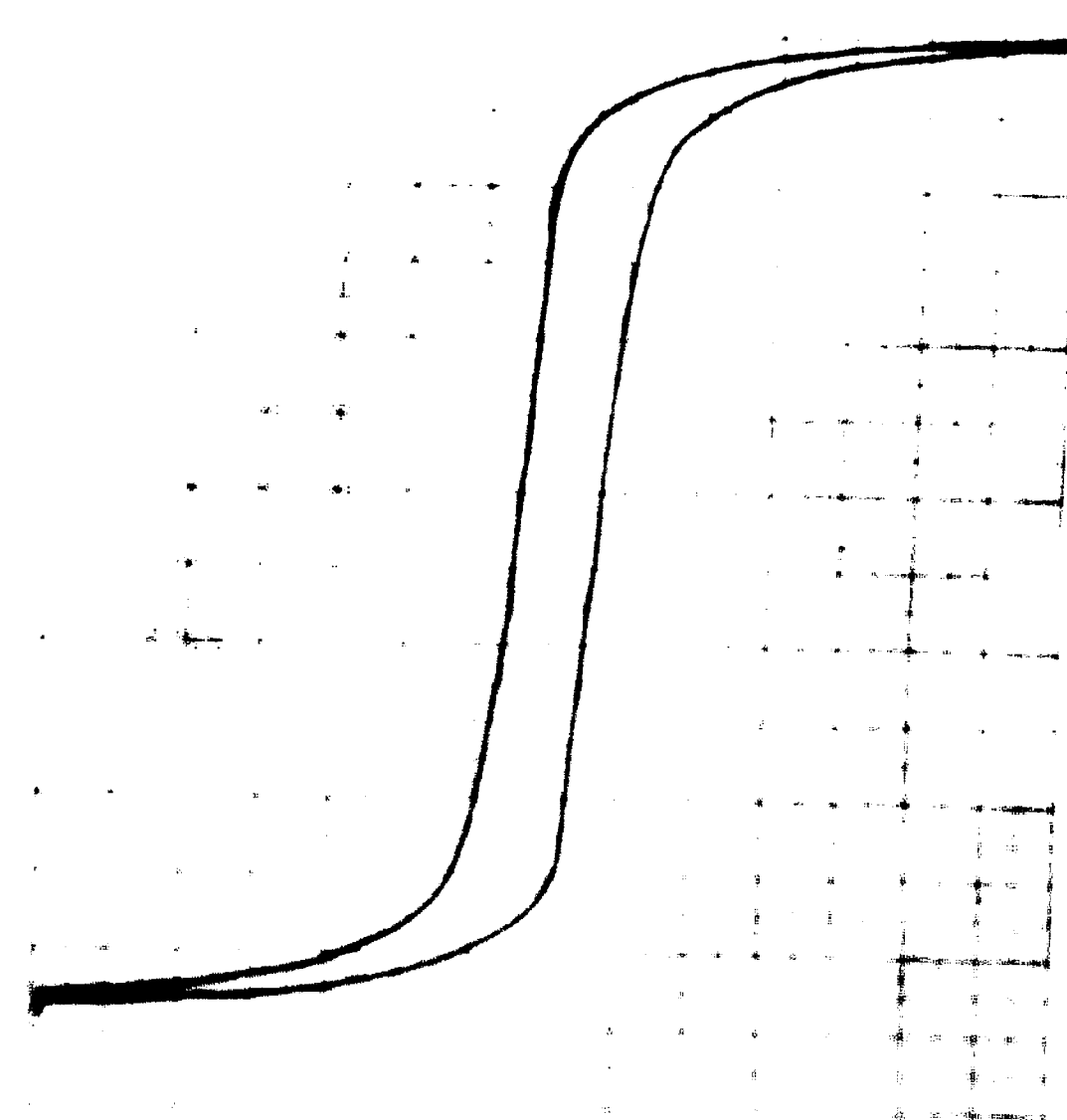
75% C.W. 700°C-2HRS.



90% C.W. NO ANNEAL



90% C.W. 500°C-1HR.



90% C.W. 800°C-2HRS.

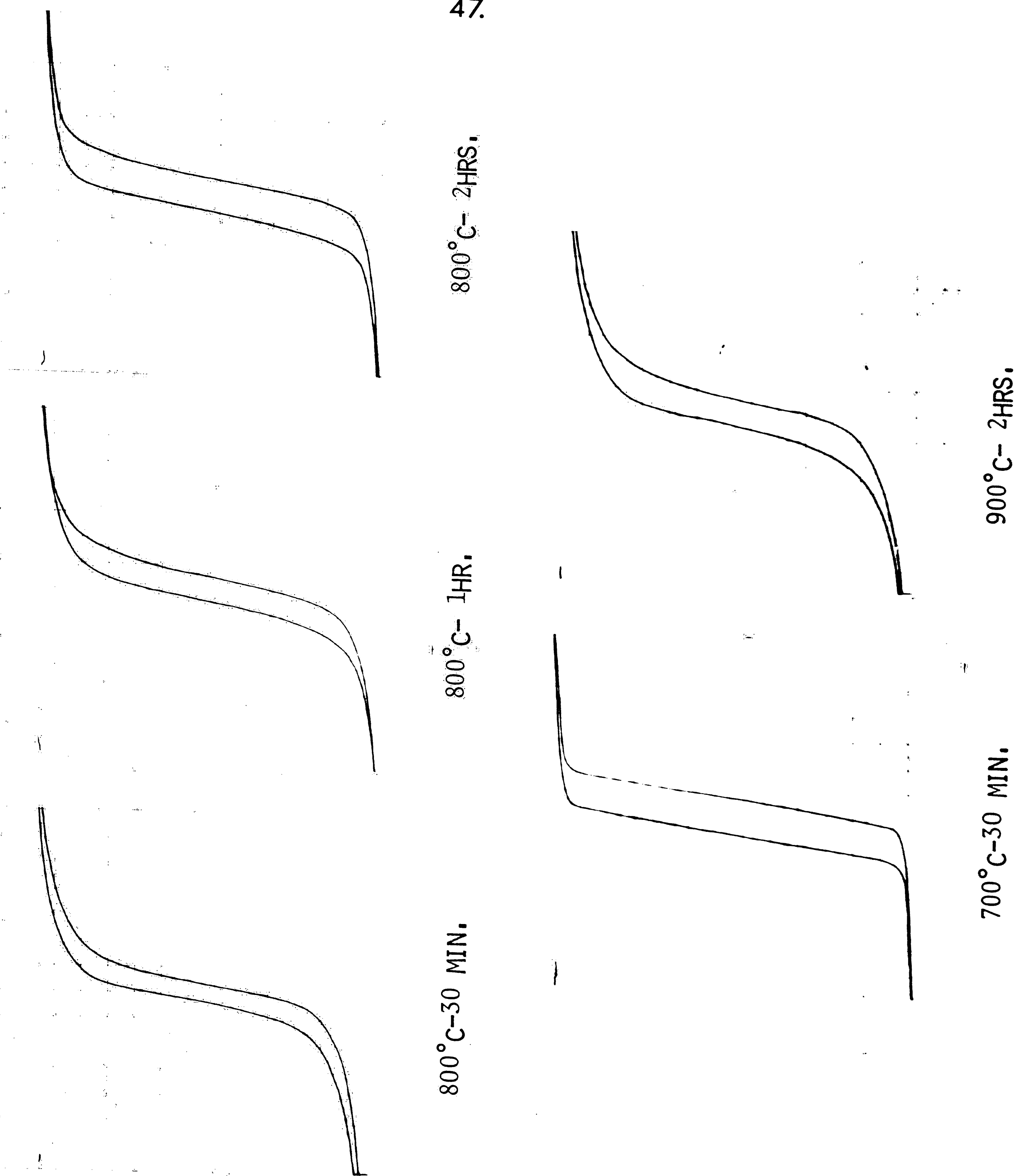


FIGURE 16
 HYSTERESIS LOOPS FOR 75% AND 90% COLD WORKED
 ALLOYS ANNEALED AS INDICATED

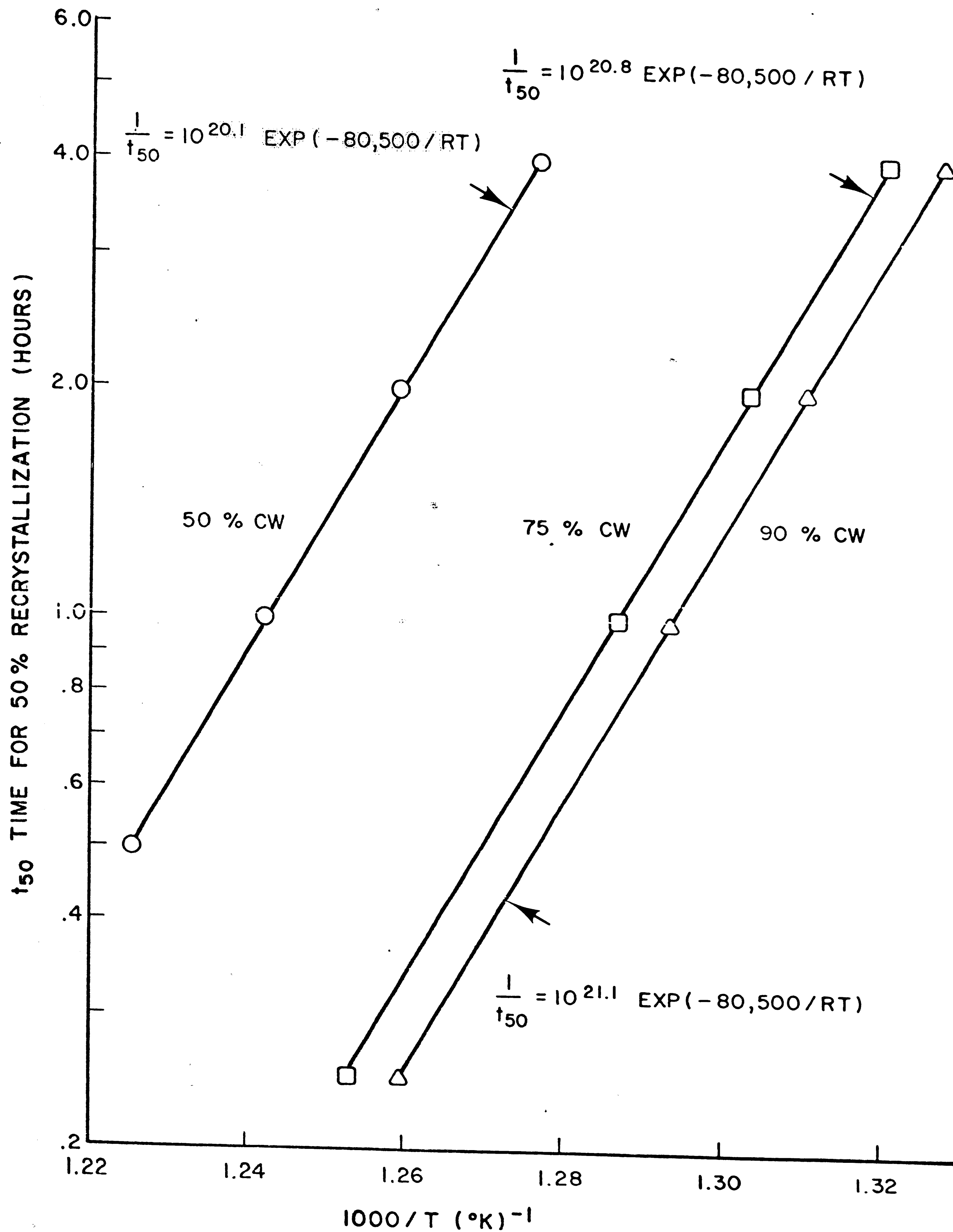
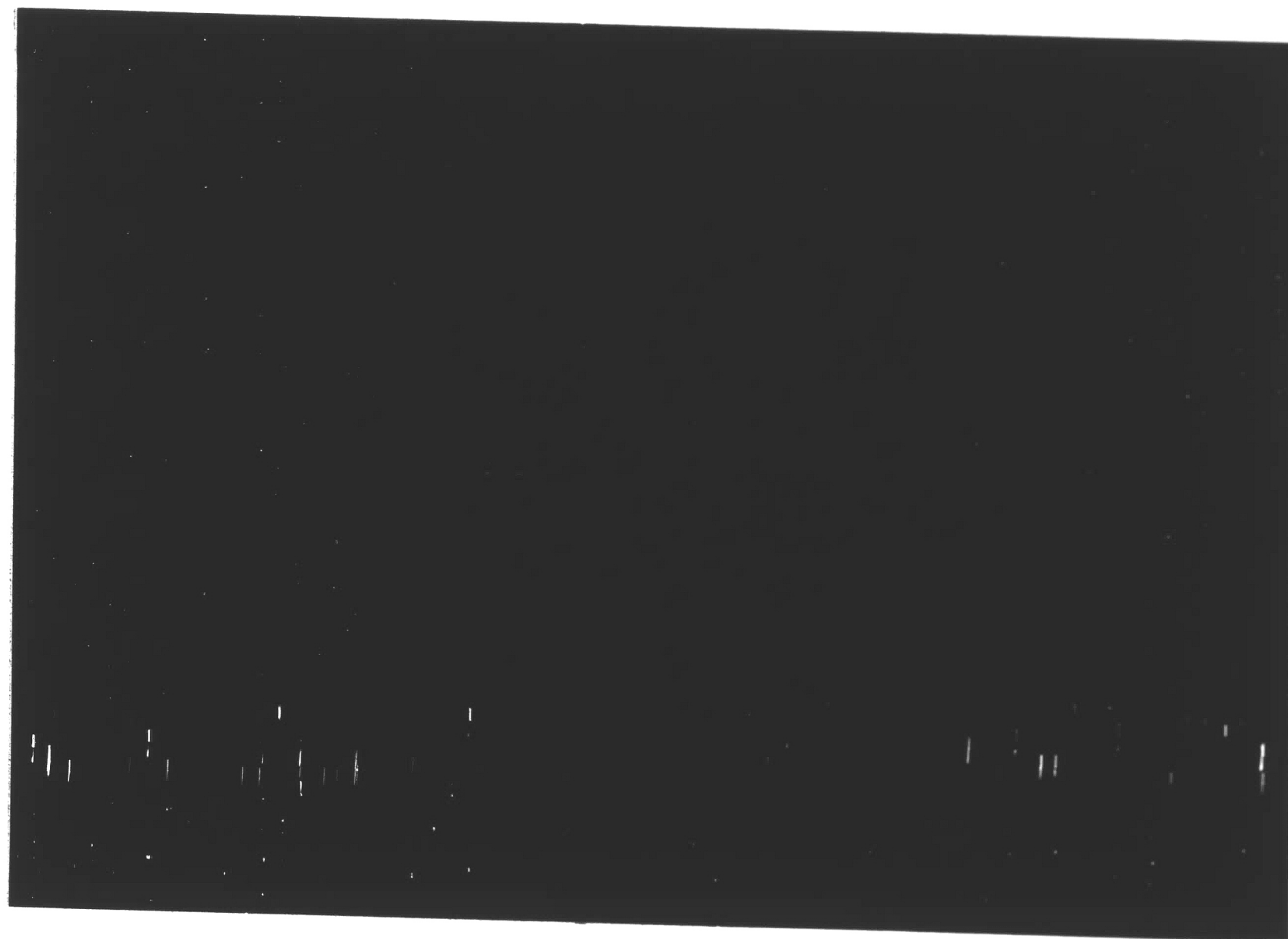


FIGURE 17
TIME FOR 50% RECRYSTALLIZATION VS $1/T$



A. 0% COLD WORK



B. 50% COLD WORK

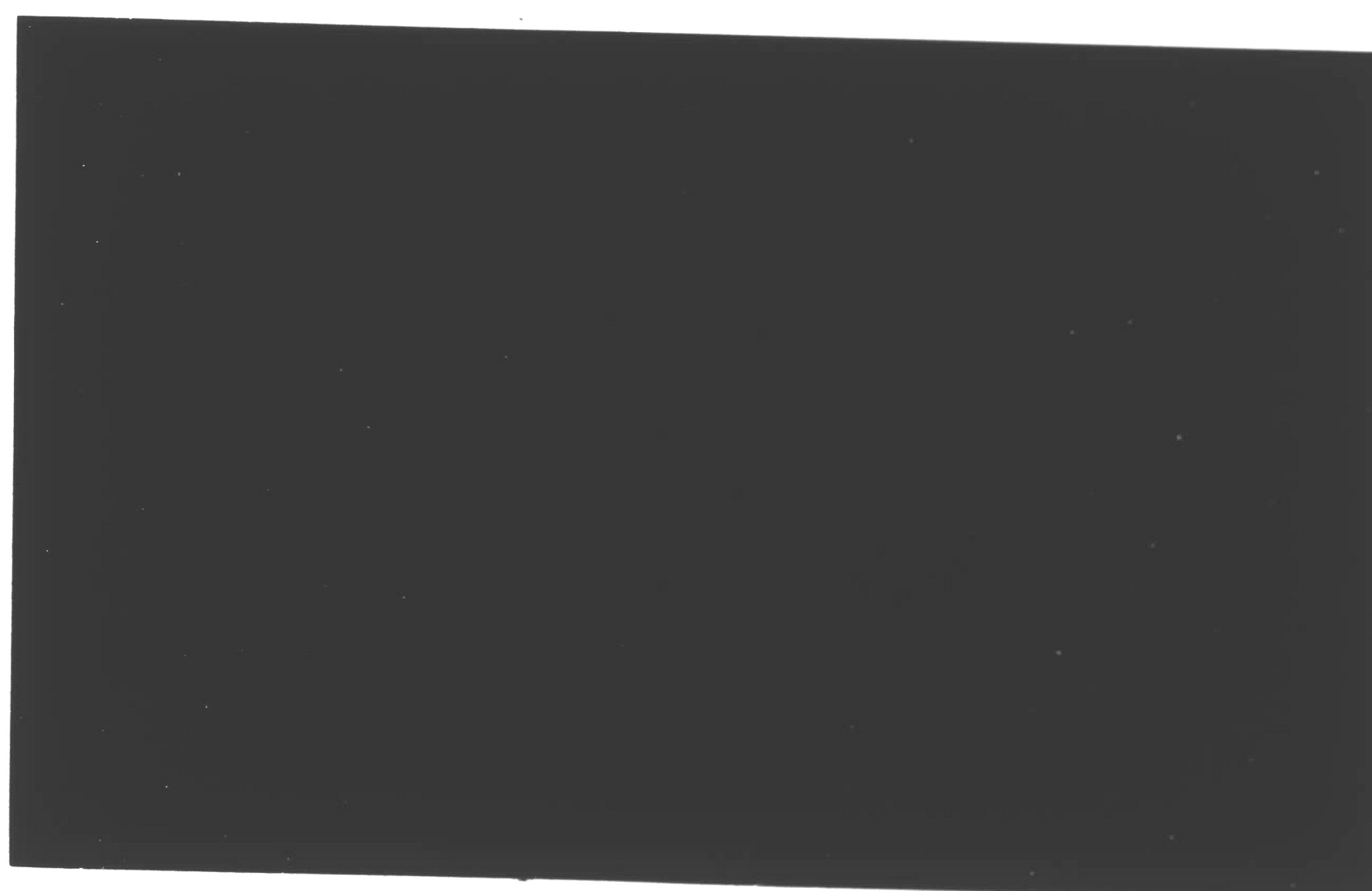
FIGURE 18
MICROSTRUCTURE OF 0% AND 50% COLD WORKED,
NO-ANNEAL ALLOYS. 10 GM. CuSO_4 - 50ML
 HCl - 50 ML H_2O ETCH. $\times 1000$.



A. 400°C

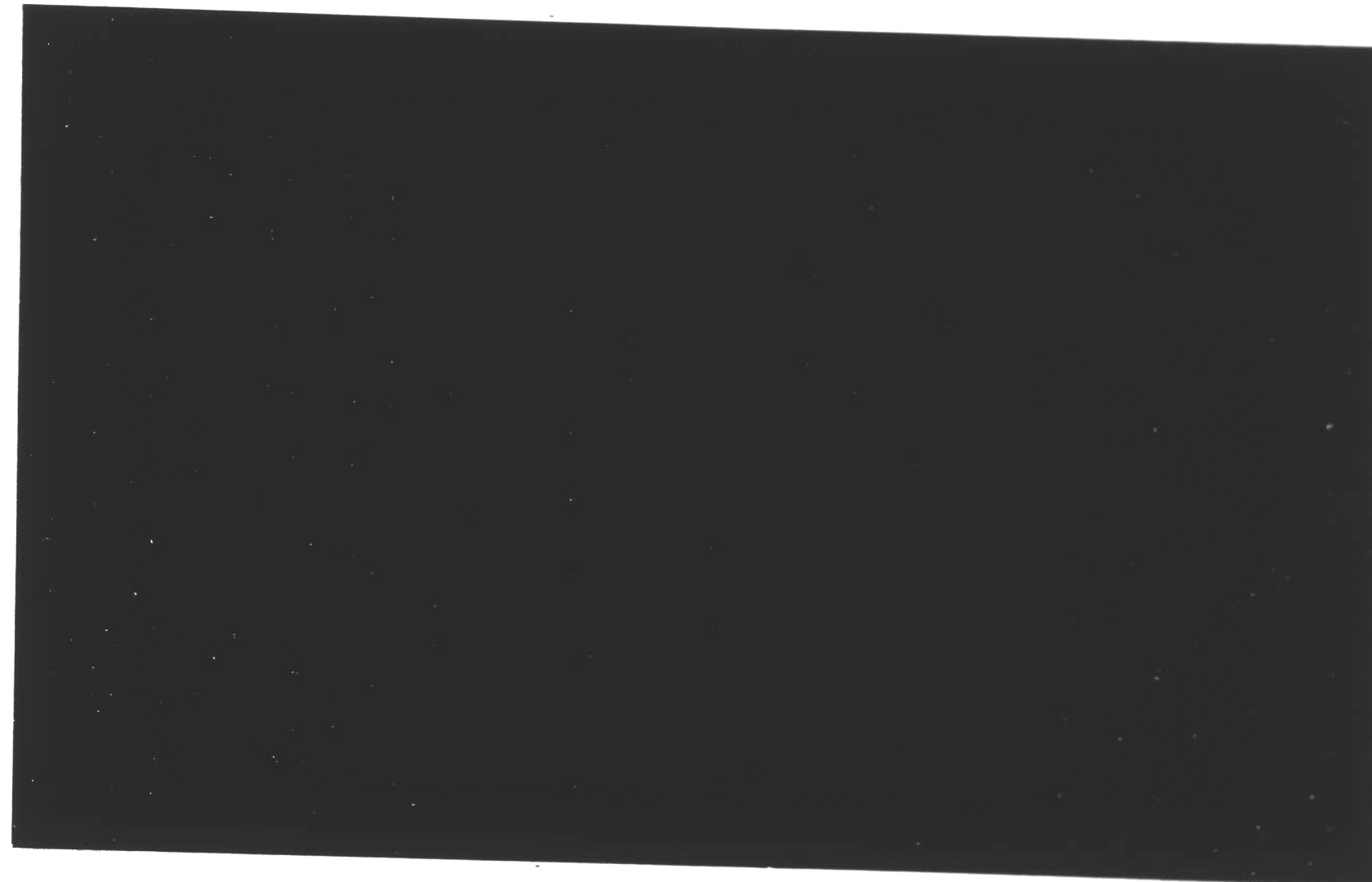


B. 500°C

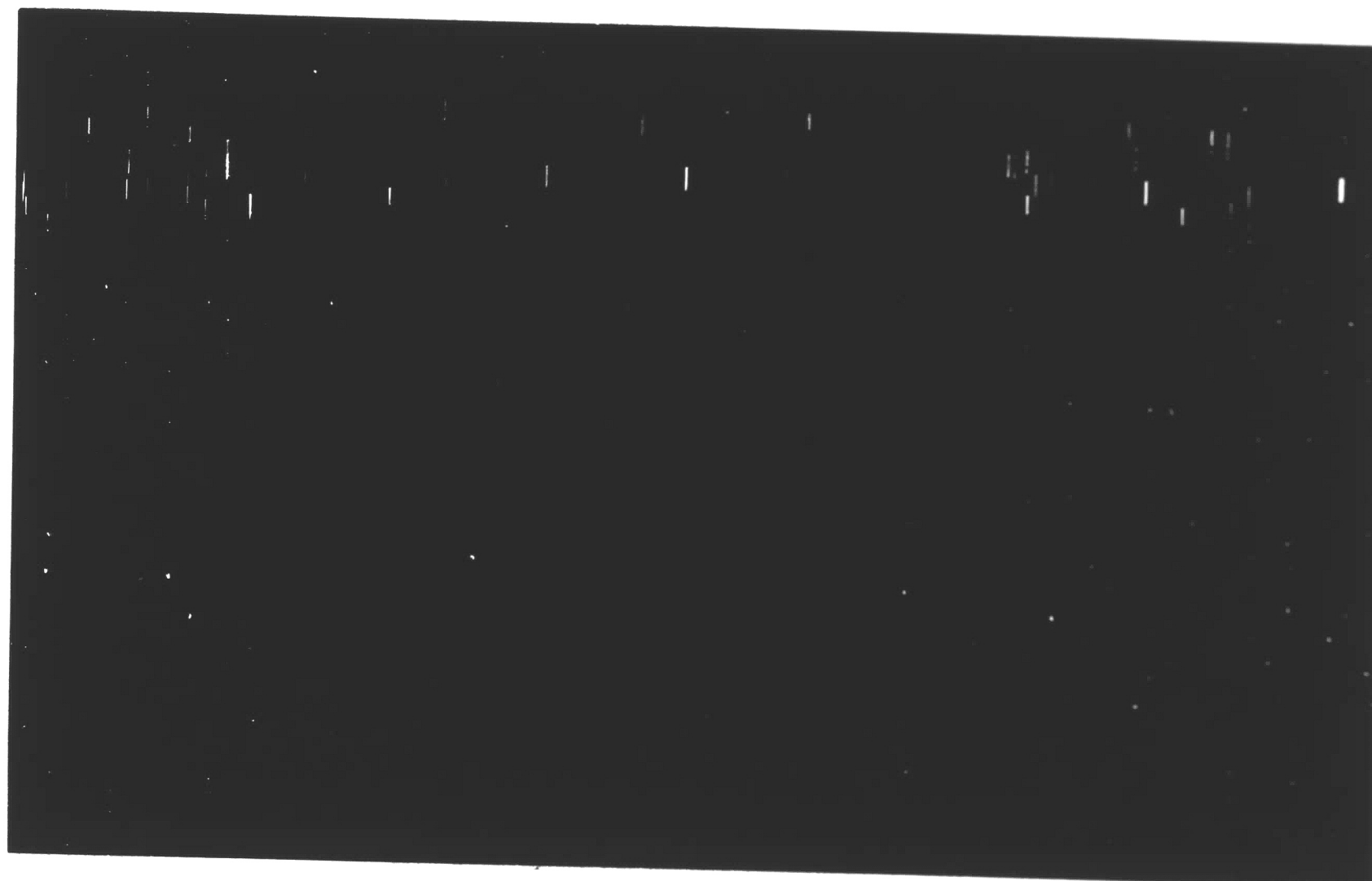


C. 800°C

FIGURE 19
 MICROSTRUCTURES OF 0% COLD WORK ALLOY ANNEALED
 FOR 15 MINUTES AT THE TEMPERATURES INDICATED.
 10 GM. CuSO_4 - 50 ML HCL - 50 ML H_2O ETCH. $\times 1000$.



A. 90% COLD WORK



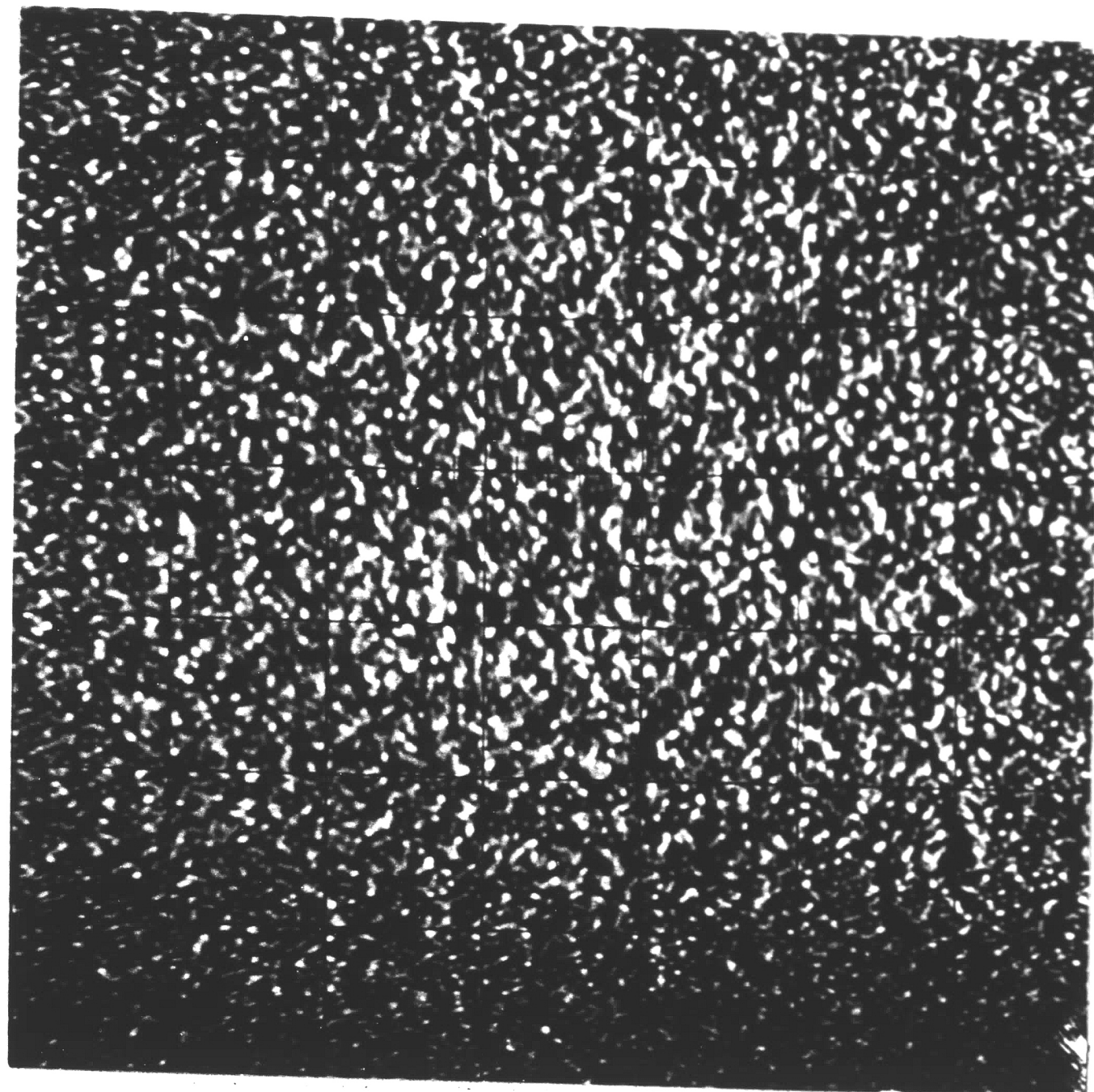
B. 50% COLD WORK



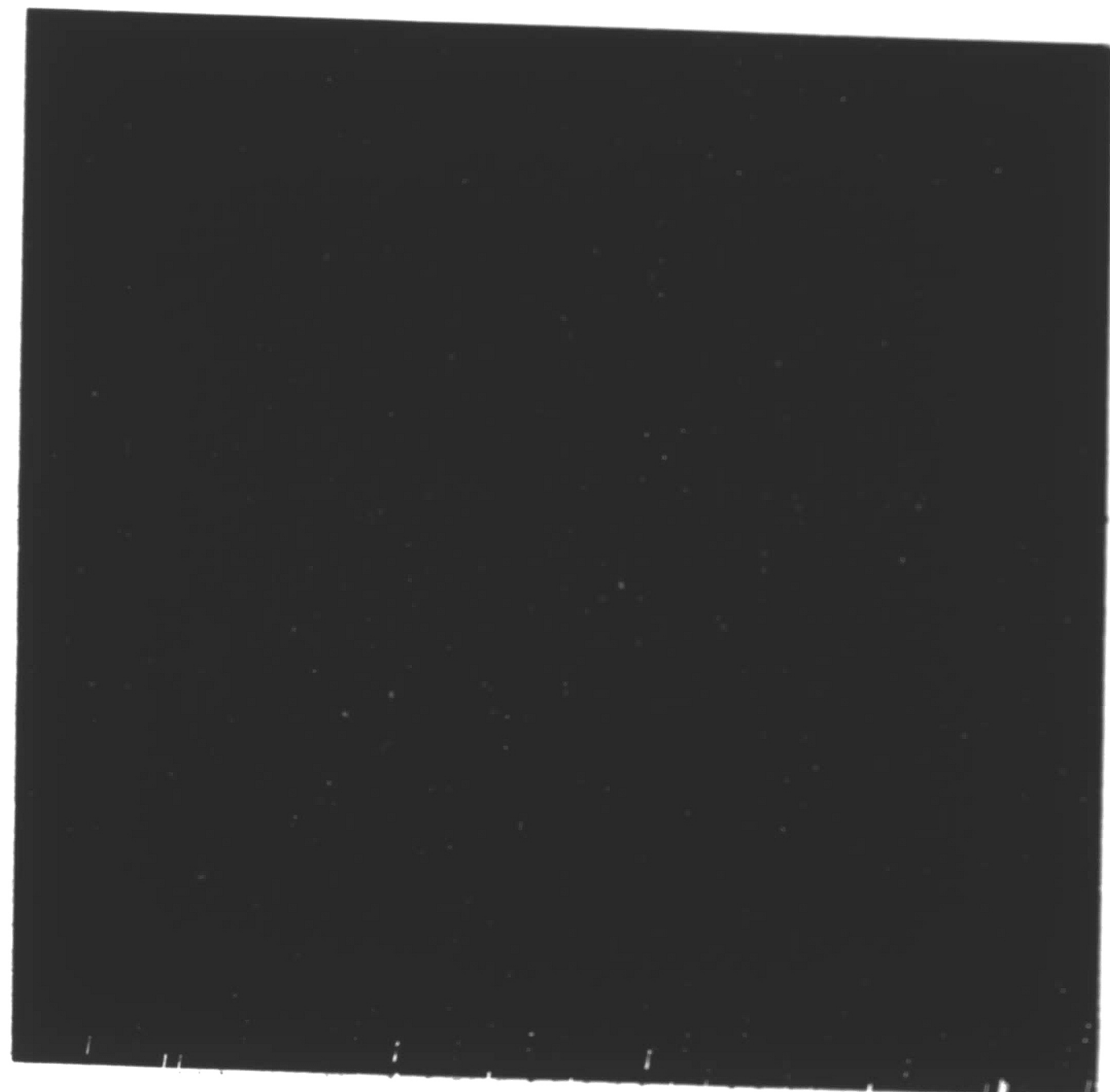
C. 0% COLD WORK

FIGURE 20

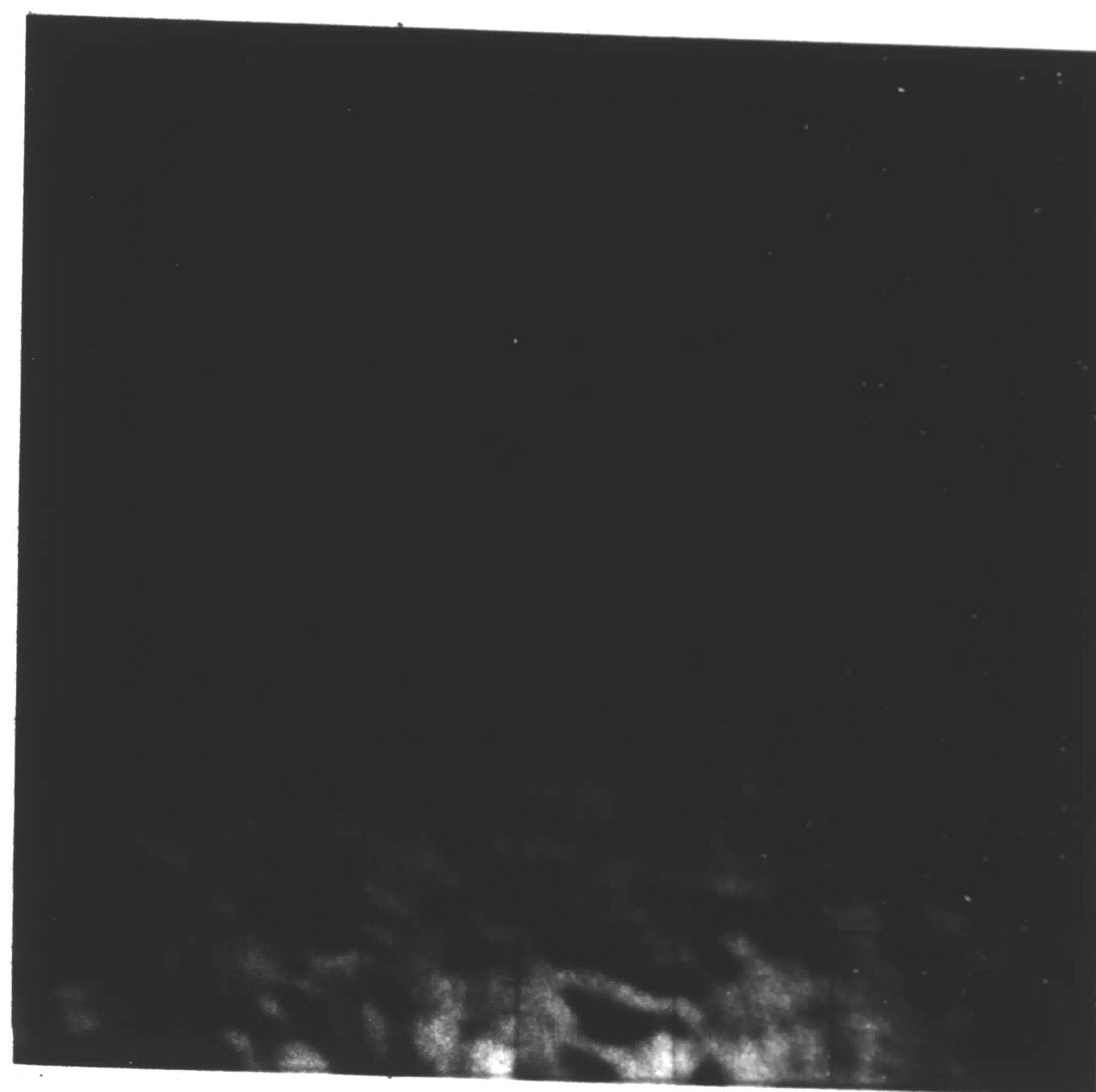
MICROSTRUCTURES OF ALLOYS ANNEALED AT 800°C
FOR 30 MINUTES. 10 GM. CuSO_4 - 50 ML HCL -
50 ML H_2O ETCH. $\times 1000$.



A. NI X-RAY DISPLAY



B. ZR X-RAY DISPLAY

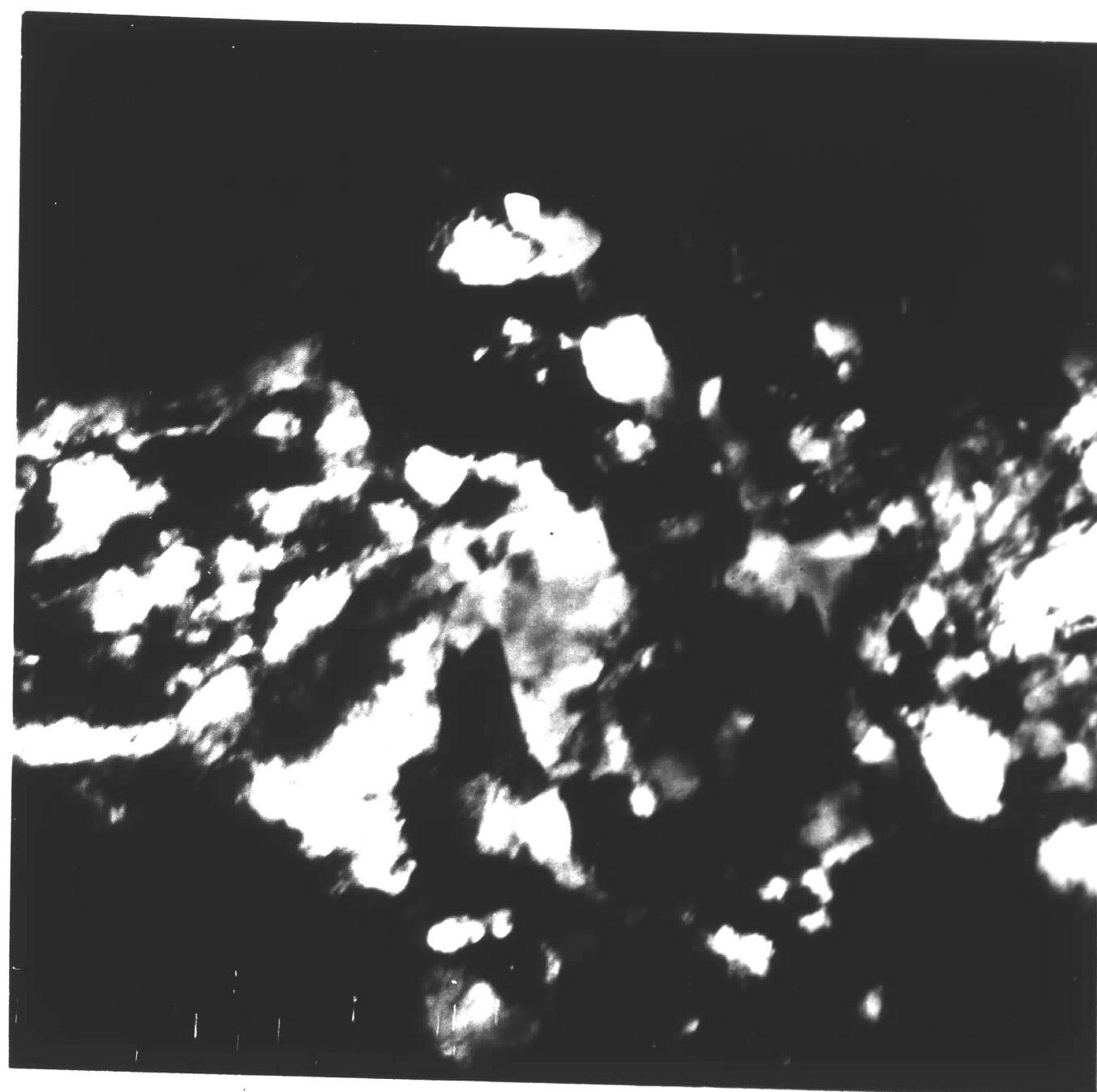


C. ELECTRON BACK-SCATTER DISPLAY

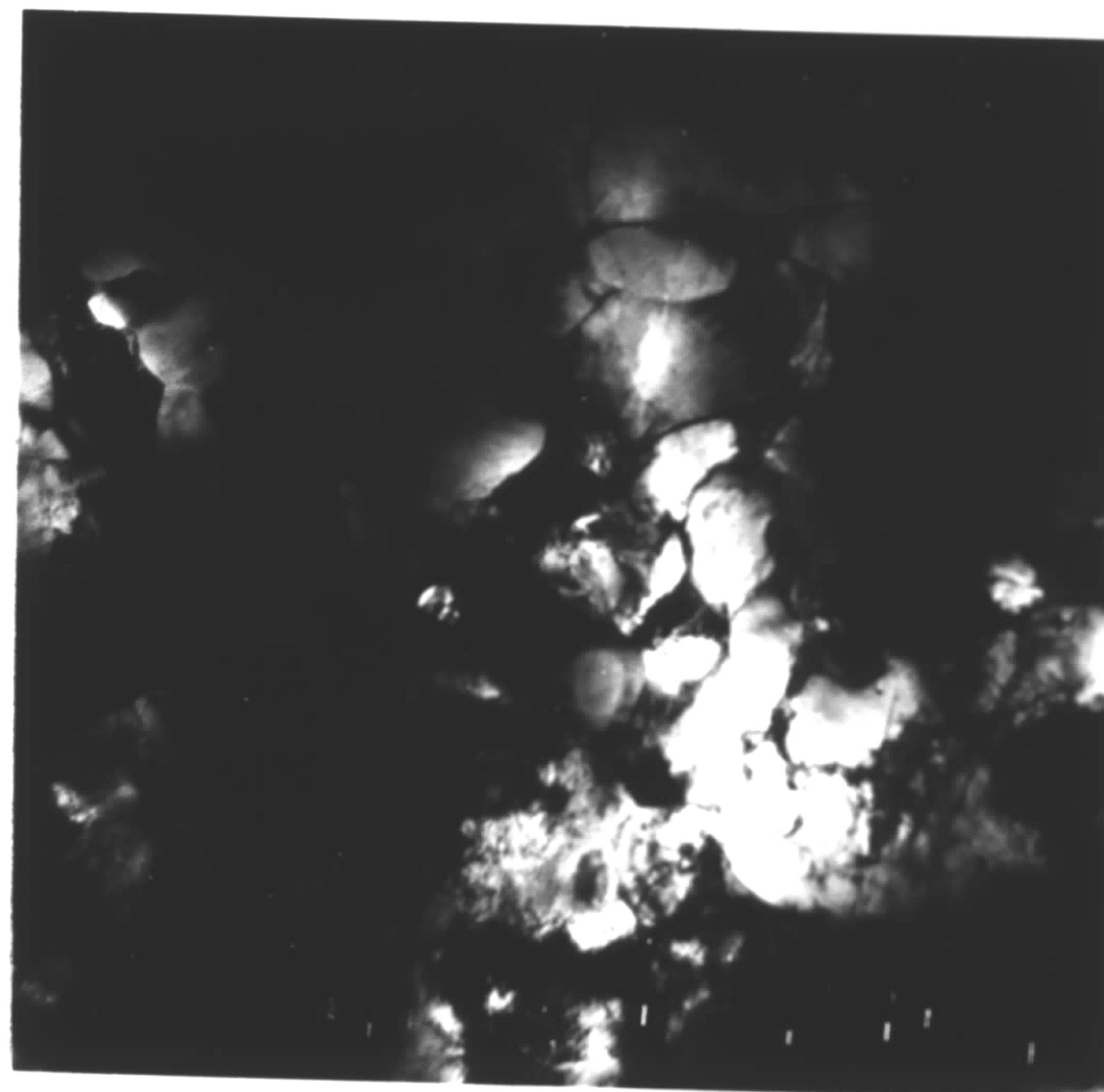
FIGURE 21

X-RAY RASTER AND BACK-SCATTER DISPLAYS
(X800) OF A 50% COLD WORKED STRUCTURE

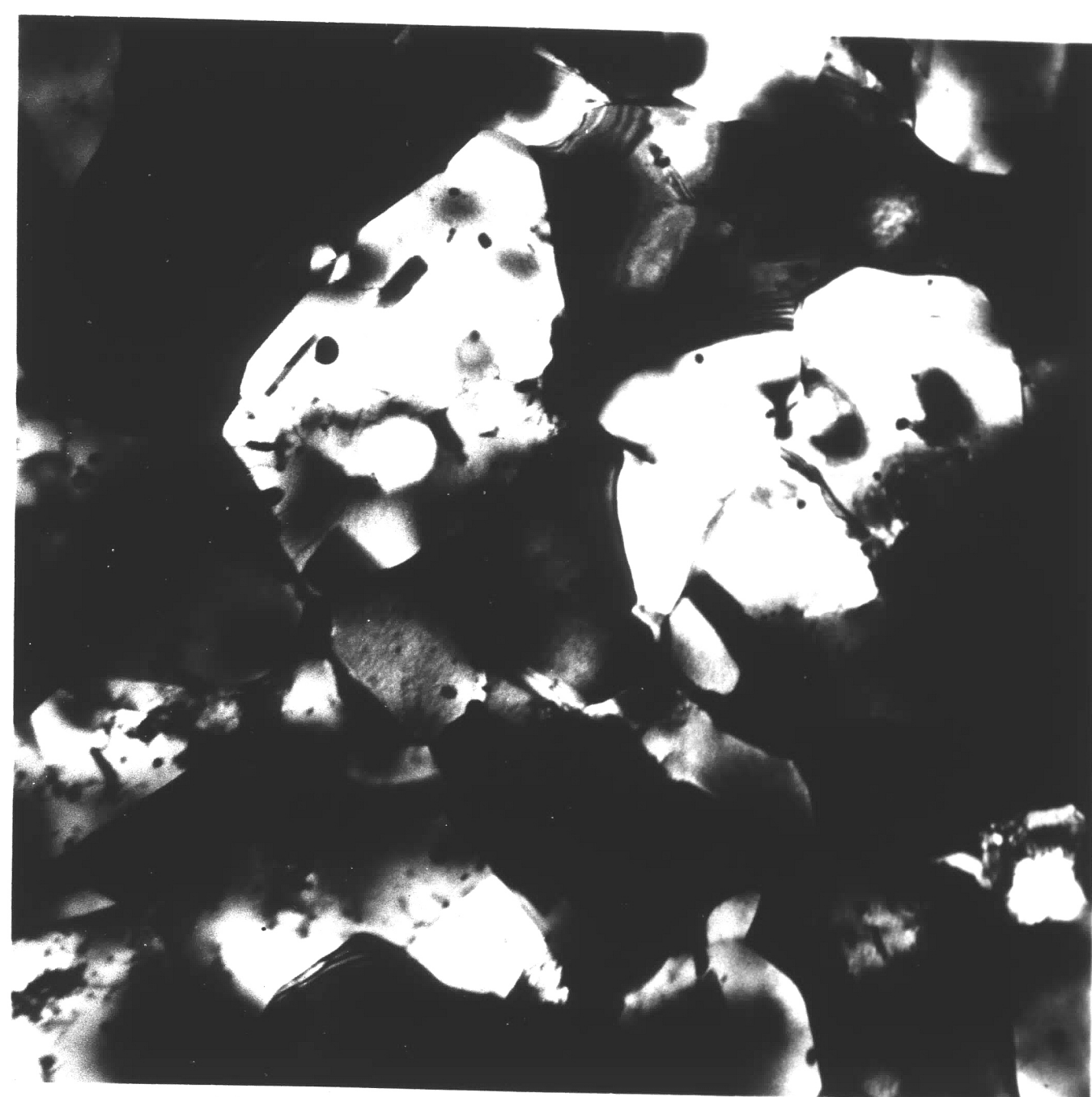
ANNEALED AT 350°C FOR 1 HOUR.



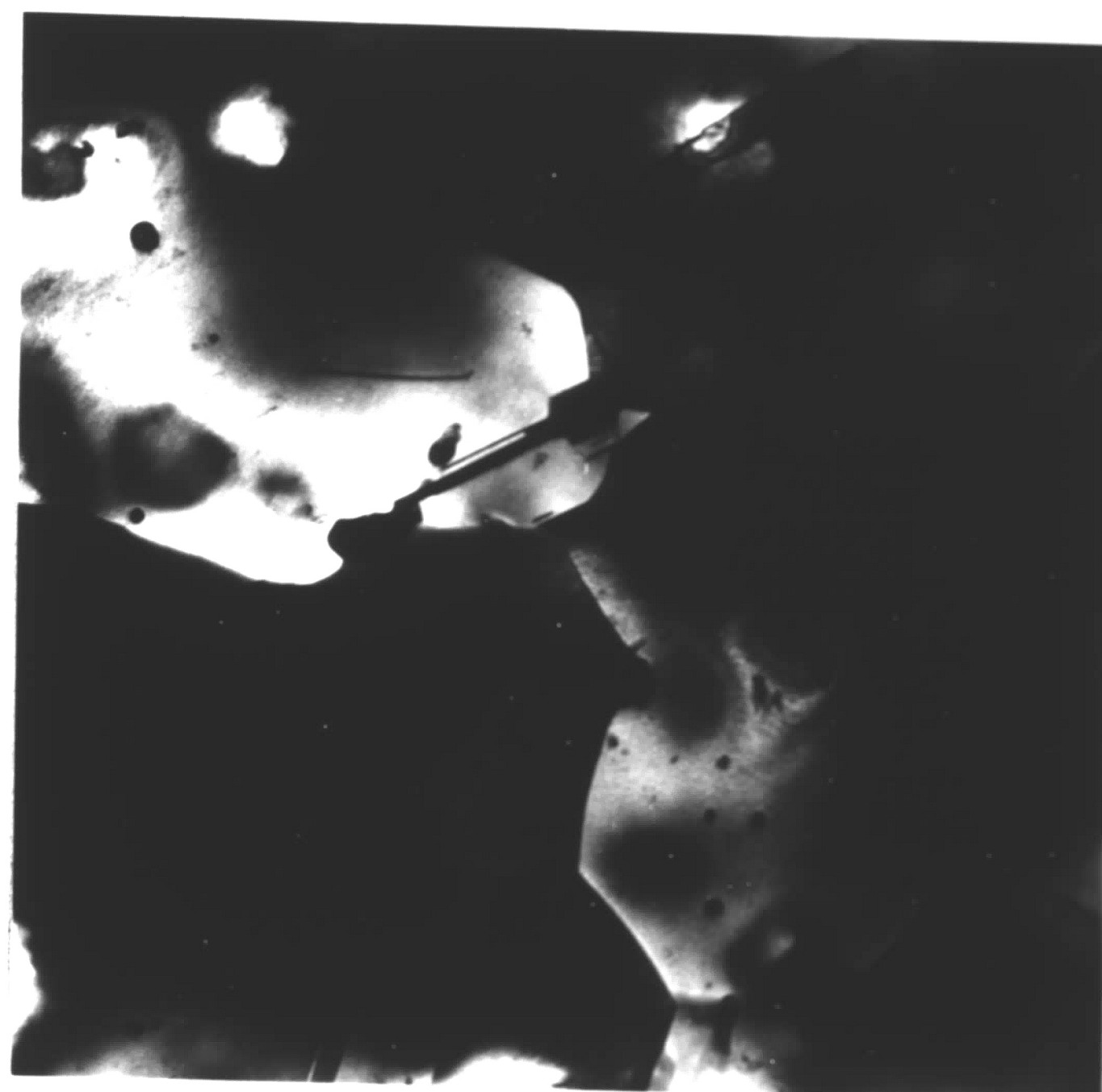
A. 15 MINUTES X20,000



B. 2 HOURS X20,000



C. 4 HOURS X10,000



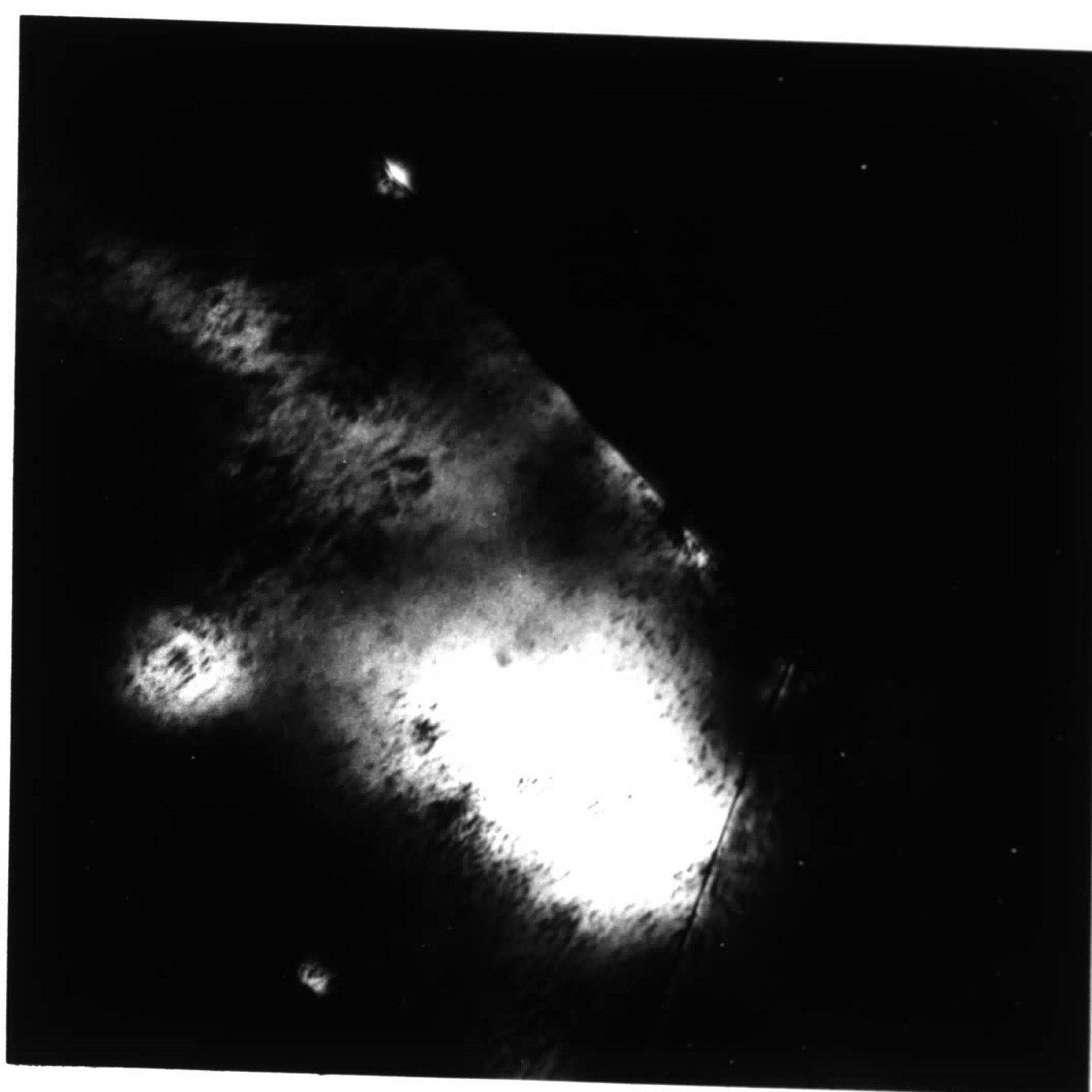
D. 4 HOURS X20,000

FIGURE 22
ELECTRON MICROGRAPHS OF 90% COLD WORKED ALLOY
ANNEALED AT 600°C FOR THE TIMES INDICATED.

54.



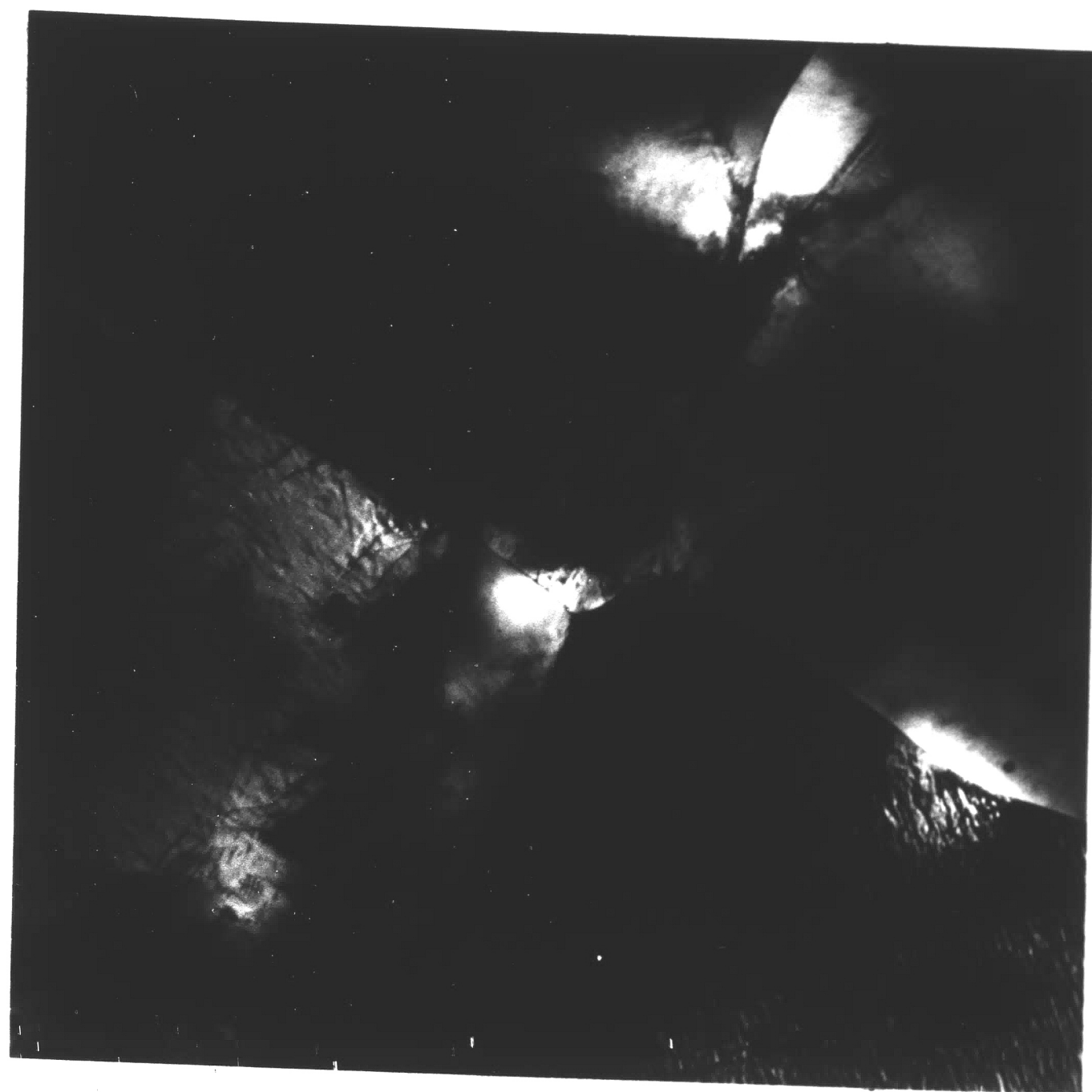
A. 850°C



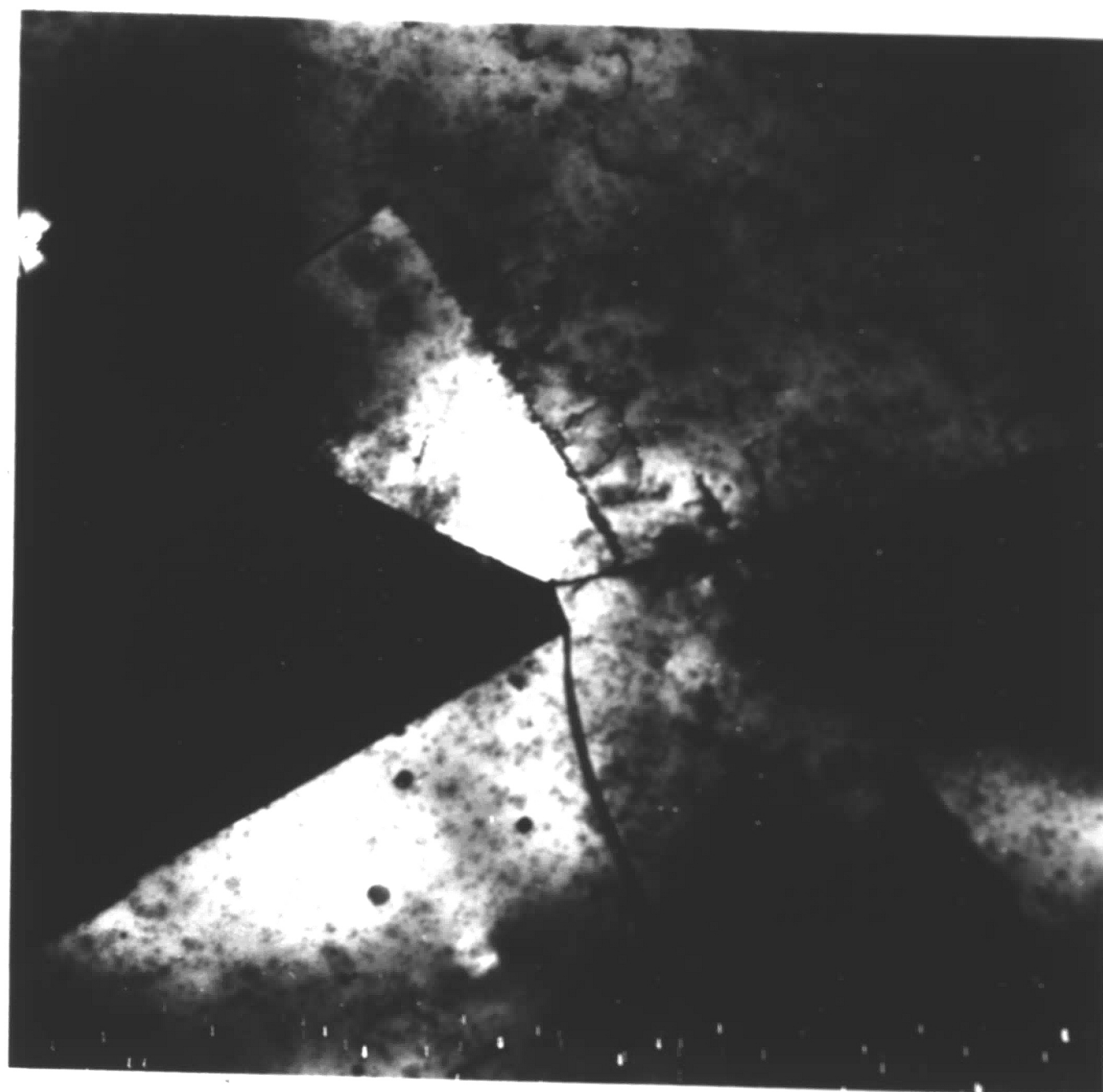
B. 900°C

FIGURE 23

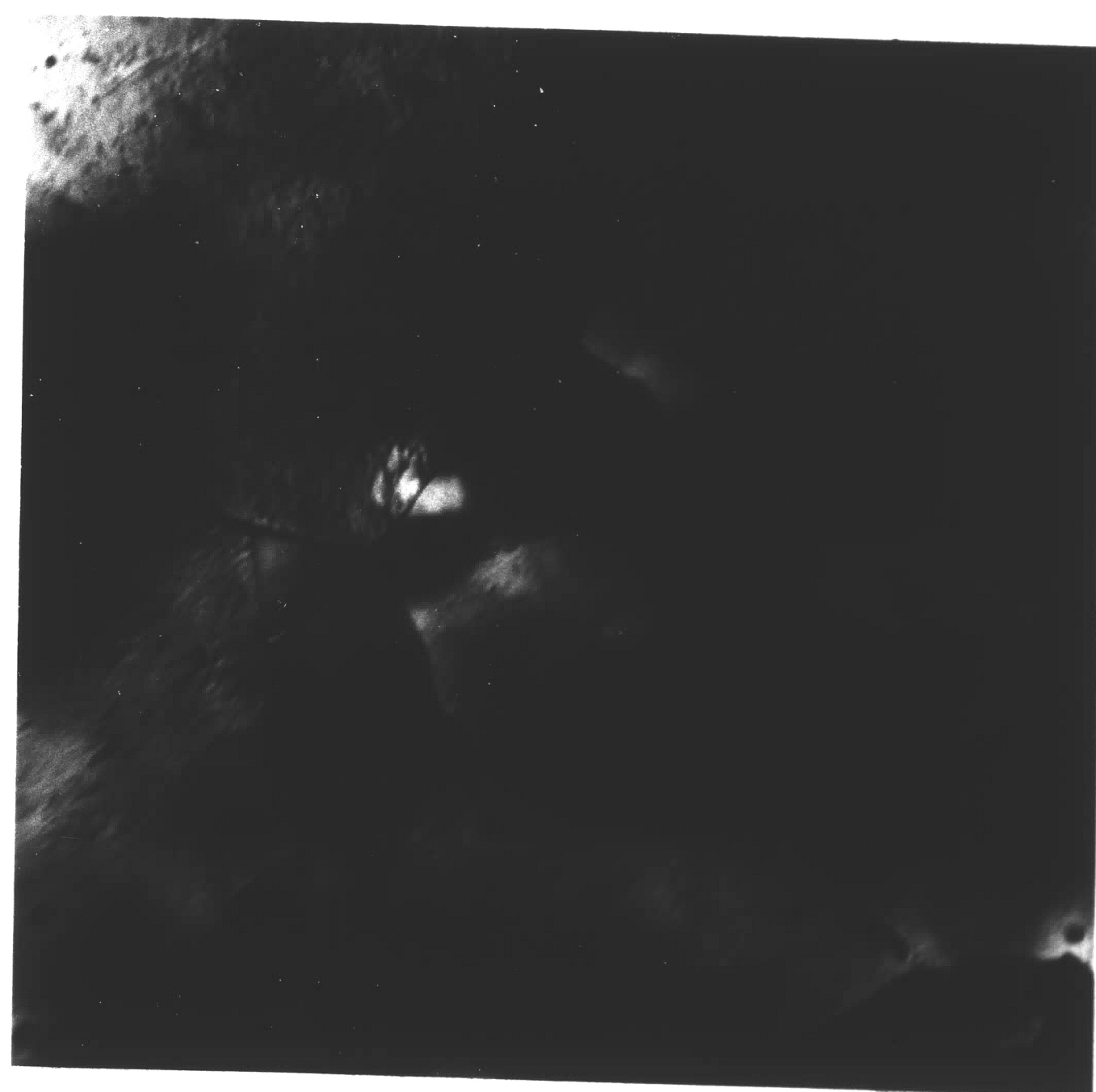
ELECTRON MICROGRAPHS OF 90% COLD WORKED ALLOY
ANNEALED FOR 2 HOURS AT TEMPERATURES INDICATED. X20,000.



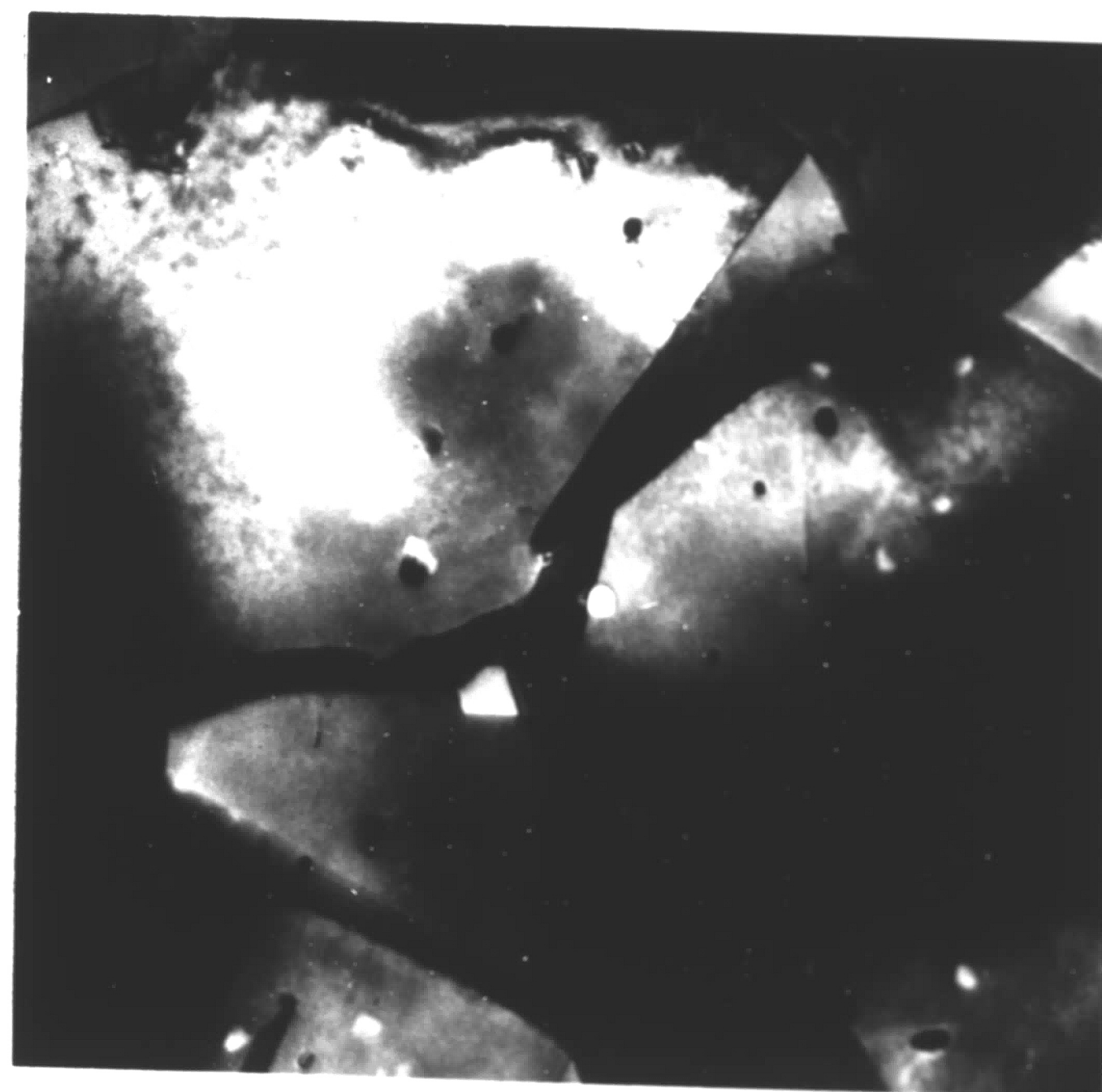
A. 30 MINUTES



B. 30 MINUTES



C. 1 HOUR

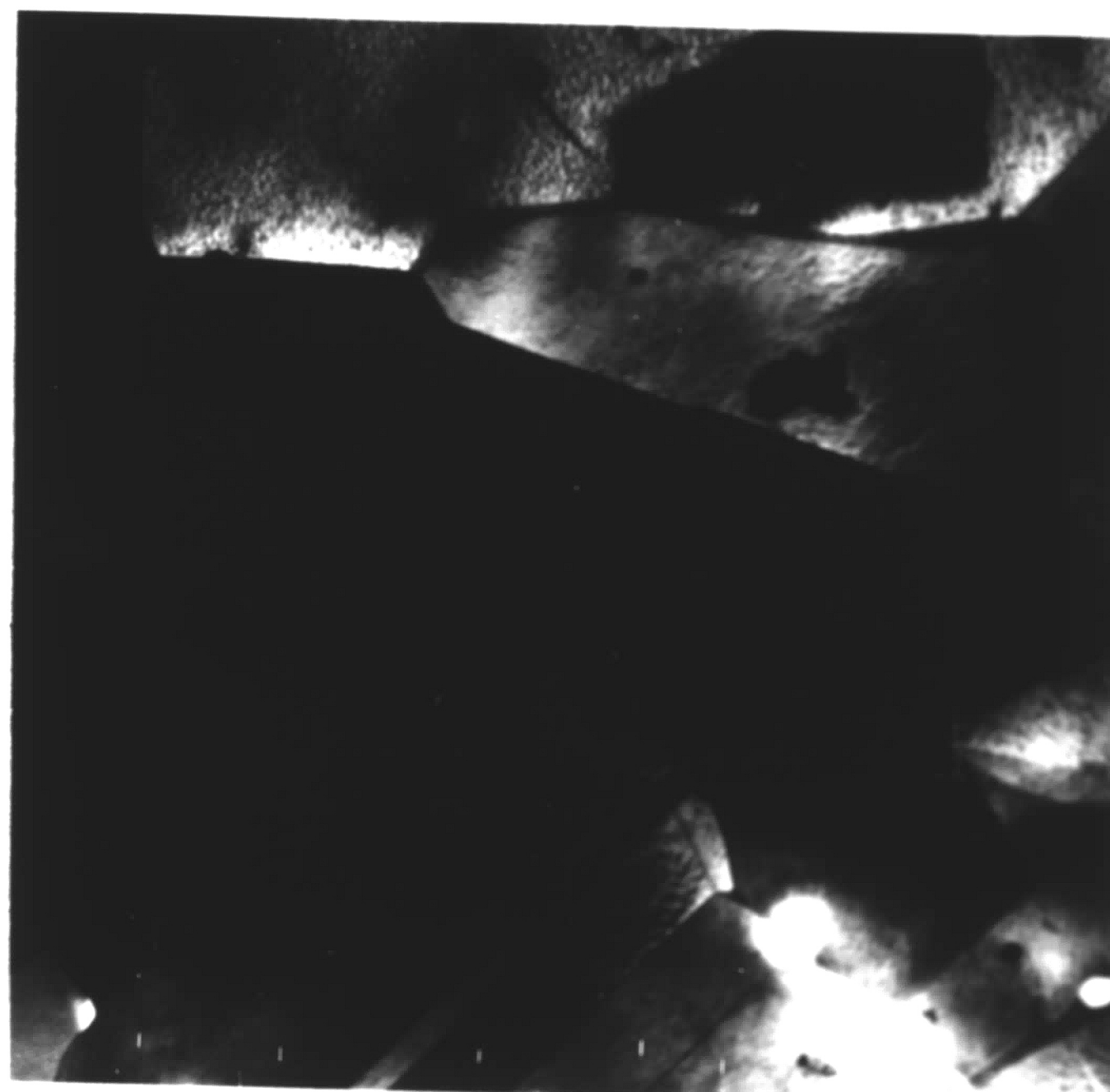


D. 4 HOURS

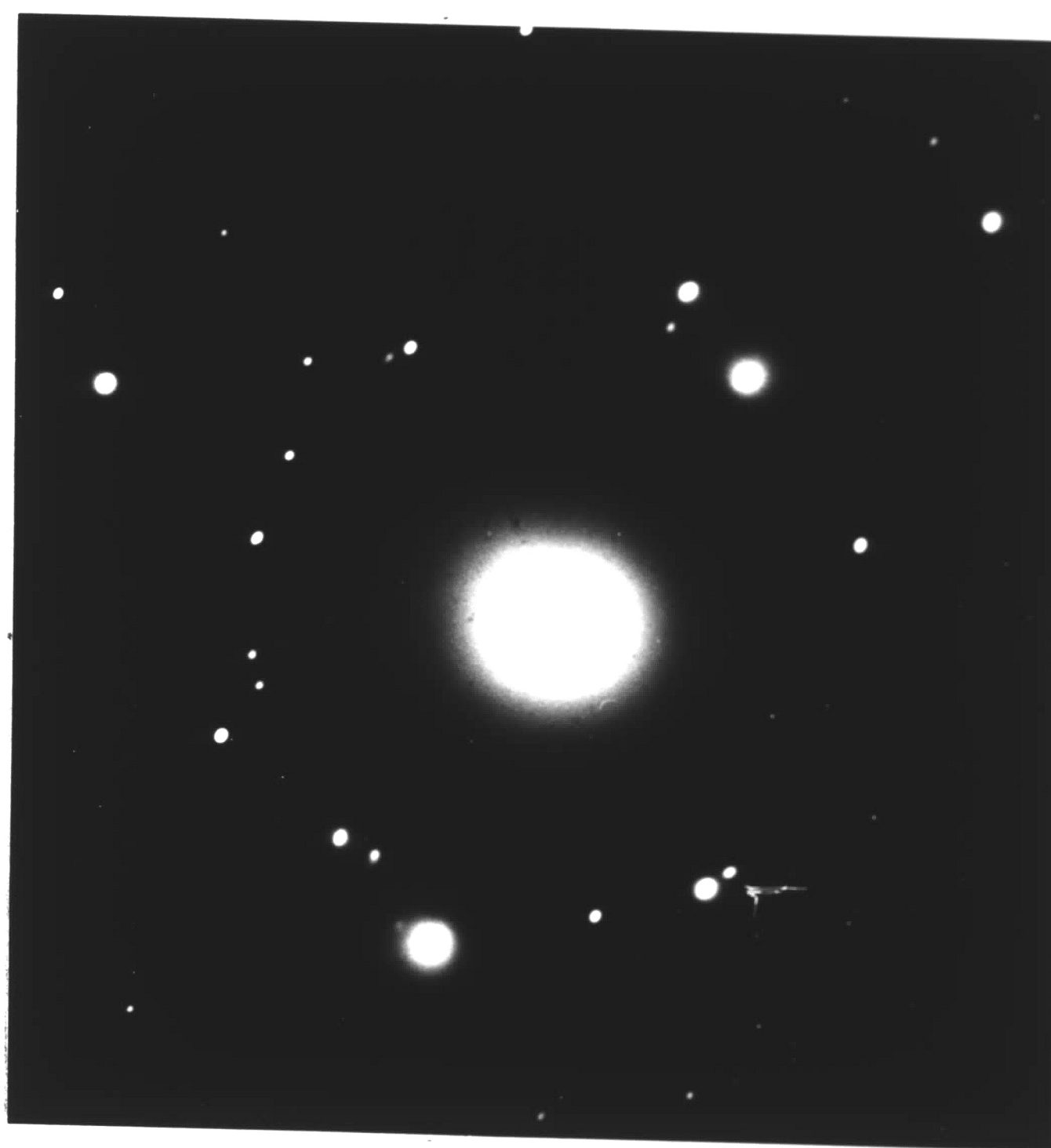
FIGURE 24
ELECTRON MICROGRAPHS OF 90% COLD WORKED ALLOY ANNEALED
AT 700°C FOR THE TIMES INDICATED. X20,000.



A. X 10,000



B. X 15,000



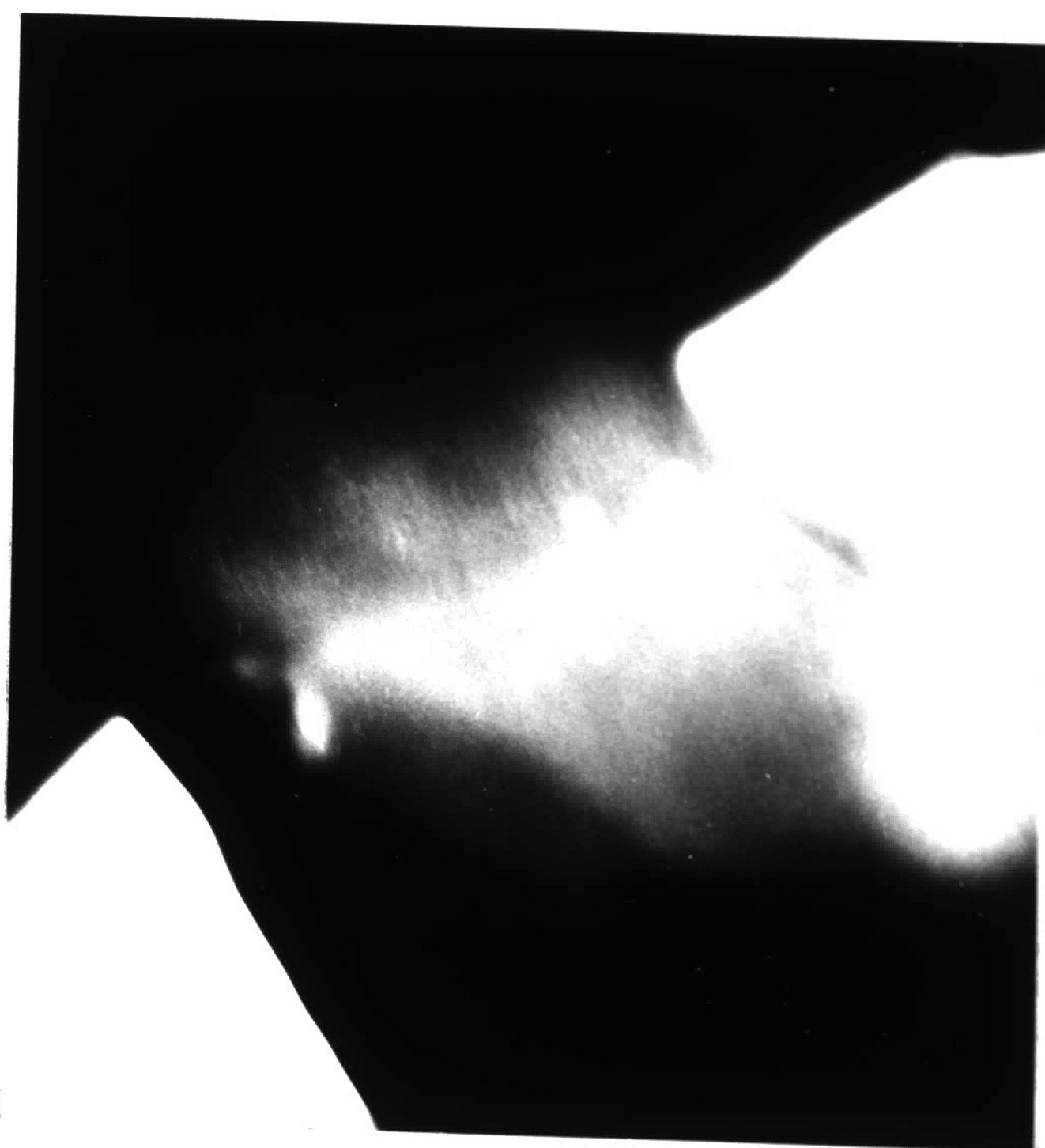
C.

FIGURE 25
ELECTRON MICROGRAPHS AND DIFFRACTION PATTERN OF 90% COLD
WORKED ALLOY ANNEALED AT 700°C FOR 30 MINUTES.

57.



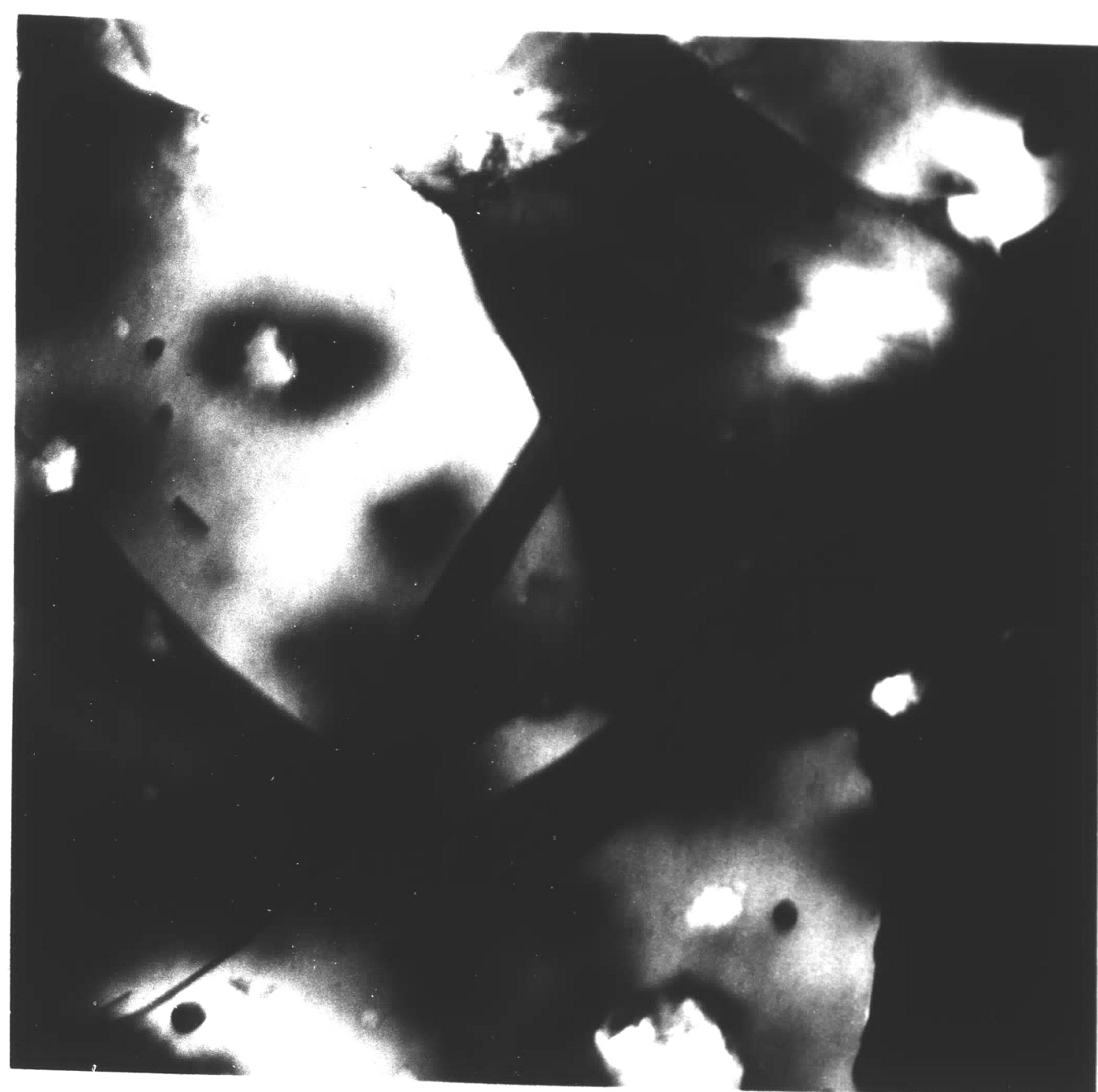
A. X 100,000



B. DARKFIELD X60,000

FIGURE 26

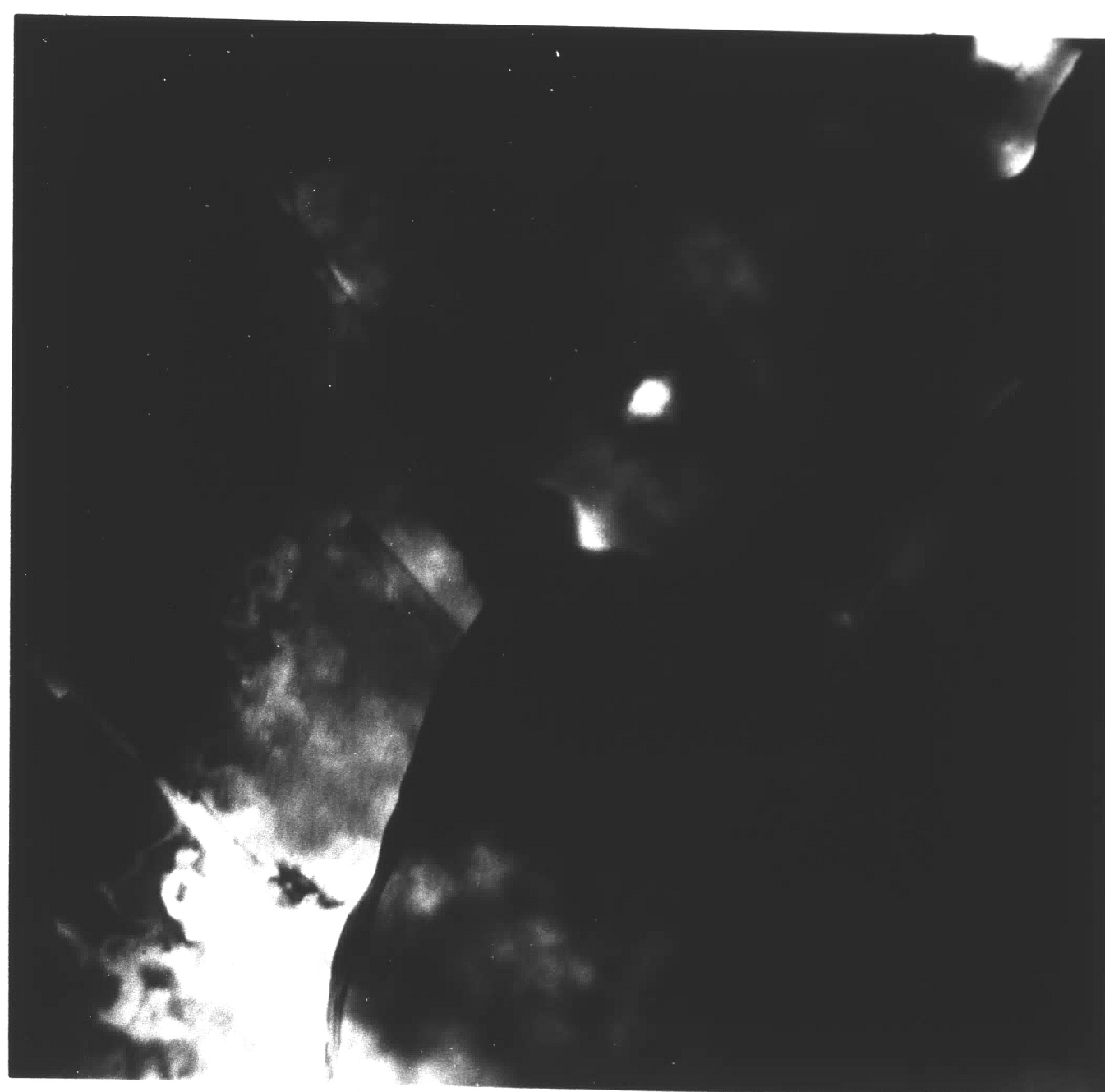
ELECTRON MICROGRAPHS OF 90% COLD WORKED ALLOY
ANNEALED AT 700°C FOR 30 MINUTES



A. 15 MINUTES X20,000



B. 30 MINUTES X20,000



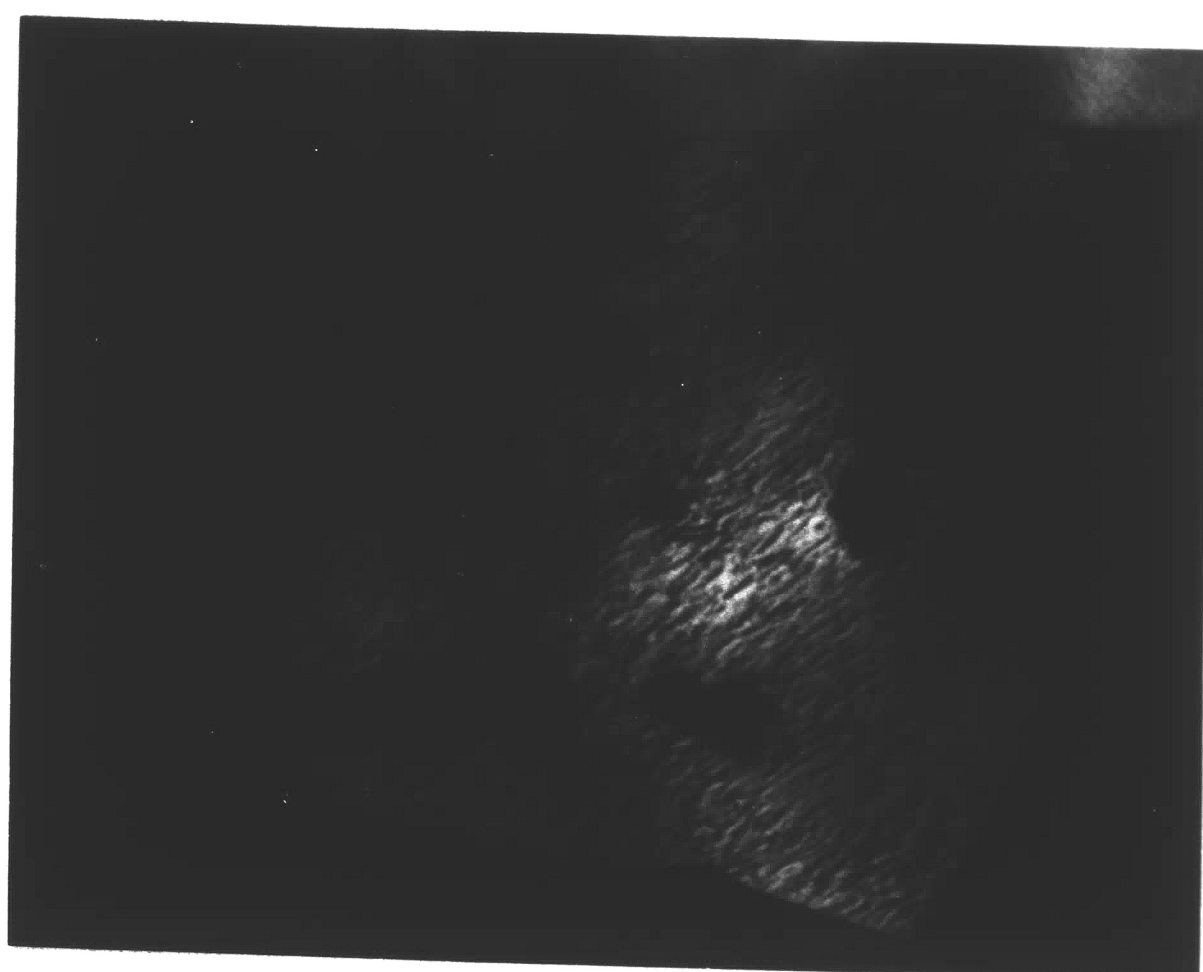
C. 1 HOUR X30,000



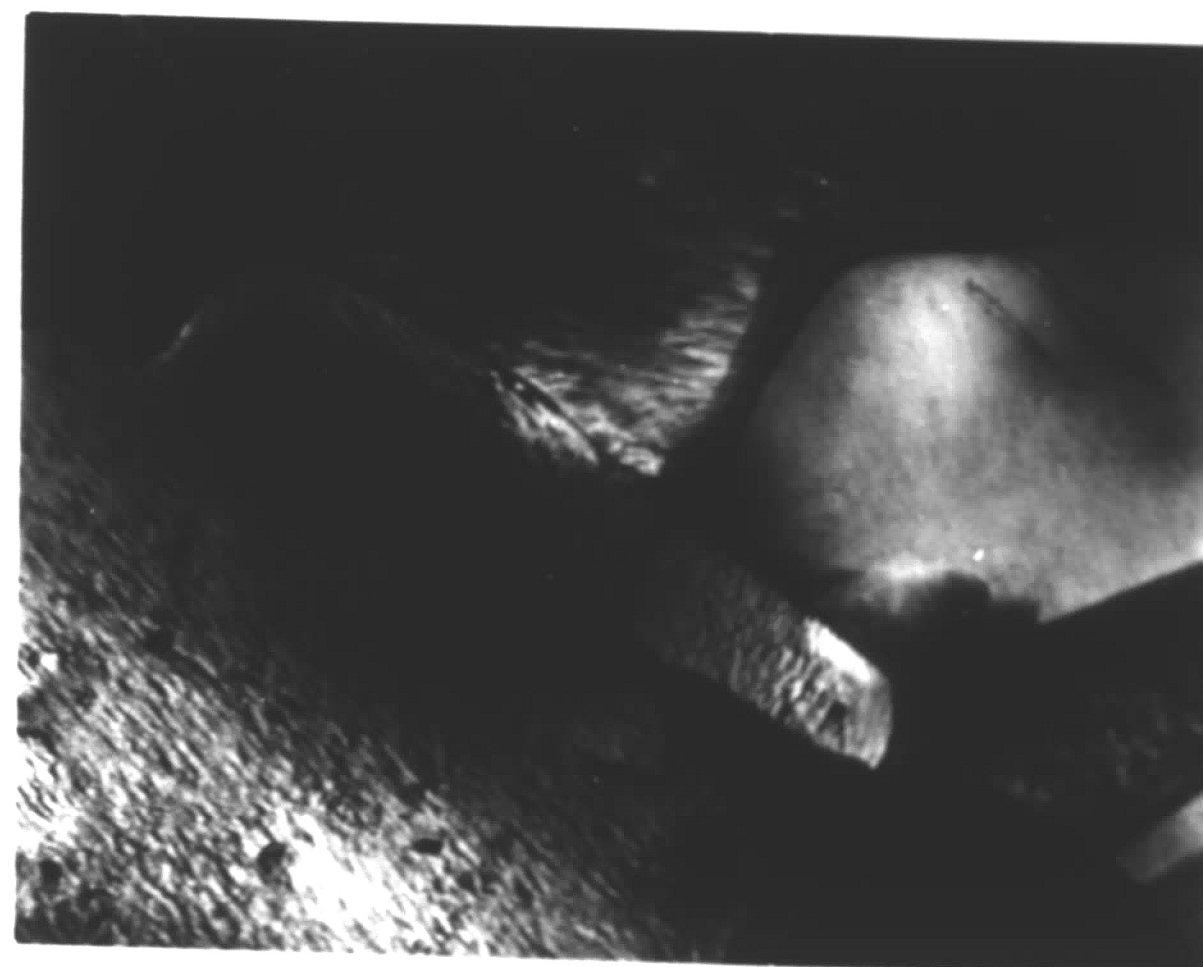
C. 2 HOURS X20,000

FIGURE 27

ELECTRON MICROGRAPHS OF 90% COLD WORKED ALLOY
ANNEALED AT 800°C FOR TIMES INDICATED.



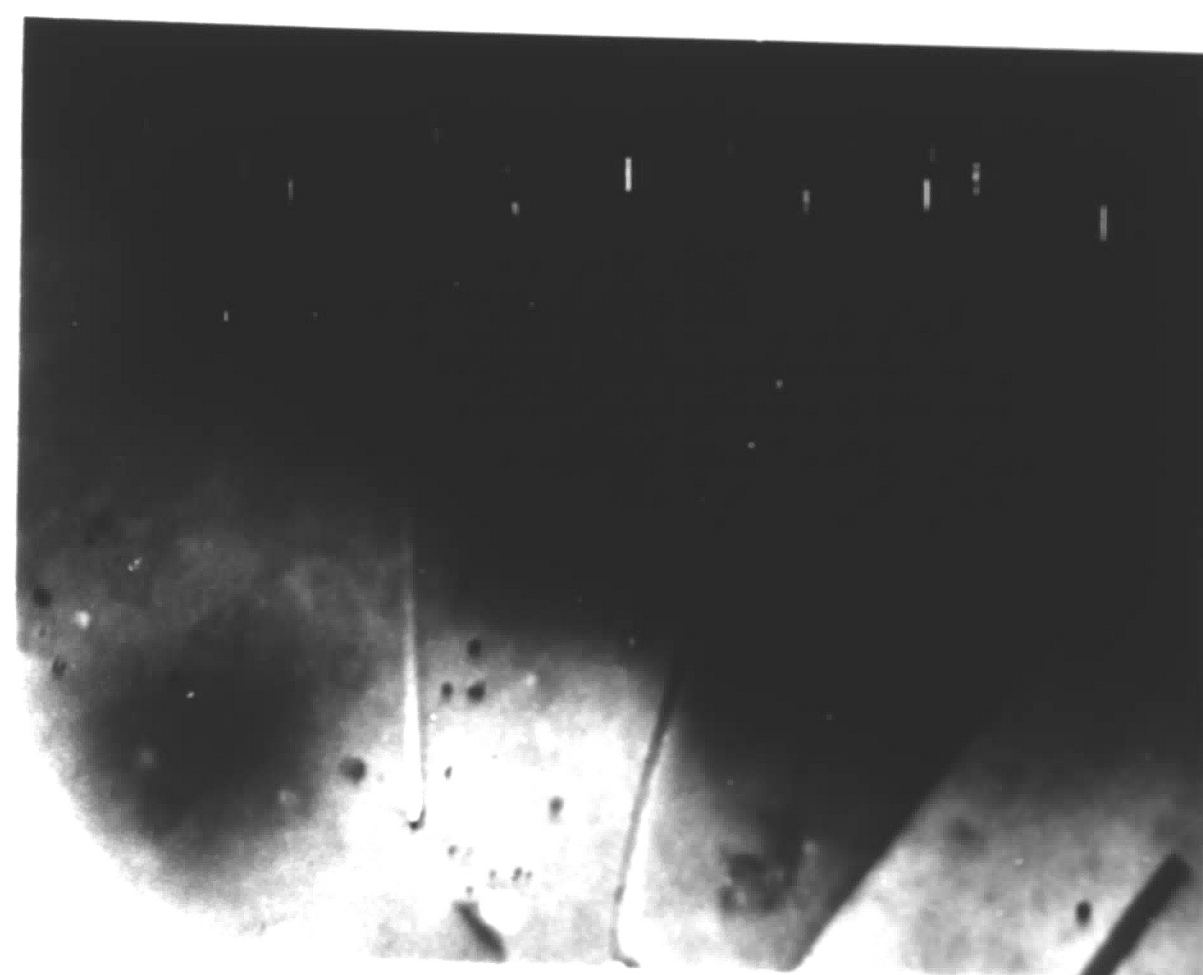
A. 700°C - 30 MIN.



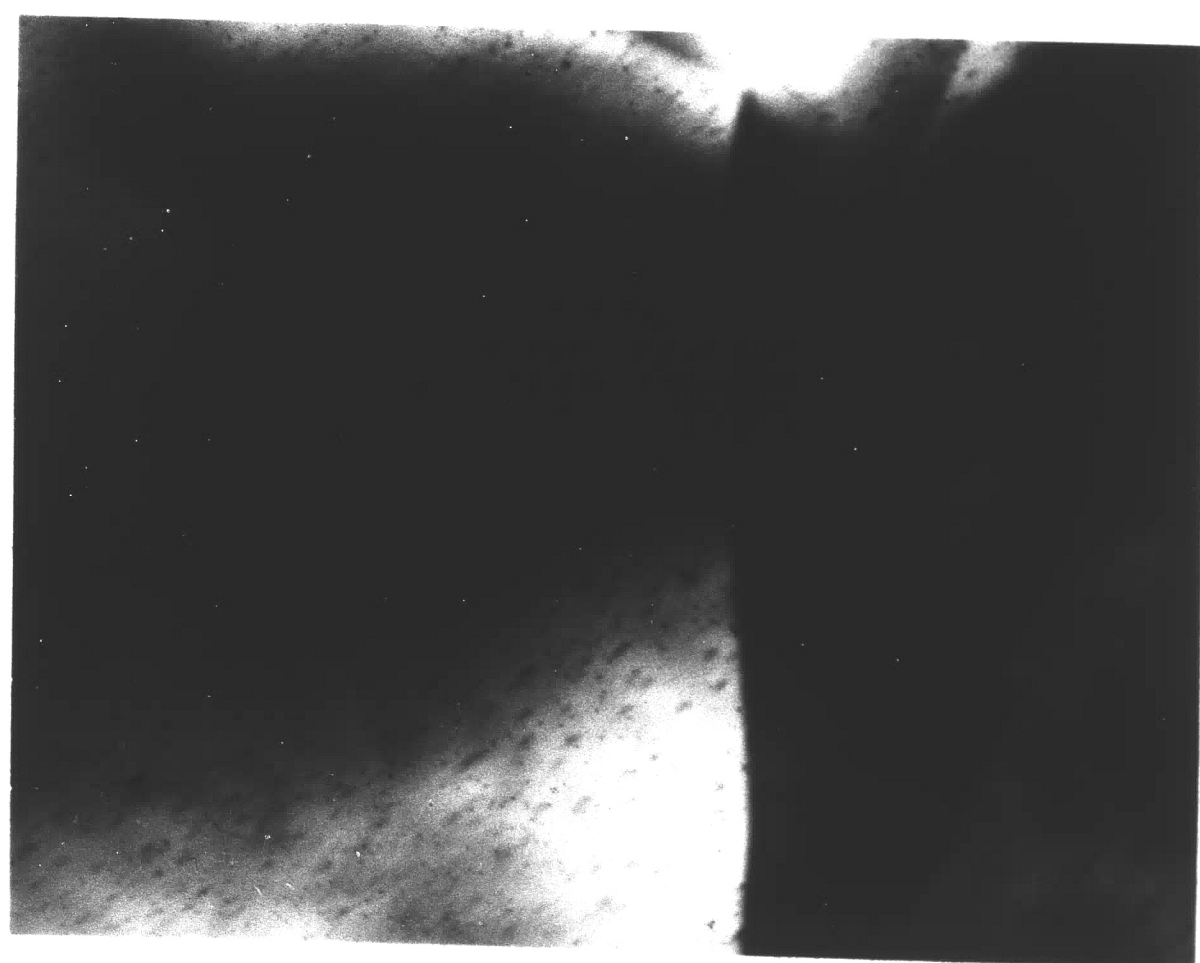
B. 700°C - 30 MIN.



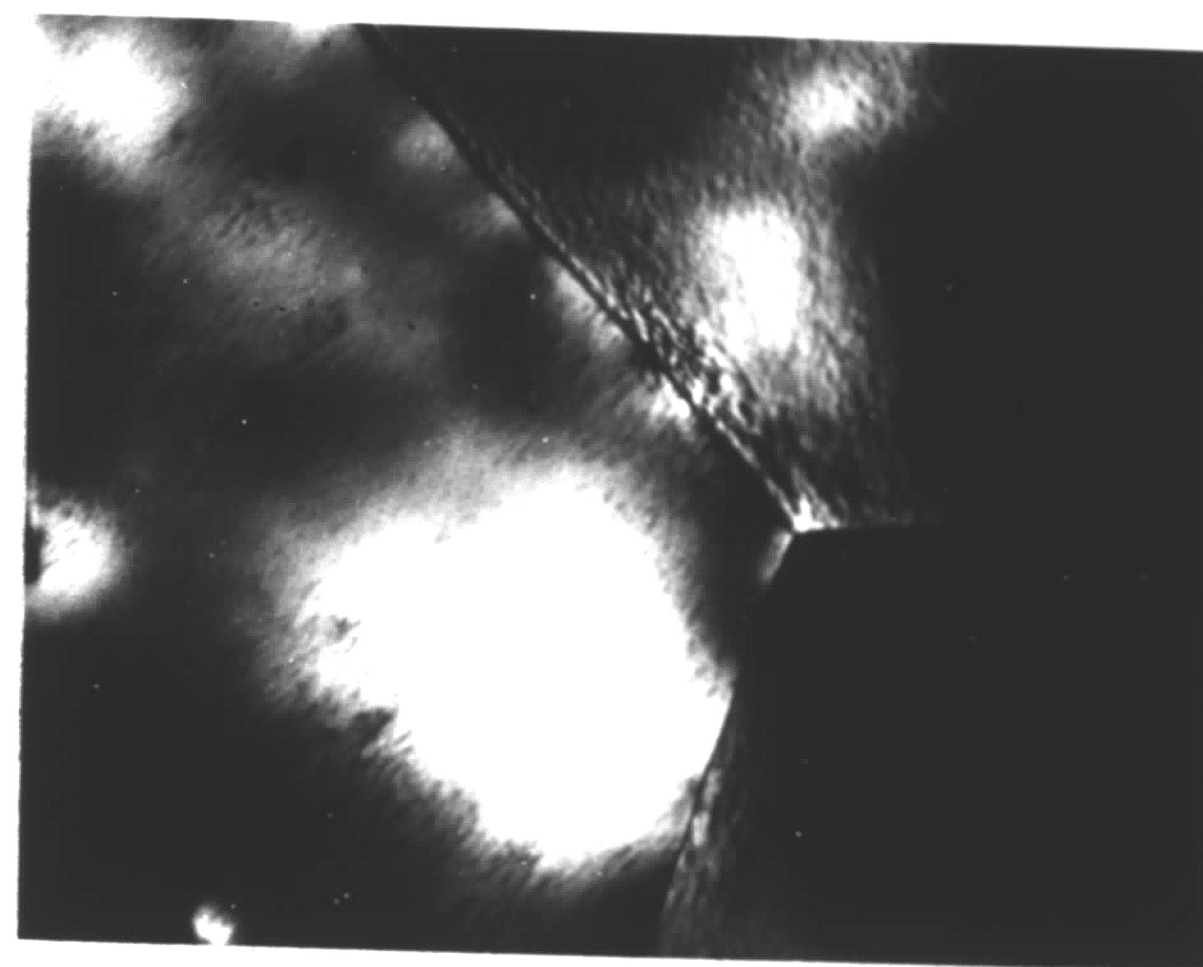
C. 800°C - 30 MIN.



D. 800°C - 30 MIN.



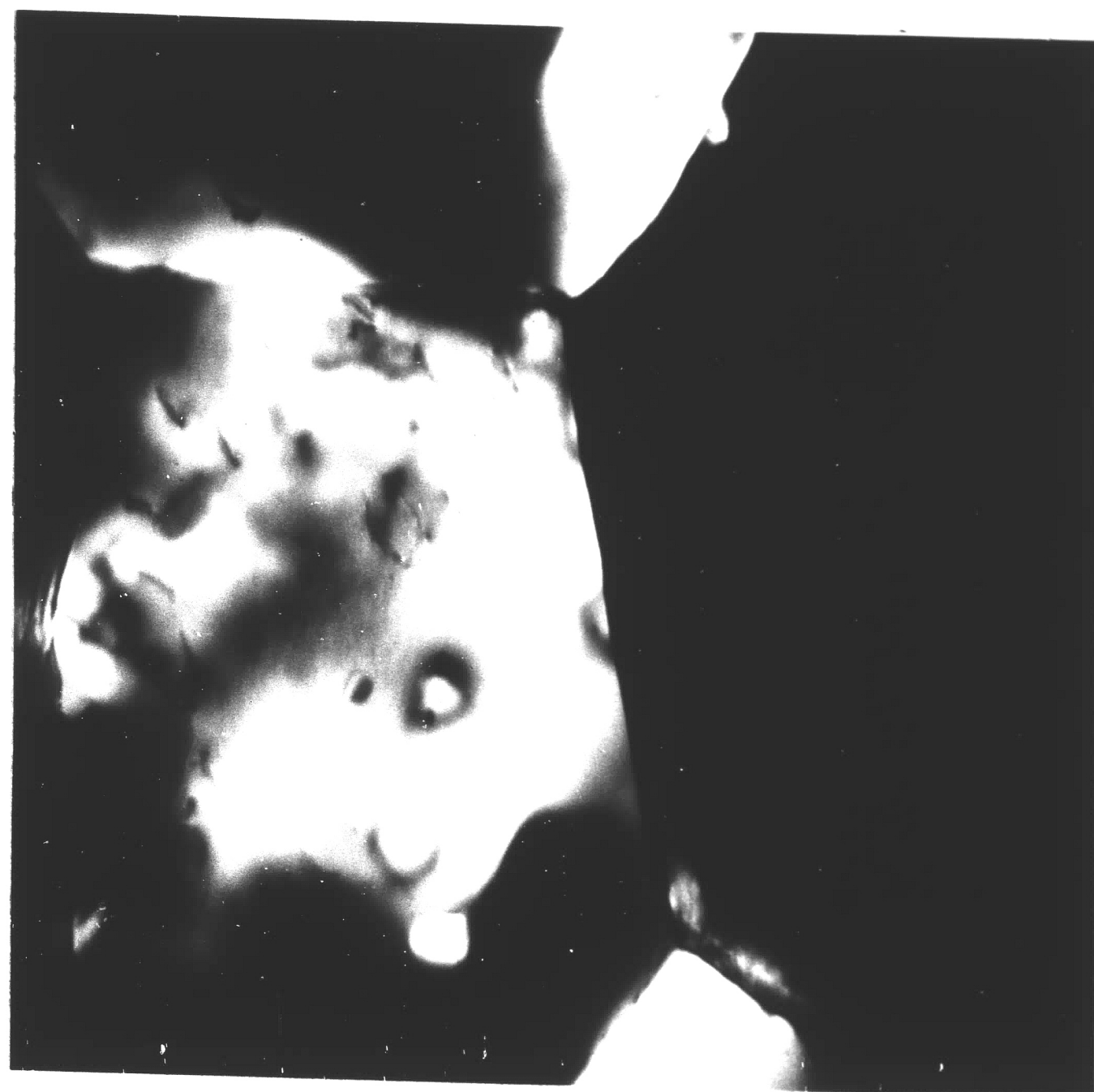
E. 900°C - 1 HR.



F. 900 °C - 2 HRS.

FIGURE 28

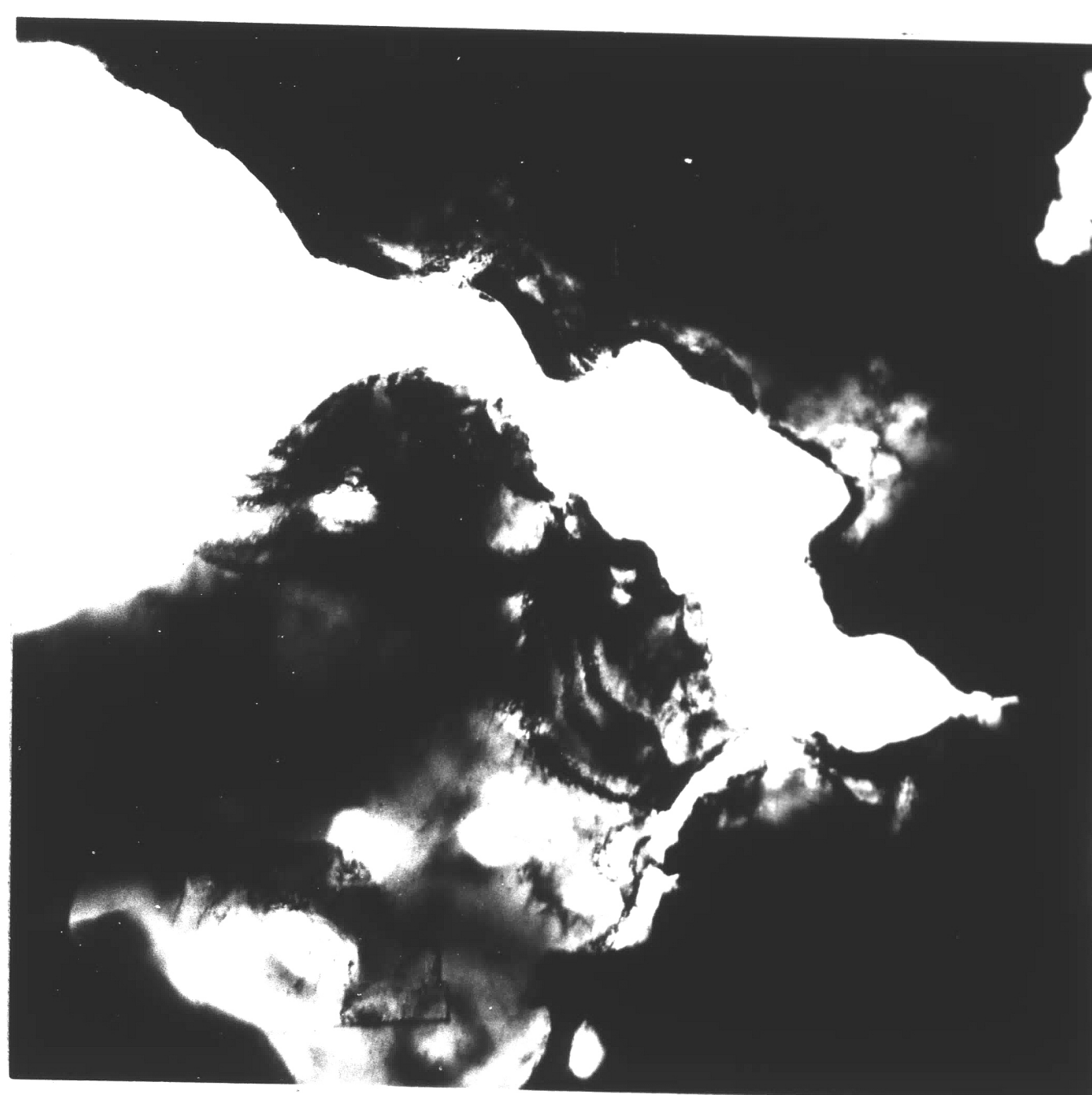
ELECTRON MICROGRAPHS OF 90% COLD WORKED ALLOY
ANNEALED AT THE TEMPERATURES AND TIMES INDICATED. X20,000



A.



B.



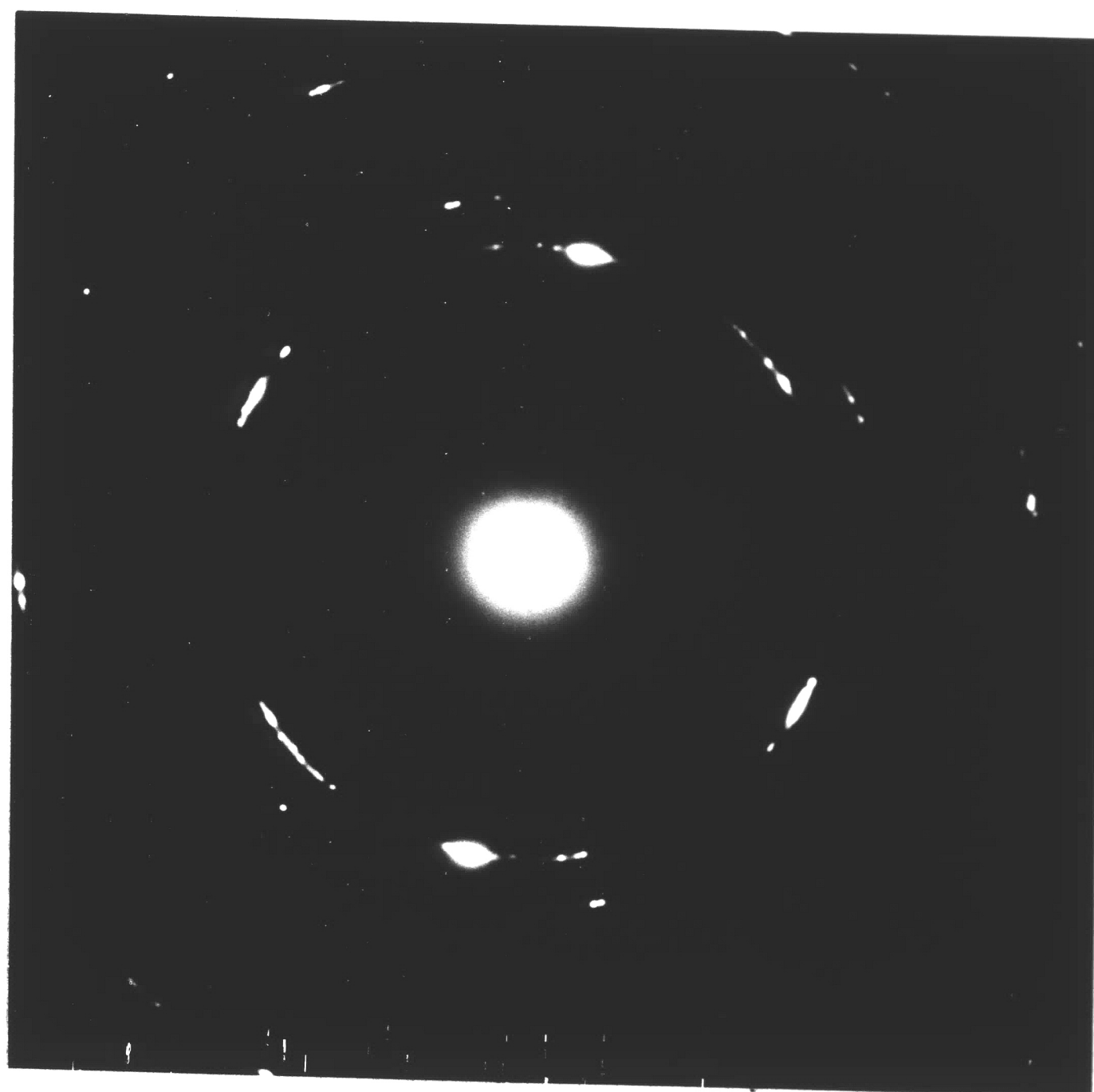
C. BRIGHTFIELD



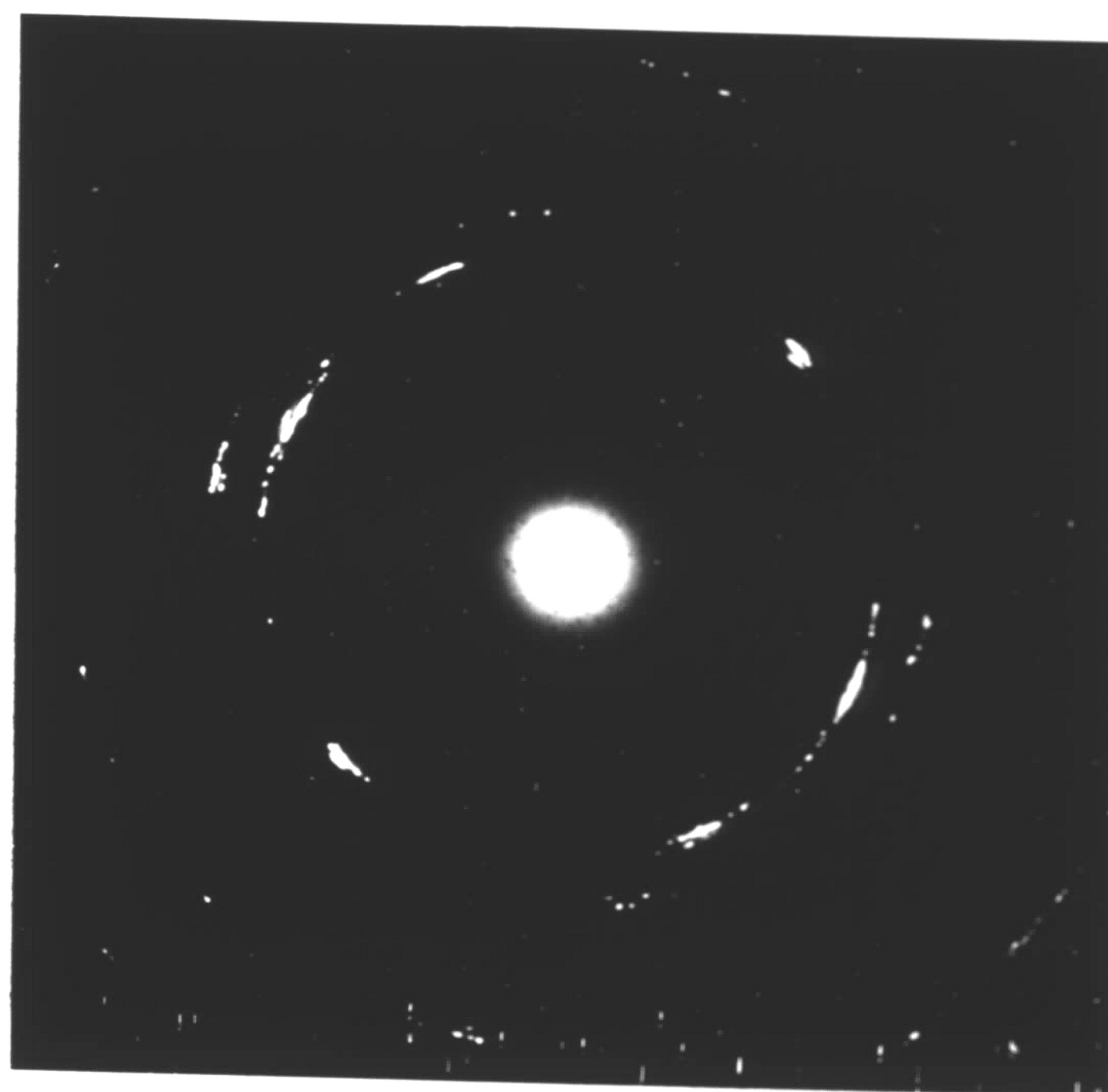
D. DARKFIELD

FIGURE 29

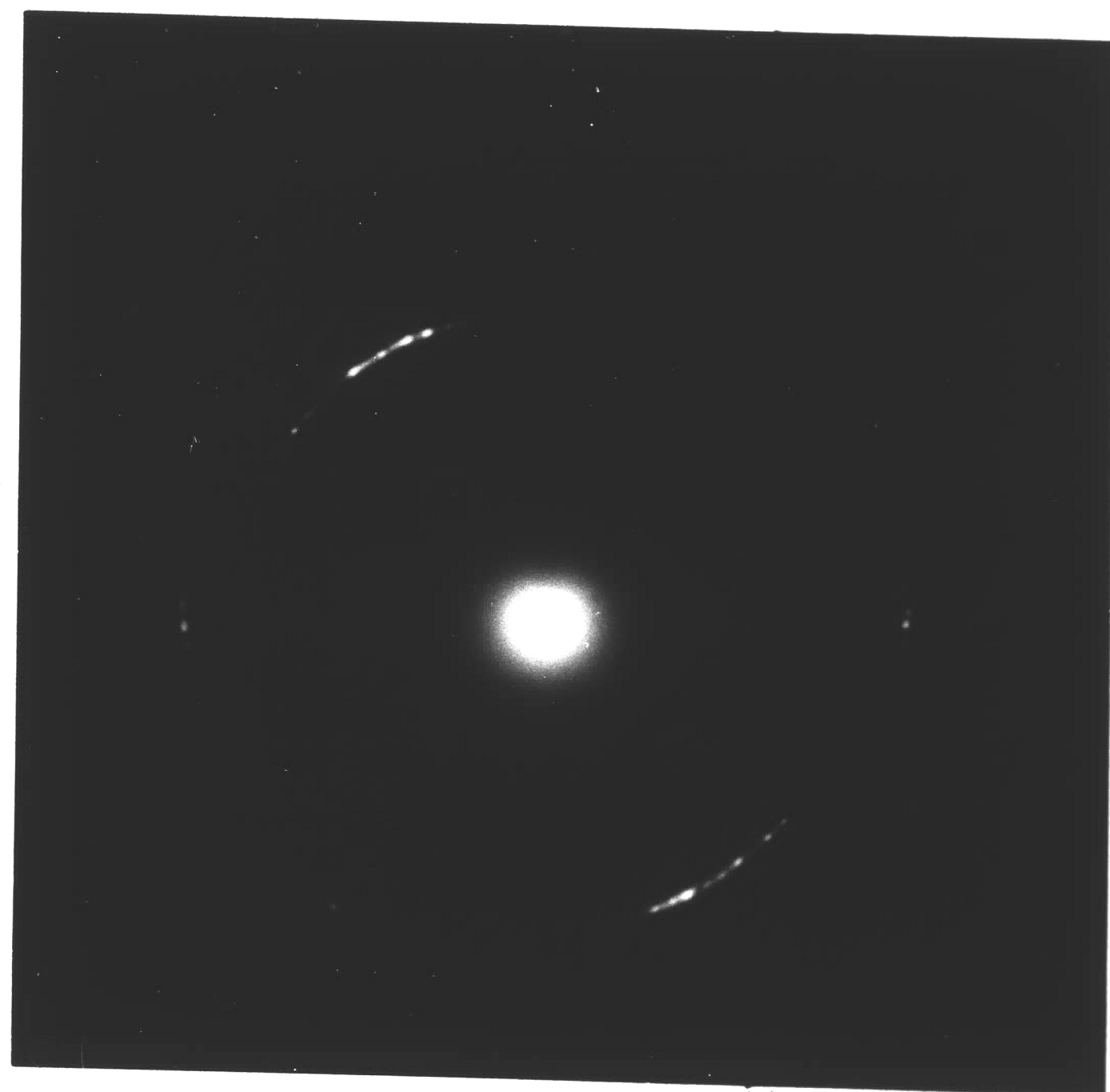
ELECTRON MICROGRAPHS OF 90% COLD WORKED ALLOY
ANNEALED AT 850°C FOR 2 HOURS. X20,000



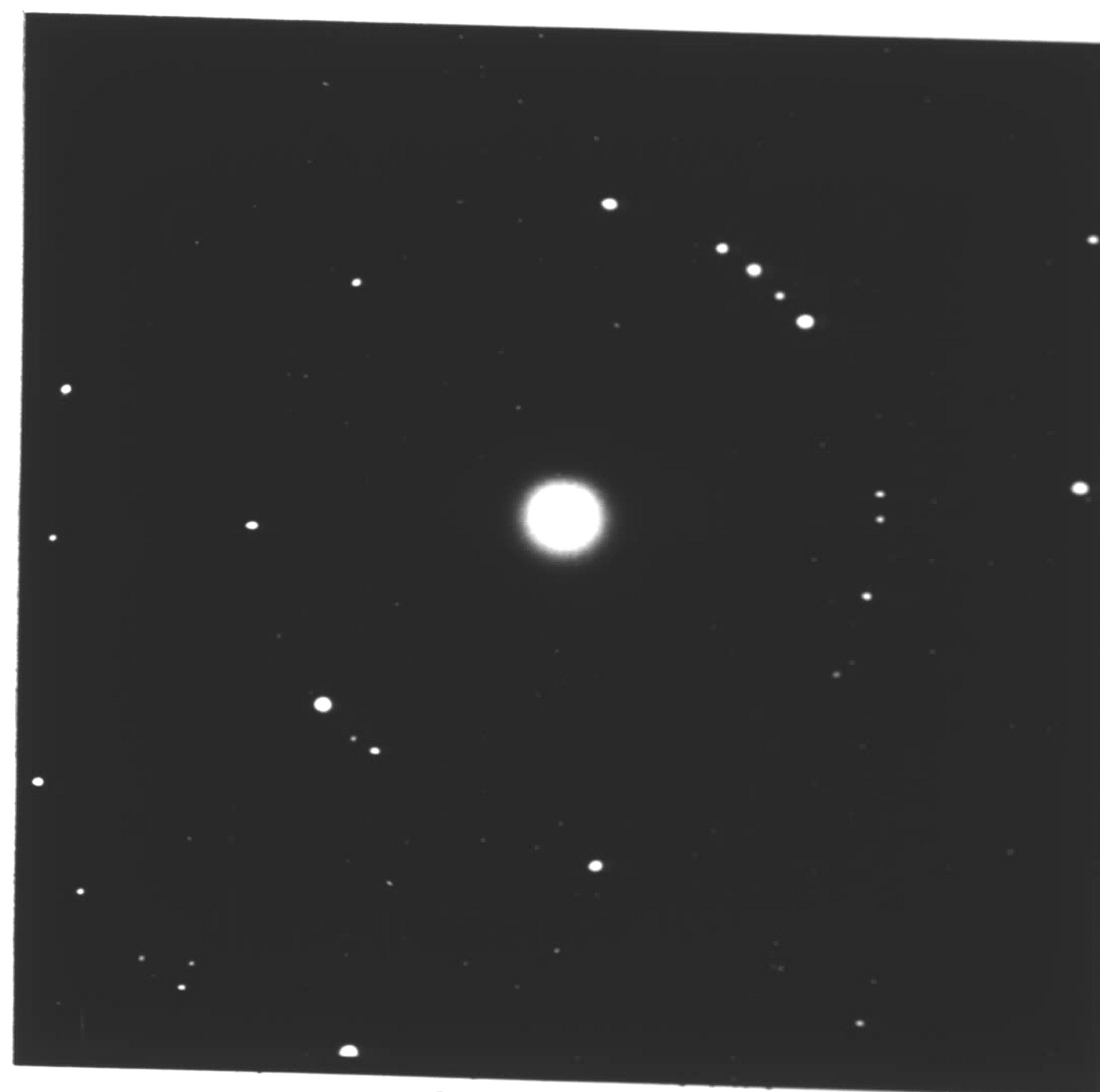
A. UNANNEALED



B. 600°C - 15 MIN.



C. 600°C - 2 HRS.



D. 700°C - 4 HRS.

FIGURE 30

ELECTRON DIFFRACTION PATTERNS OF 90% COLD WORKED
ALLOY ANNEALED AT TEMPERATURES AND TIMES INDICATED.

TABLE I

ELECTRON DIFFRACTION DATA

90% COLD WORK - UNANNEALED

MEASURED D-SPACING	OBS. I	ASTM D-SPACING	ASTM I/I ₀	COMPOUND	hkl
2.056	S	2.06	100	NiFe	111
1.776	M	1.783	30	NiFe	002
1.256	W	1.259	20	NiFe	022
1.078	M	1.073	40	NiFe	113
1.027	VW	1.027	10	NiFe	222

TABLE II

ELECTRON DIFFRACTION DATA

90% COLD WORK - 600°C - 2 HOURS

MEASURED D-SPACING	OBS. I	ASTM D-SPACING	ASTM I/I ₀	COMPOUND	hkl
2.057	S	2.06	100	NiFe	111
		2.05	100	Ni ₄ Mo	211
1.778	S	1.783	30	NiFe	002
		1.79	90	Ni ₄ Mo	310
1.455	VW	1.43	60	Ni ₄ Mo	321
1.256	M	1.259	20	NiFe	022
		1.26	90	Ni ₄ Mo	312
1.070	M	1.073	40	NiFe	113
		1.07	90	Ni ₄ Mo	213
1.029	W	1.027	10	NiFe	222
		1.03	80	Ni ₄ Mo	422

TABLE III
ELECTRON DIFFRACTION DATA

90% COLD WORK - 850°C - 2 HOURS					
MEASURED D-SPACING	OBS. I	ASTM D-SPACING	ASTM I/I ₀	COMPOUND	hkl
2.790	VW	2.80	40	Ni ₄ Mo	200
2.364	W	2.358	80	Ni ₅ Zr	220
2.050	S	2.06	100	NiFe	111
		2.05	100	Ni ₄ Mo	211
2.019	S	2.024	100	Ni ₅ Zr	311
1.892	W	1.928	80	Ni ₅ Zr	222
1.776	S	1.783	30	NiFe	002
		1.79	90	Ni ₄ Mo	310
1.681	VW	1.670	30	Ni ₅ Zr	400
1.622	VW	1.63	40	Ni ₄ Mo	301
1.534	VW	1.531	30	Ni ₅ Zr	331
1.507	VW	1.50	60	Ni ₄ Mo	202
1.471	VW	1.494	30	Ni ₅ Zr	420
1.257	S	1.259	20	NiFe	022
		1.26	90	Ni ₄ Mo	312
1.071	S	1.073	40	NiFe	113
		1.07	90	Ni ₄ Mo	213
1.024	S	1.027	10	NiFe	222
		1.03	80	Ni ₄ Mo	422

BIBLIOGRAPHY

1. Tisone, T. C., G. Y. Chin, and W. B. Grupen. "Stress Insensitive Permalloys for Memory Application." IEEE Transactions on Magnetics. September 1970. pp. 712-716.
2. Tisone, T. C., G. Y. Chin, and W. B. Grupen. "Metallurgical Control of Magnetic Properties in Co-Fe and Ni-Fe Alloys for Memory Applications." Journal of Applied Physics. March 1971.
3. Uhl, R. H. "Coercive Force and Structure in a Co-Fe-Au Alloy." Metallurgical Transactions. Vol. 1. August 1970. pp. 2157-2161.
4. Lynch, L. "The Effects of Changes in Au Concentration Upon the Microstructure and Magnetic Properties of Au-Fe-Co Alloys." Lehigh University Master's Thesis 1969.
5. Guy, A. G., Elements of Physical Metallurgy. Addison-Wesley Publishing Company, Reading, Massachusetts. 1967. pp. 418-438, 441-450.
6. Aust, K. G. and J. W. Rutter. "Grain Boundary Migration." Recovery and Recrystallization of Metals. American Institute of Mining, Metallurgical, and Petroleum Engineers. Edited by L. Himmel. Interscience Publishers. New York. 1963. pp. 142-147.
7. Wenny, D. H. Jr. and H. L. B. Gould. "The Polyform Hysteresis Loops of Thin Gage High Cobalt-Iron Alloys." Transactions of The Metallurgical Society of AIME. Vol. 233. April 1965. pp. 836-838.
8. Turnbull, D. "Role of Structural Impurities in Phase Transformations." Impurities and Imperfections. American Society for Metals. Cleveland, Ohio. 1955. pp. 136-142.
9. Hornbogen, E. "Electron Microscopical Investigation of the Recrystallization of Alloys in Which Precipitation Can Occur." Practical Metallography. Vol. 7. July 1970. pp. 349-360.
10. Chilton, J. M. and C. J. Barton. "Identification of Strengthening Precipitates in 18 Ni (250) Aluminum, Vanadium, and Titanium Maraging Steels." A.S.M. Transactions Vol. 60. 1967. pp. 528-542.

11. Thomas, G. and J. Washburn. Electron Microscopy and Strength of Crystals. Interscience Publishers. New York, 1963. pp. 542-545.
12. Hammond, C. M. and G. S. Ansell. "Gamma-Prine Precipitation in an Fe-Ni-Base Alloy." A.S.M. Transactions. Vol. 57. 1964. pp. 727-738.
13. Turnbull, D. and H. M. Treaftis. "Kinetics of Precipitation From Lead-Tin Solid Solutions." Acta Metallurgica. Vol. 3. January 1955. pp. 43-54.
14. Nesbitt, E. A. and A. J. Williams. "Effect of Precipitation on Magnetic Properties of Iron-Base Alloys." Precipitation From Iron Base Alloys. Metallurgical Conferences. Edited by Speich, G. R. and J. B. Clark. Gordon and Breach Science Publishers, Inc. New York. Vol. 28. 1963.
15. Hirsch, P. B., A. Howie, R. B. Nicholson, D. W. Pashley, and M. J. Whelan. Electron Microscopy of Thin Crystals. Plenum Press. New York. 1965. pp. 317-327.
16. Shewmon, P. G. Transformations in Metals. McGraw-Hill Book Company. New York. 1969. pp. 93-106, 212-213.
17. Hull, D. Introduction to Dislocations. Pergamon Press. Oxford. 1968. pp. 175-199, 222-227.
18. Hutchison, T. S. and D. C. Baird. The Physics of Engineering Solids. John Wiley and Sons, Inc. New York. 1968. pp. 163-168, 444.
19. Van Valack, L. H. Elements of Materials Science. Addison-Wesley Publishing Company, Inc. Reading, Massachusetts. 1964. pp. 125-126, 153-154, 311-313.
20. Moffatt, W. G., G. W. Pearsall, R. M. Rose, L. A. Shepard, and J. Wulff. The Structure and Properties of Materials. John Wiley and Sons, Inc. New York. 1967. Vol. I, pp. 139-143. Vol. IV, pp. 206-214.

VITA

Charles R. Frohlich, Jr. was born in Baltimore, Maryland in 1946, the son of Mr. and Mrs. Charles R. Frohlich. He was graduated from Parkville Senior High School in 1964 and immediately began studies in engineering at the University of Maryland. During summer employment at the Maryland Bolt and Nut Company as an engineering associate, he was involved in tool design and materials processing. In 1968 he received a B.S. degree in mechanical engineering from the University of Maryland, having been a member and officer of Pi Tau Sigma International Mechanical Engineering Honorary and Tau Beta Pi International Engineering Honorary. In June of the same year he married the former Gayle Christine Banner.

Upon graduation he accepted a position as engineer with the Western Electric Company in Baltimore and assumed engineering responsibility for semi-automatic subassembly machinery and design changes in apparatus cases for the L-4 carrier system. Transferring to the Western Electric Engineering Research Center in Princeton, New Jersey, in 1969, he was assigned to the materials analysis and characterization laboratory and promoted to development engineer. Together with research on Zr-permalloys, he pursued a Master of Science Degree in Metallurgy and Materials Science in the Lehigh-Western Electric Masters Program.